Available online at www.sciencedirect.com
ScienceDirect
Ore Geology Reviews 29 (2006) 177–241
ORE GEOLOGY REVIEWS
www.elsevier.com/locate/oregeorev

Nickel sulfide deposits in Australia: Characteristics, resources, and potential

Dean M. Hoatson *, Subhash Jaireth, A. Lynton Jaques

Geoscience Australia, GPO Box 378, Canberra, ACT, 2601, Australia

Received 26 September 2005; accepted 16 May 2006
Available online 8 August 2006

Abstract

Australia's nickel sulfide industry has had a fluctuating history since the discovery in 1966 of massive sulfides at Kambalda in the Eastern Goldfields of Western Australia. Periods of buoyant nickel prices and high demand, speculative exploration, and frenetic investment (the 'nickel boom' years) have been interspersed by protracted periods of relatively depressed metal prices, exploration inactivity, and low discovery rates. Despite this unpredictable evolution, the industry has had a significant impact on the world nickel scene with Australia having a global resource of nickel metal from sulfide ores of ~12.9 Mt, five world-class deposits (>1 Mt contained Ni), and a production status of number three after Russia and Canada. More than 90% of the nation's known global resources of nickel metal from sulfide sources were discovered during the relative short period of 1966 to 1973. Australia's nickel sulfide deposits are associated with ultramafic and/or mafic igneous rocks in three major geotectonic settings: (1) Archean komatiites emplaced in rift zones of granite–greenstone belts; (2) Precambrian tholeiitic mafic–ultramafic intrusions emplaced in rift zones of Archean cratons and Proterozoic orogens; and (3) hydrothermal-remobilized deposits of various ages and settings. The komatiitic association is economically by far the most important, accounting for more than 95% of the nation's identified nickel sulfide resources. The ages of Australian komatiitic- and tholeiitic-hosted deposits generally correlate with three major global-scale nickel-metallogenic events at ~3000 Ma, ~2700 Ma, and ~1900 Ma. These events are interpreted to correspond to periods of juvenile crustal growth and the development of large volumes of primitive komatiitic and tholeiitic magmas caused by large-scale mantle overturn and mantle plume activities. There is considerable potential for the further discovery of komatiite-hosted deposits in Archean granite–greenstone terranes including both large, and smaller high-grade (5 to 9% Ni) deposits, that may be enriched in PGEs (2 to 5 g/t), especially where the host ultramafic sequences are poorly exposed.

Analysis of the major komatiite provinces of the world reveals that fertile komatiitic sequences are generally of late Archean (~2700 Ma) or Paleoproterozoic (~1900 Ma) age, have dominantly Al-undepleted (Al_2O_3/TiO_2 = 15 to 25) chemical affinities, and often occur with sulfur-bearing country rocks in dynamic high-magma-flux environments, such as compound sheet flows with internal pathways facies (Kambalda-type) or dunitic compound sheet flow facies (Mt Keith-type). Most Precambrian provinces in Australia, particularly the Proterozoic orogenic belts, contain an abundance of sulfur-saturated tholeiitic mafic± ultramafic intrusions that have not been fully investigated for their potential to host basal Ni–Cu sulfides (Voisey's Bay-type mineralization). The major exploration challenges for finding these deposits are to determine the pre-deformational geometries and younging directions of the intrusions, and to locate structural depressions in the basal contacts and feeder conduits under cover. Stratabound PGE–Ni–Cu±Cr deposits hosted by large Archean–Proterozoic layered mafic–ultramafic intrusions (Munni Munni, Panton) of tholeiitic affinity have comparable global nickel resources to many komatiite deposits, but low-grades

* Corresponding author. Tel.: +61 2 6249 9593; fax: +61 2 6249 9983.
E-mail address: Dean.Hoatson@ga.gov.au (D.M. Hoatson).

doi:10.1016/j.oregeorev.2006.05.002

(<0.2% Ni). There are also hydrothermal nickel sulfide deposits, including the unusual Avebury deposit in western Tasmania, and some potential for 'Noril'sk-type' Ni–Cu–PGE deposits associated with major flood basaltic provinces in western and northern Australia.

Keywords: Australia; Nickel sulfide deposits; Nickel resources; Mafic–ultramafic rocks; Precambrian terranes; Mineralization potential; PGEs

Contents

1. Introduction

1.1. Evolution of Australia's nickel sulfide industry

The sampling of some curious green-stained iron-rich rocks from the shores of Lake Lefroy in the Eastern Goldfields of Western Australia represents a seminal event in the evolution of the nickel industry of Australia (Barnes, 2004a). In 1947, prospector George Cowcill collected some ferruginous samples from the spoil heaps near the Red Hill gold mine. Mapping by Western Mining Corporation Ltd (WMC: now merged into BHP Billiton) around a domal anticlinal structure (later called the Kambalda Dome) showed that the samples came from the base of an ultramafic sequence of rocks that overlay pillowed metabasalt. On the 28th of January 1966, the first drill hole (KD1) by WMC intersected 2.7 meters of massive Ni–Cu sulfide ore that assayed 8.3% Ni and 0.5% Cu from 145.7 m to 148.4 m (Gresham, 1990). Further drilling defined a significant nickel sulfide deposit (later to be called the Lunnon Shoot) hosted by komatiitic rocks, and WMC announced the discovery on the 4th of April 1966 (Marston, 1984). This significant event at Kambalda heralded the initiation of Australia's nickel sulfide industry, an industry which has defined a global resource[1] of nickel metal of ~12.9 Mt, five world-class deposits (>1 Mt contained Ni), and with laterite deposits, will produce ~212 000 t of nickel and return anticipated export earnings of A$4.2 billion in 2006–07 (ABARE, 2006b).

The early exploration successes of WMC in delineating several deposits around the Kambalda Dome and by various junior companies exploring north of Kambalda, coupled with high demand for nickel, initiated a period from 1966 to 1971 of speculative exploration known as the 'nickel boom' (Marston, 1984; Fig. 1). During the height of this boom (1969–70), most outcropping sequences of greenstone rocks in the Yilgarn Craton were being explored by prospectors, by new Australian companies that were floated solely for nickel exploration, and by various international mining groups.

Australia's nickel industry grew rapidly in the first decade with many komatiite-hosted deposits commencing production within the first two years of their discovery (Fig. 2). More than 90% of Australia's known global resources of nickel metal derived from sulfide deposits were discovered during the relative short period of 1966 to 1973 (Table 1, Fig. 1). The world-class nickel status of the Eastern Goldfields Province was established when several large deposits were discovered between 1969 and 1973; namely Mt Keith (~3.4 Mt global resource), Perseverance (~2.5 Mt), Yakabindie (~1.7 Mt), and Honeymoon Well (~1 Mt). These nickel sulfide deposits, in addition to those in the Kambalda region (~1.4 Mt), still remain to this day the largest in Australia. The combined total resource of these large deposits is ~10 Mt Ni, equivalent to almost 78% of Australia's current global nickel sulfide resources. Many other smaller (<0.2 Mt) komatiite deposits were discovered in the Kambalda–St Ives–Tramways–Widgiemooltha (e.g., Redross, Wannaway, Miitel, Foster, Mt Edwards, Spargoville, Nepean), Forrestania (New Morning, Digger Rocks, Cosmic Boy), and Menzies–Laverton (Scotia, Mt Windarra, South Windarra) regions. The period after the late 1970s saw reduced exploration activity in response to depressed global metal prices and an abrupt decline in discovery of new komatiite–nickel deposits (Fig. 1). Rocky's Reward (grouped with Perseverance), was the only major komatiite-associated deposit discovered during this period. This trend was broken in the 1990s when a significant new component to Australia's nickel inventory was the development of several large nickel laterite deposits (Murrin Murrin, Cawse, Bulong) during the 'nickel laterite boom' years of ~1996 to 2000 (Jaques et al., 2005; Fig. 1).

In addition to the komatiitic nickel discoveries, a number of different types of Ni–Cu–Co±PGE and PGE–Ni–Cu deposits associated with Precambrian mafic–ultramafic intrusions of broad tholeiitic affinity have been discovered. These include: massive sulfides in feeder conduits and along the basal contacts of mafic

[1] Global resource of nickel metal (defined as total production plus remaining reserves and/or resources, i.e., total contained nickel metal) will be used throughout this paper unless otherwise stated. Resource data for the Australian deposits are from OZMIN-Geoscience Australia's national database of mineral deposits and resources. Many nickel sulfide deposits consist of several closely adjacent orebodies, therefore the definition of deposit is somewhat arbitrary. In the case of the large mining camps of Sudbury and Noril'sk, the global resources indicated in this study are the total resources for many individual deposits.

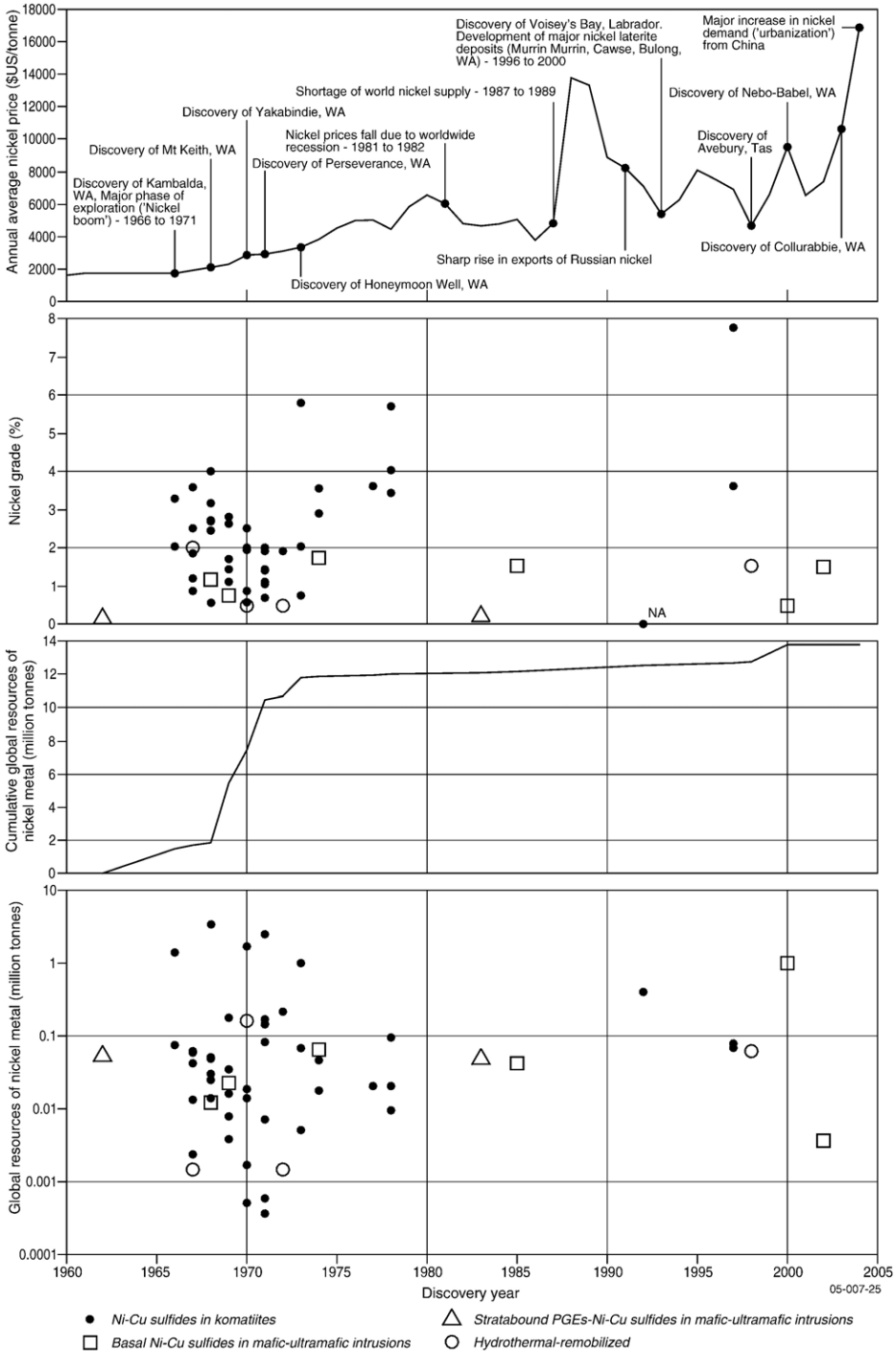

Fig. 1. Evolution of the nickel sulfide industry in Australia during the period 1962 to 2004. The plot only includes those deposits (and the Babel prospect discovered in 2000) which have published global resources of nickel metal. Resource statistics for most other deposits discovered since 2004 are yet to be released. The cumulative global resources trend indicates that more than 90% of Australia's global resources of nickel metal from sulfide deposits were discovered during a narrow time period (1966 to 1973) early in the evolution of the industry. The annual average nickel prices (in current $US/tonne) shown in the top graph are from the United States Geological Survey Mineral Commodity Summaries (nickel data compiled by P. Kuck) and the London Metal Exchange. Resource data for the Australian deposits are from Geoscience Australia's national database of mineral deposits and resources-OZMIN (see Table 1). NA=not available (a formal estimate of the nickel grade is not available for the Jericho komatiite-hosted nickel deposit discovered in 1992).

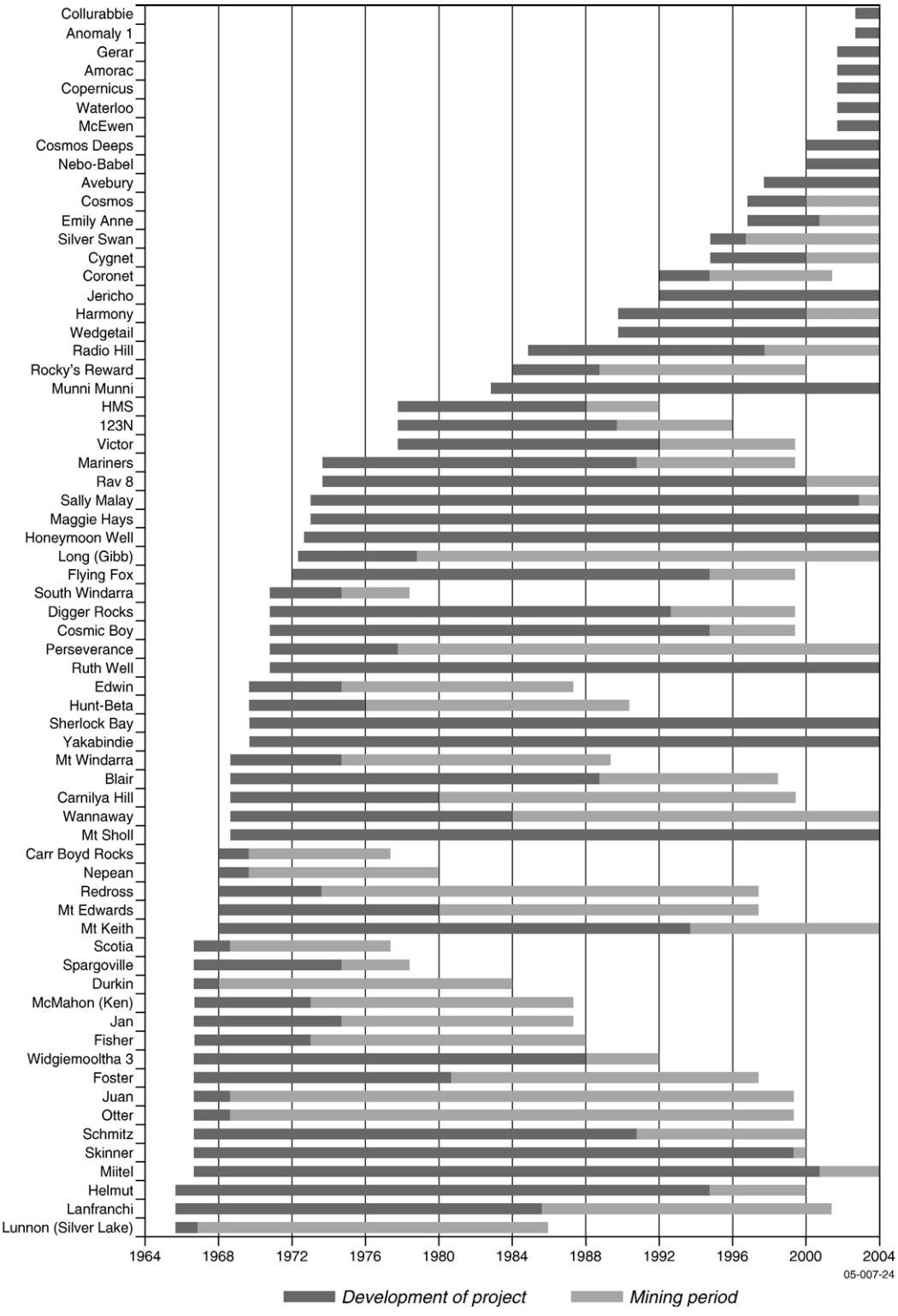

Fig. 2. Histogram summarizing the discovery and mining period(s) of Australia's nickel sulfide deposits from 1966 to 2004. Deposits with low grades of nickel (<0.15% Ni), or where nickel forms a minor by-product of other commodities, are not shown. Many of the deposits shown discovered after 2000 do not have formal resource estimates of nickel metal (hence their exclusion from Fig. 1). Data compiled from Marston (1984), Pratt (1996), Perring and Barnes (2002), Jaques et al. (2005), and various references cited in this paper.

Table 1
Global resources of nickel metal and ages of the major nickel sulfide deposits of the world

Deposit(s)	Country	Geotectonic region	Type of deposit[a]	Discovered	Age[b] (Ma)	Reference (For age)	Global Ni ore (Tonnes)	Global Ni grade (%)	Global Ni metal (Tonnes)
Armstrong (formerly Moore)	Australia	Eastern Goldfields Province	Kom	~1970	2705±4	Nelson (1997a)	2063000	1.22	25170
Avebury	Australia	Dundas Trough	Hyd	1998	?360	Newnham (2003)	11590000	1.02	118000
Babel[c]	Australia	Musgrave Block	Basal	2000	1078±3	Glikson et al. (1996)	NA	0.47	1000000
Beta	Australia	Eastern Goldfields Province	Kom	1977	2705±4	Nelson (1997a)	578000	3.63	21000
Black Swan (includes Silver Swan, Cygnet)	Australia	Eastern Goldfields Province	Kom	~1972–	2706±5	Kositcin et al. (in press)	11101000	1.93	214020
Blair	Australia	Eastern Goldfields Province	Kom	1969	2705±4	Nelson (1997a)	1326000	2.64	35000
Carnilya Hill	Australia	Eastern Goldfields Province	Kom	1968	2705±4	Nelson (1997a)	523164	2.68	14020
Carr Boyd Rocks	Australia	Eastern Goldfields Province	Basal	1968	?2700	Groenewald et al. (2000)	1018000	1.17	11950
Cliffs-Charterhall	Australia	Eastern Goldfields Province	Kom	1978	2705±4	Nelson (1997a)	2400000	4.04	97000
Copernicus	Australia	Halls Creek Orogen	Basal	2002	1844±3	Page and Hoatson (2000)	241000	1.50	3620
Corkwood [c]	Australia	Halls Creek Orogen	Hyd	1972	1844±3	Page and Hoatson (2000)	225000	0.65	1462
Cosmos	Australia	Eastern Goldfields Province	Kom	1997	2705±4	Nelson (1997a)	1017000	7.77	79 000
East Scotia	Australia	Eastern Goldfields Province	Kom	1970	2705±4	Nelson (1997a)	83900	2.00	1680
Emily Ann	Australia	Southern Cross Province	Kom	1997	>2921±4	Wang et al. (1996)	2077000	3.62	75 230
Forrestania Nickel (includes Cosmic Boy, Daybreak, Digger Rocks, Flying Fox, New Morning)	Australia	Southern Cross Province	Kom	~1971–	3000	Wang et al. (1996)	7566400	1.91	144 220
Gibb	Australia	Eastern Goldfields Province	Kom	~1973	2705±4	Nelson (1997a)	245000	2.04	5000
Honeymoon Well (includes Harrier, Wedgetail)	Australia	Eastern Goldfields Province	Kom	~1973–	2705±4	Nelson (1997a)	134800000	0.75	1011000
Jericho	Australia	Eastern Goldfields Province	Kom	1992	2705±4	Nelson (1997a)	NA	NA	405000
Kambalda (several deposits: Kambalda Dome St Ives–Tramways)	Australia	Eastern Goldfields Province	Kom	~1966–	2705±4	Nelson (1997a)	42057496	3.30	1388820
Lanfranchi	Australia	Eastern Goldfields Province	Kom	1966	2705±4	Nelson (1997a)	3650000	2.02	73870
Long	Australia	Eastern Goldfields Province	Kom	~1973	2705±4	Nelson (1997a)	1157000	5.79	67000
Maggie Hays	Australia	Southern Cross Province	Kom	~1973	>2921±4	Wang et al. (1996)	12274000	1.41	173060

Table 1 (*continued*)

Deposit(s)	Country	Geotectonic region	Type of deposit[a]	Discovered	Age[b] (Ma)	Reference (For age)	Global Ni ore (Tonnes)	Global Ni grade (%)	Global Ni metal (Tonnes)
Mariners	Australia	Eastern Goldfields Province	Kom	1974	2705±4	Nelson (1997a)	1 582 000	2.91	46 000
Marriott	Australia	Eastern Goldfields Province	Kom	1969	2705±4	Nelson (1997a)	724 000	1.10	7960
McEwen (formerly Mt Edwards 360N)	Australia	Eastern Goldfields Province	Kom	2002	2705±4	Nelson (1997a)	7 263 000	0.86	62 460
Melon	Australia	Eastern Goldfields Province	Kom	~1971	2705±4	Nelson (1997a)	350 000	2.00	7000
Miitel (includes North Miitel)	Australia	Eastern Goldfields Province	Kom	1967–	2705±4	Nelson (1997a)	1 638 440	3.60	58 970
Miriam	Australia	Eastern Goldfields Province	Kom	1969	2705±4	Nelson (1997a)	227 000	1.70	3860
Mt Edwards 166N	Australia	Eastern Goldfields Province	Kom	~1967	2705±4	Nelson (1997a)	126 160	1.85	2330
Mt Edwards 132N	Australia	Eastern Goldfields Province	Kom	1978	2705±4	Nelson (1997a)	282 262	3.45	9740
Mt Edwards 26N	Australia	Eastern Goldfields Province	Kom	1967	2705±4	Nelson (1997a)	1 700 000	2.50	42 500
Mt Edwards (includes Mt Edwards 14N)	Australia	Eastern Goldfields Province	Kom	~1967–	2705±4	Nelson (1997a)	1 080 000	1.21	13 070
Mt Keith	Australia	Eastern Goldfields Province	Kom	1968	2705±4	Nelson (1997a)	599 178 000	0.57	3 411 420
Mt Martin	Australia	Eastern Goldfields Province	Hyd	~1967	?>2500	Nelson (1997a)	72 000	2.00	1440
Mt Sholl	Australia	West Pilbara Granite–Greenstone Terrane	Basal	1969	2892±34	Frick et al. (2001)	3 029 400	0.75	22 720
Mt Windarra	Australia	Eastern Goldfields Province	Kom	1969	>2900	Barley and Groves (1990)	12 714 000	1.42	180 610
Munda	Australia	Eastern Goldfields Province	Kom	~1970	2705±4	Nelson (1997a)	45 000	2.53	1140
Munni Munni	Australia	West Pilbara Granite–Greenstone Terrane	Strat	1983	2927±13	Hoatson and Sun (2002)	24 000 000	0.20	48 000
Nepean	Australia	Eastern Goldfields Province	Kom	1968	2705±4	Nelson (1997a)	1 553 814	3.16	49 050
Panton	Australia	Halls Creek Orogen	Strat	1962	1856±2	Page and Hoatson (2000)	33 600 000	0.16	53 760
Perseverance (includes Rocky's Reward, Leinster)	Australia	Eastern Goldfields Province	Kom	~1971–	2705±4	Nelson (1997a)	236 453 000	1.05	2 480 640
Pioneer	Australia	Eastern Goldfields Province	Kom	1971	2705±4	Nelson (1997a)	32 500	1.11	360
Prospero	Australia	Eastern Goldfields Province	Kom	2004	2705±4	Nelson (1997a)	1 060 000	5.72	60 630
Radio Hill	Australia	West Pilbara Granite–Greenstone Terrane	Basal	1985	2892±34	Frick et al. (2001)	2 758 000	1.53	42 300
Ratbat	Australia	Southern Cross Province	Kom	~1971	3000	Wang et al. (1996)	250 000	1.10	2750
Rav 8	Australia	Southern Cross Province	Kom	1974	<2958±4	Nelson (1997a)	505 000	3.56	18 000

(continued on next page)

Table 1 (*continued*)

Deposit(s)	Country	Geotectonic region	Type of deposit[a]	Discovered	Age[b] (Ma)	Reference (For age)	Global Ni ore (Tonnes)	Global Ni grade (%)	Global Ni metal (Tonnes)
Ravensthorpe Nickel (includes Rav 1, 4, 5, 4w)	Australia	Southern Cross Province	Kom	~1970–	<2958±4	Nelson (1997a)	1584000	0.87	13780
Redross	Australia	Eastern Goldfields Province	Kom	1968	2705±4	Nelson (1997a)	772513	3.99	30840
Ruth Well	Australia	West Pilbara Granite–Greenstone Terrane	Kom	1971	2876±38	Meisel et al. (2001)	30000	2.00	600
Sally Malay	Australia	Halls Creek Orogen	Basal	1974	1844±3	Page and Hoatson (2000)	3736000	1.74	65010
Scotia	Australia	Eastern Goldfields Province	Kom	1967	2705±4	Nelson (1997a)	1916000	2.71	52000
Seagull	Australia	Southern Cross Province	Kom	~1971	3000	Wang et al. (1996)	970000	1.31	12710
Sherlock Bay	Australia	West Pilbara Granite–Greenstone Terrane	Hyd	1970	2866±66	Hoatson and Sun (2002)	25424000	0.40	101300
South Windarra	Australia	Eastern Goldfields Province	Kom	1971	>2900	Barley and Groves (1990)	10274000	1.44	147480
Spargoville (1a)	Australia	Eastern Goldfields Province	Kom	1967	2705±4	Nelson (1997a)	1021000	2.45	25014
Tapinos (formerly Anomaly 4 near Prospero)	Australia	Eastern Goldfields Province	Kom	2005	2705±4	Nelson (1997a)	142 000	7.4	10 500
Trough Well	Australia	Southern Cross Province	Kom	1970	3000	Wang et al. (1996)	20000	2.50	500
Victor	Australia	Eastern Goldfields Province	Kom	1978	2705±4	Nelson (1997a)	364000	5.71	20780
Victor Shoot	Australia	Eastern Goldfields Province	Kom	1973	2705±4	Nelson (1997a)	226000	5.11	11550
Wannaway	Australia	Eastern Goldfields Province	Kom	1969	2705±4	Nelson (1997a)	570400	2.81	16000
Weebo Bore	Australia	Eastern Goldfields Province	Kom	1971	2705±4	Nelson (1997a)	12000000	0.70	84000
Widgie 3	Australia	Eastern Goldfields Province	Kom	1967	2705±4	Nelson (1997a)	89000	1.89	1680
Widgie Townsite	Australia	Eastern Goldfields Province	Kom	1967	2705±4	Nelson (1997a)	2194000	1.48	32470
Yakabindie	Australia	Eastern Goldfields Province	Kom	1970	2705±4	Nelson (1997a)	290000000	0.58	1682000
Zabel	Australia	Eastern Goldfields Province	Kom	~1970	2705±4	Nelson (1997a)	979000	1.93	18890
Selebi–Phikwe	Botswana	Limpopo Orogenic Belt	Basal	1963	>2500	Eckstrand (1995)	49444000	1.04	514217
O'Toole	Brazil	Morro do Ferro Belt	Kom	1983	>2700	Brenner et al. (1990)	6600000	2.20	145200
Alexo	Canada	Abitibi Belt	Kom	1908	2707^{+5}_{-3}	Barrie et al. (1999)	57000	3.58	2040
Amax area 1 (Nose)	Canada	Thompson Nickel Belt	Kom	Pre-1975	1880±5	Hulbert et al. (2005)	7300000	1.33	97090
Bowden	Canada	Thompson Nickel Belt	Kom	1962	1880±5	Hulbert et al. (2005)	80000000	0.60	480000
Bucko	Canada	Thompson Nickel Belt	Kom	1961	1880±5	Hulbert et al. (2005)	2500000	2.23	55750

Table 1 (*continued*)

Deposit(s)	Country	Geotectonic region	Type of deposit[a]	Discovered	Age[b] (Ma)	Reference (For age)	Global Ni ore (Tonnes)	Global Ni grade (%)	Global Ni metal (Tonnes)
Canalask	Canada	Kluane Mafic–Ultramafic Belt	Basal	Pre-1955	232±1	Hulbert (1997)	500 000	1.68	8400
Dumont	Canada	Abitibi Belt	Kom	~1969	2710	Naldrett (1989)	150 000 000	0.50	750 000
Expo-Ungava	Canada	Cape Smith Belt	Kom	Pre-1979	1918^{+9}_{-7}	Parrish (1989)	6 300 000	0.86	54 180
Giant Mascot	Canada	Cordillera	Basal	~1923	Cretaceous	Eckstrand et al. (2003)	2 050 000	1.40	28 700
Gordon Lake	Canada	Abitibi Belt	Kom	Pre-1958	2750–2697	Ayer et al. (2002)	1 070 000	1.62	17 334
Great Lakes	Canada	Southern Province	Basal	Pre-1986	1108.8^{+4}_{-2}	Davies and Sutcliffe (1985)	45 600 000	0.18	83 448
Langmuir (No. 1 and 2)	Canada	Abitibi Belt	Kom	~1973	2710–2703	Ayer et al. (2002)	1 600 000	2.09	33 440
Lorraine	Canada	Belleterre–Angliers Belt	Basal	Pre-1981	2694±30	Barnes et al. (1993)	661 000	0.39	2578
Lynn Lake	Canada	Lynn Lake Belt	Basal	1941	Proterozoic	Eckstrand et al. (2003)	20 151 000	1.02	206 145
Macassa	Canada	Limerick Township	Basal	1961	Proterozoic	Eckstrand (1995)	1 800 000	0.91	16 380
Manibridge	Canada	Thompson Nickel Belt	Kom	1963	1880±5	Hulbert et al. (2005)	1 409 000	2.55	35 929
Marbridge	Canada	Abitibi Belt	Kom	~1957	2719–2710	Ayer et al. (2002)	7 740 00	2.82	21 826
Montcalm	Canada	Abitibi Belt	Basal	1976	2702±2	Barrie and Naldrett (1989)	3 560 000	1.44	51 264
Namew Lake	Canada	Thompson Nickel Belt	Kom	1984	1847±6	Cumming and Kristic (1991)	2 600 000	2.44	63 440
Raglan	Canada	Cape Smith Belt	Kom	~1931	$?1918^{+9}_{-7}$	Parrish (1989)	24 700 000	2.72	671 840
Redstone	Canada	Abitibi Belt	Kom	Pre-1989	2710–2703	Ayer et al. (2002)	1 220 000	2.39	29 158
Shebandowan	Canada	Abitibi Belt	Kom	Pre-1972	2750–2697	Ayer et al. (2002)	15 000 000	1.50	225 000
St. Stephen (3 zones)	Canada	Appalachian–Caledonian Orogen	Basal	1880	Devonian	Paktunc (1987)	1 000 000	1.05	10 500
Sudbury	Canada	Superior–Southern–Grenville Provinces	Astro	1856	1850±1	Krogh et al. (1984)	1 648 000 000	1.20	19 776 000
Texmont	Canada	Abitibi Belt	Kom	Pre-1971	2710–2703	Ayer et al. (2002)	3 190 000	0.93	29 667
Thompson	Canada	Thompson Nickel Belt	Kom	1956	1880±5	Hulbert et al. (2005)	150 300 000	2.32	3 486 960
Voisey's Bay	Canada	Torngat Orogen	Basal	1993	1333±1	Amelin et al. (1999)	136 700 000	1.59	2 173 530
Wellgreen	Canada	Kluane Mafic–Ultramafic Belt	Basal	1952	>232±1	Hulbert (1997)	669 000	2.04	13 648
Jinchuan	China	Sino–Korean Craton	Basal	1958	827±8	Li et al. (2004)	515 000 000	1.06	5 459 000
Hitura	Finland	Kotalahti Nickel Belt	Kom	1963	>1877±2	Papunen and Vorma (1985)	12 300 000	0.56	68 880
Kotalahti	Finland	Kotalahti Nickel Belt	Basal	1954	1883	Papunen and Vorma (1985)	23 200 000	0.70	162 400

(continued on next page)

Table 1 (*continued*)

Deposit(s)	Country	Geotectonic region	Type of deposit[a]	Discovered	Age[b] (Ma)	Reference (For age)	Global Ni ore (Tonnes)	Global Ni grade (%)	Global Ni metal (Tonnes)
Monchegorsk	Russia	Baltic Shield, Kola Peninsula	Basal	pre-1935	2493±7	Neradovsky et al. (1997)	47000000	0.70	329000
Noril'sk (N)–Talnakh (T)	Russia	Siberian Platform	F B	~1926 (N), 1960 (T)	251±0.3	Kamo et al. (2003)	1257000000	1.84	23128800
Pechenga	Russia	Baltic Shield, Kola Peninsula	Basal	1912	1977±55	Hanski et al. (1990)	339000000	1.18	4000200
Merensky Reef	South Africa	Kaapvaal Craton, Transvaal Basin	Strat	1924	2060±3	Kruger et al. (1986)	4209000000	0.15	6313500
Platreef	South Africa	Kaapvaal Craton, Transvaal Basin	Basal[d]	1925	2060±3	Kruger et al. (1986)	1597000000	0.41	6547700
Kabanga	Tanzania	Kibaran Orogenic Belt	?Basal	1976	1275±11	Deblond and Tack (1999)	11700000	1.72	201240
Duluth	USA	Mid-Continent Rift System	F B	1948	1099±0.7	Paces and Miller (1993)	4000000000	0.20	8000000
Great Dike	Zimbabwe	Zimbabwe Craton	Strat	1925	2587±8	Mukasa et al. (1998)	2574000000	0.21	5405400
Hunter's Road	Zimbabwe	Zimbabwe Craton	Kom	1974	2700	Prendergast (2003)	30000000	0.70	210000
Shangani	Zimbabwe	Shangani Greenstone Belt	Kom	1969	2700	Prendergast (2003)	22000000	0.71	156200
Trojan	Zimbabwe	Mazoe Greenstone Belt	Kom	1956	2700	Prendergast (2003)	20350000	0.68	138380

Sources of Ni resource data:
Australian deposits — OZMIN (Geoscience Australia's national database of mineral deposits and resources, April 2006).
Other deposits — Eckstrand (1995) and Naldrett (2002).
NA=not available.

[a] Kom=Ni–Cu sulfides in komatiites; Bas=basal Ni–Cu sulfides in mafic–ultramafic intrusion; Strat=stratabound PGEs–Ni–Cu sulfides in mafic–ultramafic intrusion; Hyd=hydrothermal-remobilized; F B=Ni–Cu sulfides in intrusions related to flood basalts; Astro=astrobleme-associated Ni–Cu sulfides.

[b] Age can refer to the age of a specific nickel sulfide deposit (e.g., Kambalda), or the general age of the metallogenic province containing nickel deposits that are similar to a dated deposit (e.g., 2705 Ma komatiite-hosted deposits in the Eastern Goldfields Province: see Fig. 10).

[c] Deposits shown in italics contain preliminary resources only.

[d] Some deposits may not be representative, *sensu stricto*, of the indicated deposit type (e.g., Platreef is not a basal sulfide deposit similar to Voisey's Bay, but for convenience it is classified in this category).

intrusions in the Halls Creek Orogen (Sally Malay, Copernicus), Pilbara Craton (Radio Hill, Mt Sholl), and Musgrave Province (Nebo–Babel, Mt Harcus); stratabound PGE–Ni–Cu sulfides in mafic–ultramafic intrusions in the Pilbara (Munni Munni) and Yilgarn (Weld Range) cratons; and stratabound PGE–Ni-bearing chromitites in mafic–ultramafic intrusions in the Halls Creek Orogen (Panton, Lamboo, Eastmans Bore) (Figs. 2 and 9). Sally Malay and Radio Hill are the only tholeiitic-hosted deposits currently mined.

Since the late 1990s, there have been several new nickel deposits and prospects reported with more unusual magmatic (Collurabbie, Collurabbie South, Beasley) and hydrothermal-remobilized (Avebury) settings. Deposits such as Nebo–Babel and Avebury, and the Collurabbie prospect, have also had profound impacts by defining new metallogenic provinces in areas previously considered to have low potential to host a major deposit. During the last five years, nickel exploration in Australia has been stimulated by record nickel prices (at least ~US$29 600/tonne) that are largely driven by a major increase in demand for this metal by China and a shortfall in supply. Nickel exploration expenditures are currently approaching their highest levels since the boom period of 1966–1971 and record numbers of companies are exploring throughout Australia.

1.2. Objectives and methodology

This paper summarizes the distribution, characteristics, resources, and potential of Australia's nickel sulfide deposits. We examine the elements considered

important for the formation of nickel sulfide mineralizing systems and suggest exploration strategies relevant to Australia's Archean and Proterozoic terranes. With the exception of Pratt (1996), very few publications have described these deposits and compiled their resource attributes at a national scale. The growth in Australia's base-metal resources, including nickel sulfide deposits, for the period 1976 to 2005 is reviewed by Jaques et al. (2005). Our study draws on the comprehensive synthesis studies of Western Australia's nickel sulfide deposits by Marston (1984), Hill et al. (1987), Gresham (1990), Harrison (1990), Hudson (1990), Groves and Hudson (1990), Townsend and Preston (1991), Dowling and Hill (1998), Barnes (2004b), Abeysinghe and Flint (2005), Flint et al. (2005), and the many deposits described in *Economic Geology* (1981, special issue, volume 76, no. 6; 2005, 100th Anniversary Volume), Lesher (1989), Hughes (1990), Solomon and Groves (1994), Berkman and Mackenzie (1998), and the references listed in this paper. The geological setting and resources of Australia's nickel laterite deposits have been described by Reid (1996), Brand et al. (1998), Elias (2002), Flint et al. (2005), Freyssinet et al. (2005), and Abeysinghe and Flint (2005) and will not be discussed in detail here.

The nickel resource data used in this paper for Australia's deposits are from OZMIN-Geoscience Australia's national database of mineral deposits and resources — and includes only those deposits that have published global resources of nickel metal. Such a resource statistic enables more meaningful comparisons between deposits and provinces since it provides an indication of the total metal in the deposit or province prior to mining activities. Formal resource estimates for recently discovered high-profile prospects, such as Nebo–Babel and Collurabbie in Western Australia, have not been published up to mid-2006. Resource data for foreign deposits are from Naldrett (2002) and Eckstrand (1995).

2. Global distribution, endowment, and ages of nickel sulfide deposits

All magmatic Ni–Cu±PGE sulfide deposits are spatially and genetically related to bodies of mafic or ultramafic rocks (Naldrett, 1997). Such deposits form when mantle-derived mafic and ultramafic magmas become saturated in sulfide and segregate immiscible sulfide liquid, commonly following interaction with crustal rocks (Arndt et al., 2005). The sulfides generally constitute a small volume of the host rock(s) and are dominated by a simple major mineralogy of pyrrhotite (Fe_7S_8), pentlandite ($[Fe,Ni]_9S_8$), and chalcopyrite ($CuFeS_2$). Nickel, Cu, Co, and the PGEs are the main commodities of economic interest, whereas gold, silver, chromium, and lead can be minor associated metals.

Relative to other deposit types, magmatic Ni–Cu ±PGE deposits are rare; in total there are only 142 deposits and camps in the world that contain more than 100 000 tonnes of global resources of metal (Hulbert and Eckstrand, 2005). The world's nickel sulfide resources are dominated by two 'unique' geological settings; namely subvolcanic mafic intrusions related to flood basalts at Noril'sk (~23.1 Mt), Siberia, and the astrobleme-associated mafic-intrusion deposits at Sudbury (~19.8 Mt), Canada (Fig. 3). Deposits from both these mining camps account for about 42% of the total global nickel resources (~103.1 Mt) for the sulfide deposits/camps listed in Table 1. These significant contributions not only reflect the large number of deposits and their considerable metal endowments, but also their protracted mining histories, e.g., sulfide ores from Sudbury have been mined since 1886 (Giblin, 1984).

Nickel sulfide deposits occur on most continents, but Russia, Australia, Canada, and southern Africa contain the major deposits (Fig. 3). In contrast, most nickel laterite deposits lie in Indonesia, New Caledonia, Brazil, and the Philippines (i.e., within a band about 22° of latitude either side of the equator) by virtue of their formation in humid tropical conditions and tectonically active plate collision zones (Elias, 2002). In these settings, large obducted ophiolite sheets are exposed to intense chemical weathering which enhances supergene enrichment processes. Controls on the formation of nickel laterite deposits include bedrock lithology, tectonic setting, age of weathering, paleoclimatic history, and geomorphology (Freyssinet et al., 2005). The Eastern Goldfields Province of the Yilgarn Craton is one of the few provinces in the world which contains both large sulfide and large laterite deposits, but even here these deposit types are generally not spatially coincident. A notable exception is the Honeymoon Well sulfide deposit which also has significant resources of nickel in the laterite profile.

Diverse geotectonic settings and a wide range of formation ages from the Archean to the Permo-Triassic are also characteristic features of nickel sulfide deposits. The settings range from rift- and continental flood basalt-associated mafic sills (Noril'sk, Duluth), astrobleme-associated mafic intrusions (Sudbury), komatiitic volcanic flows and related intrusions (Kambalda, Thompson), to tholeiitic mafic intrusions (Voisey's Bay). Naldrett (1989, 1997) has also broadly classified

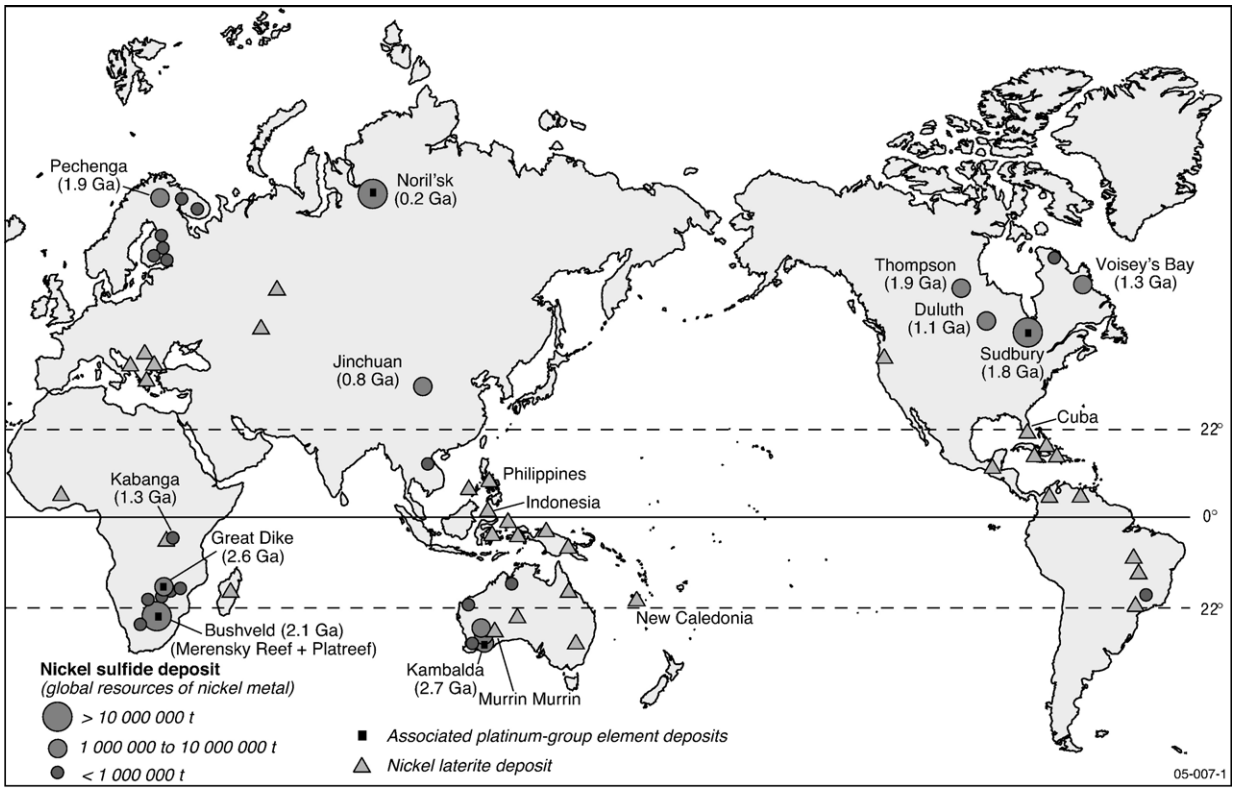

Fig. 3. World distribution of significant sulfide and laterite nickel deposits. Sulfide deposits containing important by-products of PGEs or have associated PGE–Ni deposits are also shown. Distribution of laterite deposits after Elias (2002).

magmatic nickel sulfide deposits on the basis of whether the host bodies were emplaced in: (1) rifted continental margins; (2) cratonic–intracontinental environments; (3) active orogenic belts; and (4) synvolcanic greenstone belts. It is also apparent from Fig. 3 that the largest nickel sulfide deposits/camps (Noril'sk, Sudbury, Kambalda, Bushveld), irrespective of their geotectonic setting, also contain significant resources of PGEs. Lesher (2004) has emphasized the diverse nature of nickel sulfide deposits in regard to their different geological ages, different tectonic settings in continent-related extensional environments, association with a wide range of mafic–ultramafic magma types, and their interaction with country rocks in a variety of different ways. Different classifications of nickel sulfide deposits throughout the world can be found in Naldrett (1989, 1997, 2004), Eckstrand (1995), Lesher and Keays (2002), Lesher (2004), and Arndt et al. (2005).

The identified nickel resources of the world are very large. Kuck (2006) estimates that the identified land-based resources averaging 1% Ni or greater is at least 130 Mt of nickel. Approximately 40% of these resources are in sulfide deposits and 60% are in laterites. In addition, extensive deep-sea resources of nickel are contained in manganese crusts and nodules covering large areas of the ocean floor, particularly in the Pacific and Indian Oceans. Deep-sea nickel resources are estimated at 290 Mt, more than double the identified resources contained in land-based nickel deposits (Pratt, 1996). With regard to the countries listed in Table 1, Canada (28.4 Mt) has slightly more global resources of sulfidic nickel than Russia (27.5 Mt), followed by Australia (12.9 Mt), South Africa (12.9 Mt), USA (8 Mt), Zimbabwe (5.9 Mt), China (5.5 Mt), and Finland (0.23 Mt). When including laterite deposits, Australia has the largest nickel resources with 37% of the world's nickel economic demonstrated resources, followed by Russia (10%), Cuba (9%), and Canada (7%) (Geoscience Australia, in press).

Fig. 4 compares the nickel sulfide resources for the fifteen largest Australian deposits with the major foreign deposits. The Australian deposits shown in this figure are exclusively of the komatiite–sulfide association, whereas the foreign deposits are represented by a very diverse group of deposits. The magnitude of the contributions from the Noril'sk and Sudbury mining camps is also

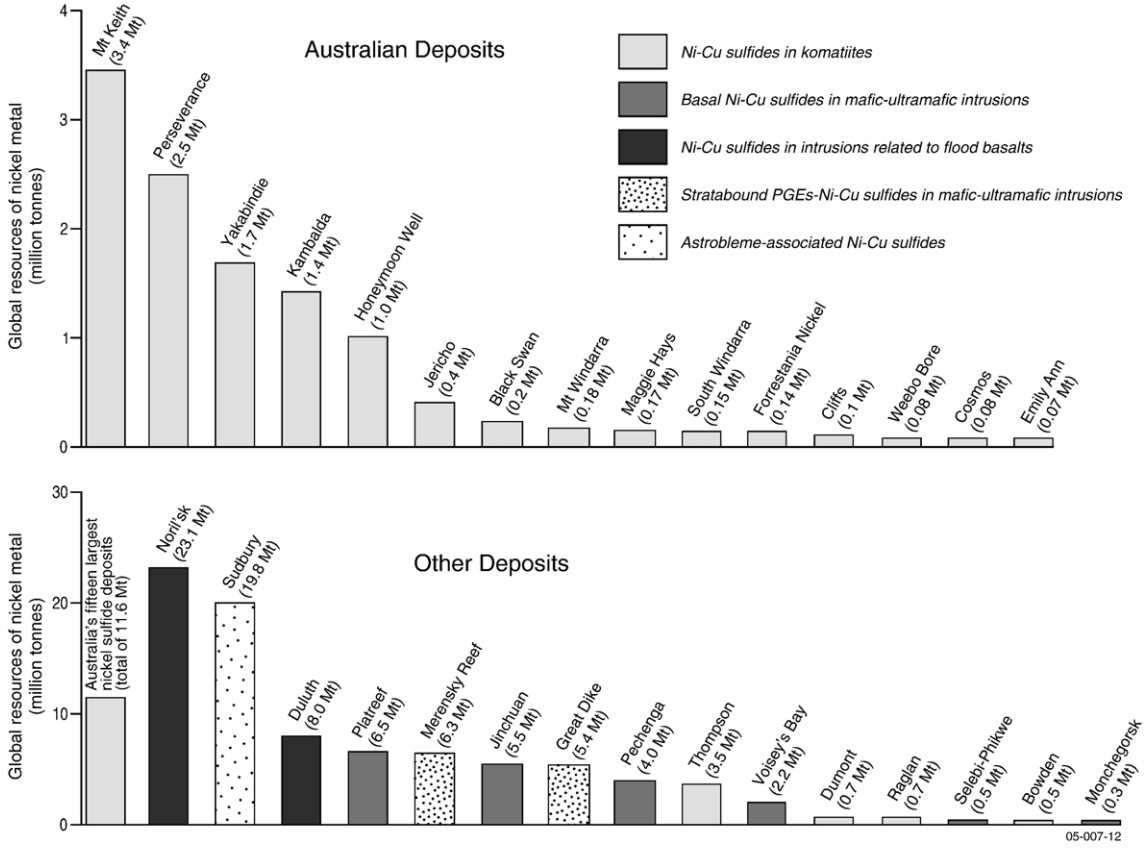

Fig. 4. Histogram comparing the global resources of nickel metal for Australia's fifteen largest deposits with the fifteen largest foreign deposits. The graphs highlight the dominance of the komatiite–nickel association in Australia compared with the different associations for the foreign deposits, and also the significant resources contained in the Noril'sk and Sudbury mining camps. Some deposits shown are grouped under but may not be representative of, *sensu stricto*, the indicated deposit type. The locations of the Australian deposits in the top histogram are shown in Fig. 9.

highlighted by being nearly twice the size of the cumulative tonnage of Australia's fifteen largest deposits.

Grade and global resource statistics for the major nickel sulfide deposits of the world (Fig. 5) indicate that Australia is particularly well endowed with world-class komatiite-associated deposits, and a number of small-tonnage, but high-grade (5 to 9%) komatiite deposits (e.g., Cosmos, Prospero, Long, Victor, Silver Swan-included in Black Swan in Fig. 5). However, deposits hosted by mafic–ultramafic intrusions, although of similar grade, are up to two orders of magnitude smaller in contained metal relative to the larger foreign deposits. Stratabound PGE–Ni–Cu±Cr deposits in large Archean–Proterozoic layered mafic–ultramafic intrusions (Great Dike, Merensky Reef and Platreef in the Bushveld) contain significant resources of nickel (5 to 7 Mt) but at subeconomic grades (<0.4% Ni).

Komatiite-associated Ni–Cu deposits are of specific Archean and Proterozoic ages (Fig. 6) with the largest deposits formed at ~2700 Ma (Kambalda, Mt Keith, Abitibi belt) and ~1900 Ma (Thompson and Cape Smith belts). Barren komatiites are widespread in the early Archean (e.g., ~3200–3500 Ma, South Africa: Maier, 2004; >3000 Ma, Aldan Craton, Siberia: Puchtel et al., 1993) and, rarely, in the Phanerozoic (270 Ma, Song Da, Vietnam: Hanski et al., 2004; 89 Ma, Gorgona Island, Colombia: Walker et al., 1999). Basal Ni–Cu sulfide deposits (Voisey's Bay, Jinchuan, Sally Malay, Radio Hill) do not appear to be age dependent, although the larger deposits are younger than ~2060 Ma. Large deposits/mining camps associated with continental flood basalt (Noril'sk, Duluth) and astrobleme (Sudbury) events appear to have a very restricted representation in the geological record.

3. Australia's status in the global nickel industry and current exploration trends

Australia produced an estimated 12.8% (~190 000 t; ABARE, 2006a) of the world's annual total nickel

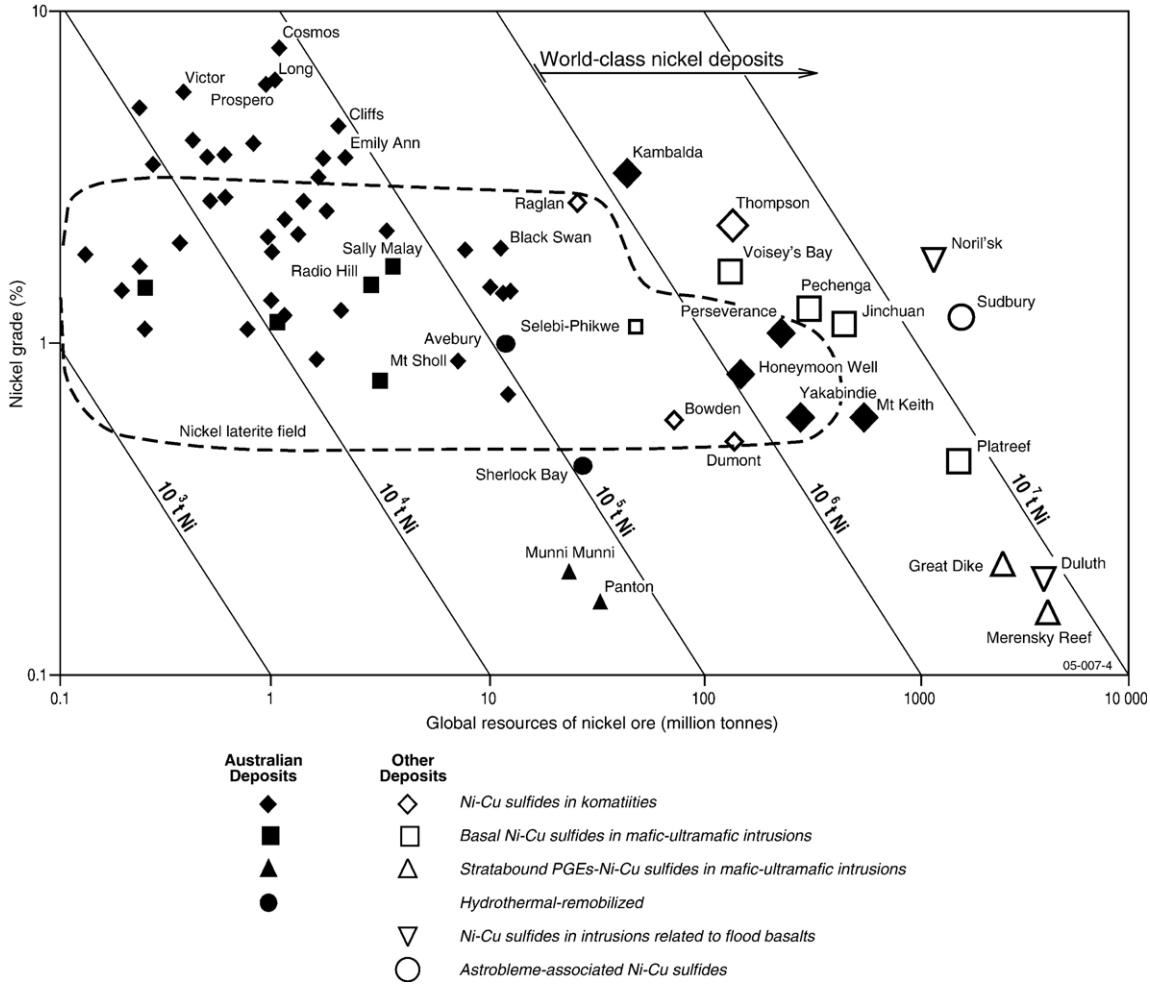

Fig. 5. Logarithmic plot of nickel grade (wt.%) versus global resources of nickel ore (production plus reserves and resources in million tonnes) for the major nickel sulfide deposits of the world. Australian deposits are shown with filled symbols and the major foreign deposits with open symbols. The grey diagonal lines indicate contained nickel metal in tonnes. The field enclosed by the dash line corresponds to the major nickel laterite deposits of the world. (Elias, 2002). World-class deposits shown in large symbols are defined as those containing more than one million tonnes of contained nickel metal. Data for Australian deposits compiled from OZMIN, and other deposits from Naldrett (2002) and Eckstrand (1995).

output (~1.48 Mt from sulfide and laterite sources) in 2005, which equates to number three after Russia (21.3%) and Canada (13.2%, Kuck, 2006). Traditionally, Russia has dominated world output, however, in recent years Australia and Canada have regularly interchanged positions. ABARE has also forecasted that Australia's mine production from sulfide and laterite sources will rise 15% to 212 000 t in 2006–07 (ABARE, 2006b). Higher output is expected when nickel sulfide mines, such as Flying Fox, Maggie Hays, Miitel, Redross, Mariners, Cosmos Deeps, Black Swan, Waterloo, Yakabindie, Cliffs, Sally Malay (all in WA), and Avebury (Tasmania) come into production or ramp up toward capacity. Australia's nickel production is dominated by komatiite-hosted deposits (~82%) with minor contributions from mafic–ultramafic intrusions (~3%) and laterite (~15%) sources (Fig. 7A). Abeysinghe and Flint (2005) have shown that the most productive (nickel production in tonnes) nickel sulfide deposits during 2004-05 were: Perseverance–Leinster (35 079; does not include June 2005 quarter), Mt Keith (31 833), Cosmos (11 025), Emily Ann (9882), Long (8869), Miitel (6884), Silver Swan (6165), Beta and Hunt (4758), Sally Malay (4582), and Radio Hill (2109). Laterite deposits, such as Murrin Murrin (28 631 t) in the Yilgarn Craton, that are amenable to large-scale lower cost open-pit mining account for nearly 70% of the nation's nickel resources (Fig. 7B).

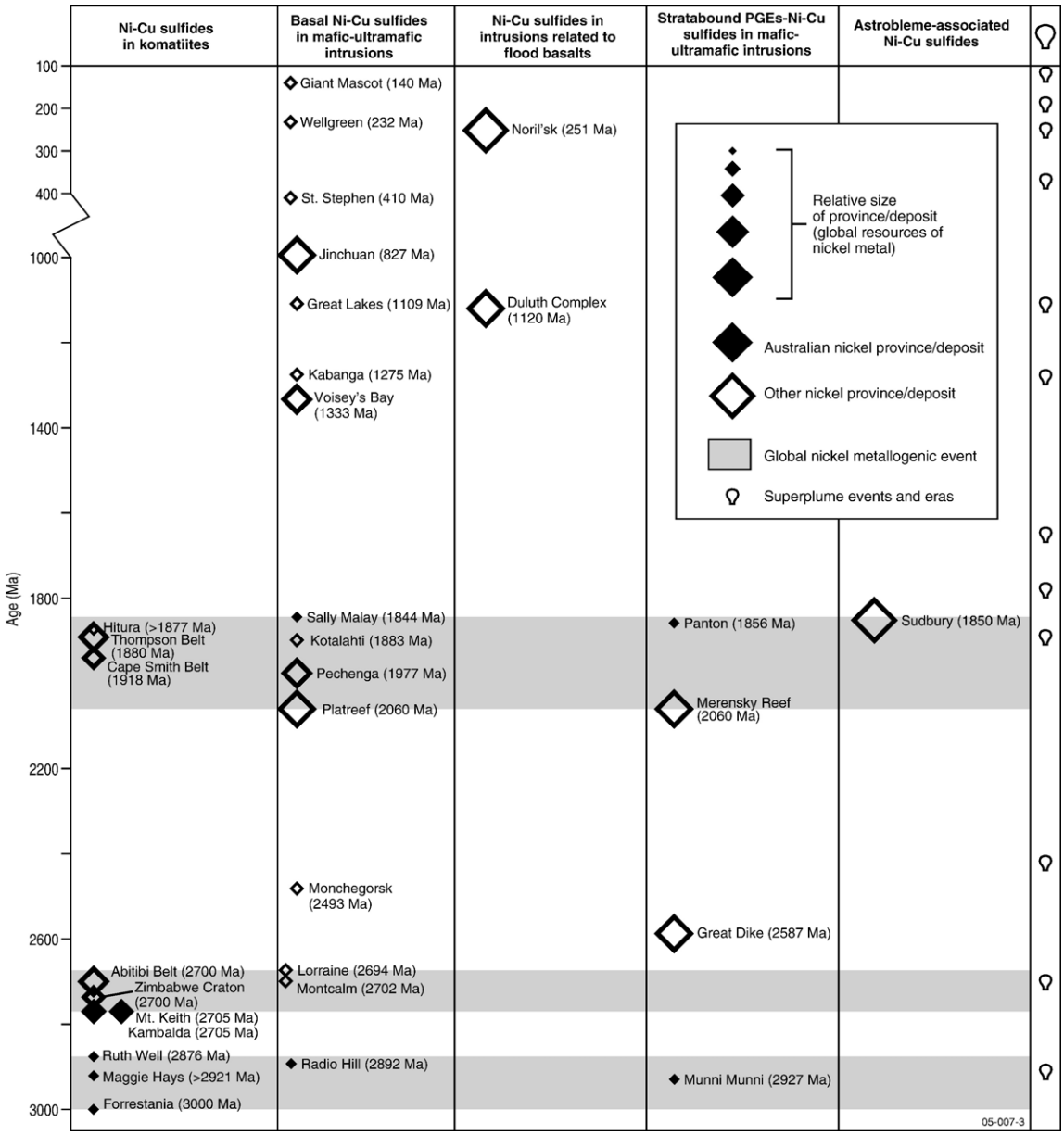

Fig. 6. Time–nickel sulfide metallogenic event plot showing approximate ages and relative sizes of nickel sulfide deposits and nickel sulfide camps/provinces in the world. The concentration of different types of nickel deposits forming during a particular geological period defines three major global nickel-metallogenic events at 1840 Ma to 2060 Ma, 2690 Ma to 2705 Ma, and 2875 Ma to 3000 Ma. The geological periods of the major superplume events are from Abbott and Isley (2002).

There is also potential for considerable expansion of laterite production with significant operations (annual production of ~50 000 t) planned for the Ravensthorpe and Kalgoorlie nickel projects in the southern Yilgarn Craton.

Komatiite-hosted sulfide deposits (96%) dominate Australia's global resources of nickel metal associated with sulfide deposits (Fig. 8A). This is in contrast to the world situation where komatiite deposits (18%) provide the fourth largest contribution after flood basalt (30%), astrobleme (20%), and basal sulfide (20%) associations (Fig. 8B). The Eastern Goldfields Province (63%) dominates world nickel resources hosted by komatiites (Fig. 8C). However, the number of deposits shown in Table 1 is not complete for all countries outside Australia and consequently the relative contributions

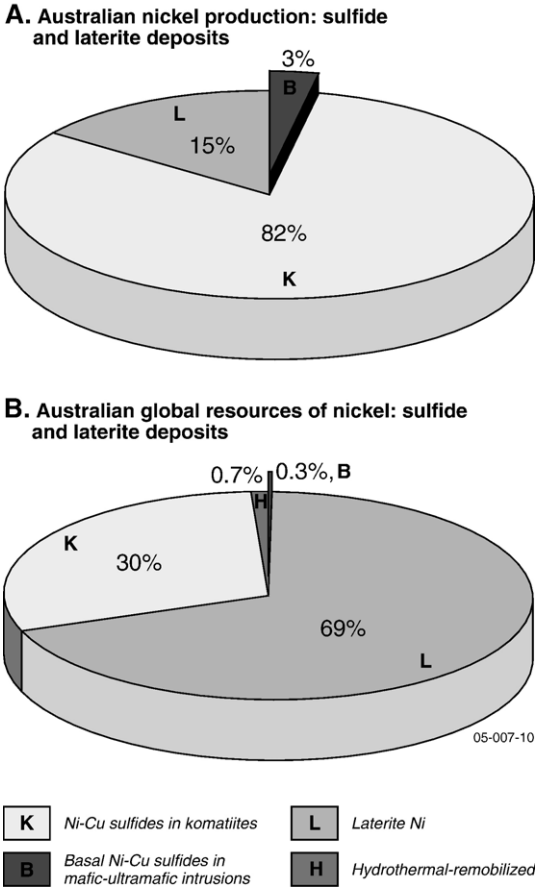

Fig. 7. Australia's nickel production and resources related to sulfide and laterite deposits (data from ABARE and OZMIN). (A) Nickel production is mainly derived from komatiite-hosted deposits (82%) that are associated with Archean greenstone sequences in the Yilgarn Craton of Western Australia. (B) In contrast, global resources of nickel metal are dominated by laterite deposits (69%), with komatiite deposits constituting most of the balance (30%) of the nation's nickel resource. Mafic–ultramafic intrusions account for only a few per cent of nickel production and resources.

shown in Fig. 8C are biased towards the two Australian provinces.

Exploration for nickel sulfides has been very active since 2001 in most Precambrian provinces of Australia. Total expenditure for Ni–Co exploration (sulfide and laterite) in Australia has risen sharply during this period. During 2005, expenditure was up 42% from the previous year to A$168.1 million (Australian Bureau of Statistics, 2006). Western Australia (A$152.2 million) dominates the exploration investment with this state alone accounting for more than 90% of the nation's Ni–Co exploration expenditure.

More than 170 major and junior companies were actively exploring for nickel in Western Australia in

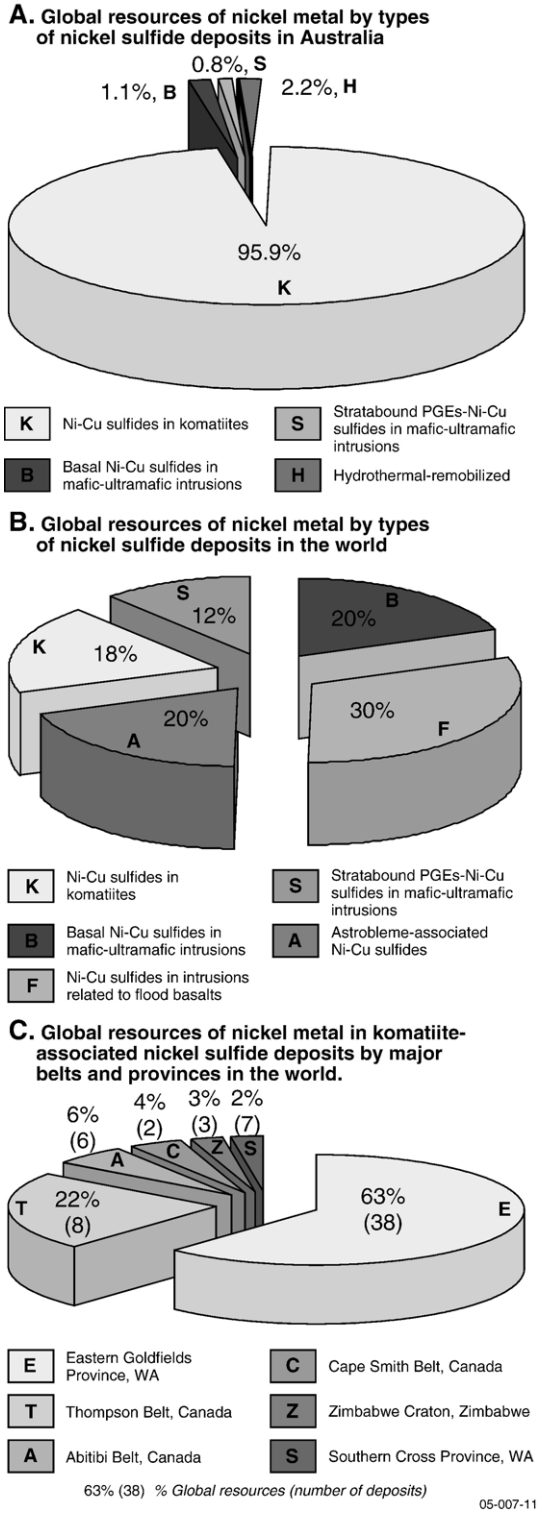

Fig. 8. Global resources of nickel metal by: (A) types of nickel sulfide deposits in Australia; (B) types of nickel sulfide deposits in the world; and (C) major komatiite provinces/belts in the world.

2006. The main areas of interest include Archean greenstone belts in the Yilgarn Craton (near Kambalda, Leonora, Leinster, and Forrestania), the northern margins of this craton, the western part of the Pilbara Craton, and the Proterozoic Kimberley, Musgrave, Albany–Fraser, Hamersley, and Bangemall provinces. Recent exploration successes include the discovery of: (1) increased resources at previously known deposits (many deposits around the Kambalda Dome, Flying Fox, Radio Hill); (2) delineation of deep and covered mineralized komatiite sequences (Cosmos Deeps, Prospero, Wedgetail-grouped with Honeymoon Well, Flying Fox-T5-grouped with Forrestania Nickel); (3) new mineralized Precambrian mafic± ultramafic intrusions (Nebo–Babel, Copernicus, Billy Ray, Mt Harcus); and (4) new styles of mineralization and new provinces (Avebury, Collurabbie, Beasley).

Exploration targets have now broadened to include deposits at greater depths, under cover, and in remote regions previously considered to have low prospectivity, such as Neoproterozoic basins (e.g., Officer Basin, Western Australia) and younger Phanerozoic provinces (western Victoria, Tasmania). This change of direction for exploration has led to a greater diversity of nickel deposits and prospects being found. These include those with the highest nickel grades in the world (5–9%: Cosmos, Cosmos Deeps, Prospero, Silver Swan, Flying Fox-T5), multi-element ores (Ni, PGEs, Cu, Co, Au, Ag: Collurabbie, Daltons), and other deposits having unusual settings (Avebury).

4. Nickel sulfide associations in Australia

Australia's nickel sulfide deposits are associated with ultramafic and/or mafic igneous rocks in three major geotectonic settings: (1) Archean komatiites emplaced in rift zones of granite–greenstone belts; (2) Precambrian tholeiitic mafic–ultramafic intrusions emplaced in rift zones of Archean cratons or Proterozoic orogens; and (3) hydrothermal-remobilized occurrences with no apparent age or tectonic constraints. The deposits are widely distributed throughout Australia, but are most abundant in the older Precambrian provinces of Western Australia (Fig. 9). The largest, and economically the most important, deposits are associated with komatiitic rocks in the Archean greenstone belts of the Yilgarn Craton of Western Australia.

Most of Australia's nickel sulfide deposits can be classified into two orthomagmatic associations that reflect the dominant chemical affinities of the host magma, namely komatiitic (*Type 1*) and tholeiitic (*Type 2*). A third relatively minor association encompasses hydrothermal-remobilized mineralizing systems (*Type 3*). The three associations are further divided largely according to the spatial distribution of the mineralization (e.g., basal, internal, feeder conduit, compositional contacts, discordant pipes, remobilized). The relatively simple classification shown in Table 2 (based primarily on magma-type association) avoids the use of somewhat equivocal criteria that are often used in other classifications, such as geotectonic settings (Naldrett, 1981, 1989; Barnes and Lightfoot, 2005), ambiguous lithological terms (dunite versus peridotite: Marston, 1984; Lesher, 1989), and also does not depend on detailed petrographic descriptions of ore types (e.g., blebby, cloudy, interstitial, offset: Lesher and Keays, 2002) that can be found in a single deposit, and/or uncertain genetic qualifiers (intrusive versus extrusive, stratiform versus stratabound: Marston, 1984; Lesher, 1989; Arndt et al., 2005). The classification introduced here can easily be expanded to include foreign deposits and it provides a useful framework for exploration.

There are other deposits in Australia that contain nickel sulfide assemblages but, because of their low nickel contents (<0.15% Ni), absence of defined global resources, and/or equivocal origins, they are not included in the classification of Table 2. Such deposits include PGE–Ni–Cu sulfides in alkaline–ultramafic intrusions (Mordor intrusion — Arunta Region: Barnes et al., 2004b; Hoatson et al., 2005a), sediment-hosted polymetallic deposits (Browns deposit, Rum Jungle: McCready et al., 2004), Ni–Ag–Cu sulfides associated with an interpreted gabbroic feeder conduit (Barrow Creek Prospect D-Arunta Region: Mithril Resources Limited, 2005). Other deposits containing nickel-oxide assemblages, such as oceanic manganese nodules and seamount crusts (Dampier Ridge–Lord Howe Rise: Pratt, 1996), are also not included in Table 2.

4.1. Komatiitic association

Australia's nickel sulfide production is dominated by the ~2705 Ma komatiite-hosted deposits in the Eastern Goldfields Province of the Yilgarn Craton (Figs. 9 and 10). This province contains the largest concentration of Archean komatiite-hosted nickel deposits in the world, and includes such world-class examples as Mt Keith, Kambalda, and Perseverance (Jaques et al., 2002). Other mineralized komatiite sequences occur in the Southern Cross (~3030 Ma to 2720 Ma) and Northeastern Goldfields (>?2900 Ma to 2710 Ma) provinces, however, those from the Murchison (~3000 Ma to 2750 Ma) and South West (~2670 Ma) provinces appear to be poorly

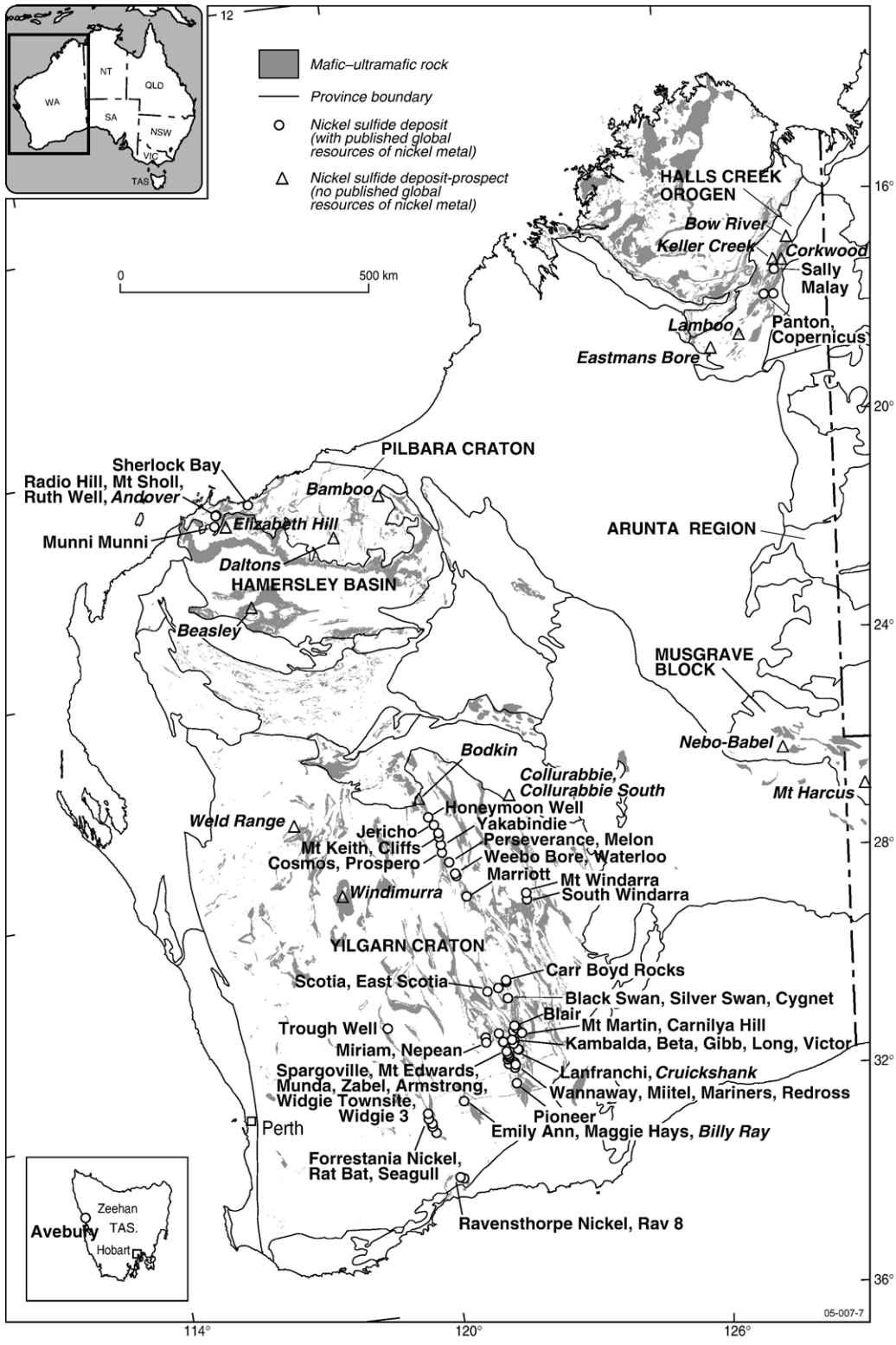

Fig. 9. Distribution of outcropping mafic–ultramafic rocks in the western part of Australia and the locations of nickel sulfide deposits that have published global resources of nickel metal in OZMIN. Nickel prospects (with no global metal resource) that are described in the text are shown in italics. Inset: location of the Avebury deposit in western Tasmania.

Table 2
Classification of Australia's nickel sulfide deposits

Association	Deposits/prospects	Geodynamic setting	Age (Ma)	Metal association	Ni:Cu	Typical size	Status	Reference(s)
1. Komatiitic								
1A. Massive and/or matrix sulfides at base of olivine cumulate (peridotite) sequences in preferred lava pathways	*Kambalda, WA; Maggie Hays, WA; Cosmos, WA*	Rift zones in granite–greenstone belts of Archean cratons	~2900–2700	Ni–Cu± Au± PGE±Co	7–20	0.05–50 Mt @ 1–10% Ni, 0.1–0.4% Cu	Mine	Marston (1984) Hill et al. (1987) Lesher and Keays (2002)
1B. Disseminated sulfides in central parts of thick olivine cumulate (dunite) sequences in preferred lava pathways	*Mt Keith, WA; Black Swan, WA; Honeymoon Well, WA*	Rift zones in granite–greenstone belts of Archean cratons	~2900–2700	Ni–Cu± PGE±Co	>20	5–300 Mt @ 0.5–1.5% Ni, 0.01–0.04% Cu	Mine	Marston (1984) Hill et al. (1987) Lesher and Keays (2002)
Other komatiitic deposits								
— Sulfides at basal contact of olivine cumulate sequences associated with comagmatic flood basalts	*Beasley, WA*	Archean continental flood basalts	?2770	Ni–Cu–PGE	NA	NA	Prospect	AUSQUEST Limited (2003)
— PGE-enriched sulfides associated with komatiitic and tholeiitic mafic–ultramafic rocks	*Collurabbie*, WA; ?Daltons, WA	Rift zones in granite–greenstone belts of Archean cratons	?2900–2700	PGE–Ni–Cu	<2	NA	Prospect	Dundas (2004)
2. Tholeiitic								
2A. Massive and disseminated sulfides in feeder conduit and/or depressions along basal contacts of mafic± ultramafic intrusions	*Radio Hill, WA; Sally Malay, WA; Mt Sholl, WA; Nebo–Babel, WA*	Rift zones in Archean–Proterozoic cratons or Proterozoic orogenic belts	~2925–2700, ~1850, ~1080	Ni–Cu–Co±PGE	0.5–7	1–5 Mt @ 0.5–3% Ni, 1–2% Cu, 0.2% Co	Mine	Thornett (1981) Hoatson and Blake (2000) Hoatson and Sun (2002) Dundas (2004)
2B. Stratabound disseminated sulfides near ultramafic–gabbroic zone contacts of mafic–ultramafic intrusions	*Munni Munni, WA; Weld Range, WA; Windimurra, WA*	Rift zones in Archean–Proterozoic cratons or Proterozoic orogenic belts	~2925–2800, ?1850	PGE–Cu–Ni	<2	5–25 Mt @ 3 g/t PGE, 0.3% Cu, 0.2% Ni	Prospect	Hoatson et al. (1992) Hoatson and Sun (2002)
2C. Stratabound chromitite layers near ultramafic–gabbroic zone contacts of ultramafic–mafic intrusions	*Panton, WA; Eastmans Bore, WA; Salt Creek–Plumridge, WA*	Proterozoic orogenic belts	~1850, ~1300	PGE–Ni–Cu–Au–Cr	5	30–75 Mt @ 2 g/t PGE, 0.2% Ni, 0.04% Cu	Prospect	Perring and Vogt (1991) Hoatson and Blake (2000)
2D. Discordant bronzitite breccia pipes in mafic–ultramafic intrusions	*Carr Boyd Rocks, WA*	Rift zones in Archean cratons	?2700	Ni–Cu	3	1 Mt @ 1.2% Ni, 0.5% Cu	Mine (closed)	Purvis et al. (1972) Marston (1984)
3. Hydrothermal-remobilized								
3A. Hydrothermal-remobilized–ultramafic host or ?skarn	*Avebury, Tas*	Phanerozoic troughs	?360	Ni	Ni>Cu	12 Mt @ 1% Ni	Mine	Newnham (2003)

(continued on next page)

Table 2 (*continued*)

Association	Deposits/prospects	Geodynamic setting	Age (Ma)	Metal association	Ni:Cu	Typical size	Status	Reference(s)
3. Hydrothermal-remobilized								
3B. Hydrothermal-remobilized–metasedimentary rock host	*Sherlock Bay, WA; Cruickshank, WA*	Rift zones in Archean cratons	~2925–2700	Ni–Cu	5	25 Mt @ 0.4% Ni, 0.1% Cu	Prospect	Miller and Smith (1975) Ruddock (1999)
Other hydrothermal-remobilized deposits								
— Hydrothermal-remobilized–felsic±mafic±ultramafic rock hosts	*Elizabeth Hill, WA; ?Andover, WA*	Faults in Archean cratons	<2870	Ag–Pb–Ni–Cu±PGE	NA	0.02 Mt @ 0.4% Ag, minor Ni	Mine (closed)	Barnes (1995) Hoatson and Sun (2002)
— Remobilized–metamorphic–metagabbro host	*Corkwood, WA; Bow River, WA*	Proterozoic orogenic belts	~1865	Ni–Cu–Co	3	0.2 Mt @ 0.6% Ni, 0.2% Cu, 0.03% Co	Prospect	Marston (1984) Hoatson and Blake (2000)
— Hydrothermal arsenical–auriferous-bearing quartz-carbonate veins	*Mt Martin, WA; Bamboo, WA*	Rift zones in Archean cratons	NA	Ni–As–Au	Ni>>Cu	0.2 Mt @ 2% Ni, 2.3% As	Prospect	Marston (1984)

Type examples of deposits/prospects are indicated in italics.
NA=not available.

mineralized (Fig. 10). Therefore, the favorable age range for mineralized komatiites from the Yilgarn Craton appears to be ~2700 Ma to ~3000 Ma. Weakly mineralized komatiite sequences in the Pilbara Craton are generally older (~3460 Ma to 2880 Ma) and thinner than those in the Yilgarn Craton (Table 3). Only two Australian komatiite occurrences are known outside the West Australian Craton. The ~2520 Ma Lake Harris Komatiite in the central Gawler Craton is the youngest of these, and the easternmost known occurrence of komatiitic rocks in Australia (Hoatson et al., 2005b). Komatiitic flows coeval with the Lake Harris Komatiite also occur near Mt Hope on the western Eyre Peninsula of the southern Gawler Craton. Neither komatiite sequence is known to be mineralized.

The komatiite-hosted nickel sulfide deposits of Australia have been divided into two major groups (1A and 1B) on the basis of the style of mineralization (massive versus disseminated) and the location of the sulfides (basal contact versus intra-unit). These economically important groups are based on the subdivision of deposits in the Yilgarn Craton by Dowling and Hill (1998), Barnes et al. (1999), and Beresford and Rosengren (2004). Other relatively minor komatiite deposits are associated with comagmatic flood basalts and tholeiitic intrusions. *Type 1A nickel deposits* (Kambalda, Perseverance, Cosmos, Wedgetail, Waterloo, Maggie Hays) are prominent throughout the Eastern Goldfields and Southern Cross provinces of the Yilgarn Craton. Typical deposits generally contain small-tonnage ores (0.5 to 5 Mt) of moderately high nickel grade (2 to 4% Ni), although some deposits (Cosmos, Silver Swan) have the highest primary magmatic nickel grades (up to 9% Ni) in the world. The most important *type 1B nickel deposits* (Mt Keith, Yakabindie, Honeymoon Well) occur in the northern part of the Norseman–Wiluna greenstone belt of the Eastern Goldfields Province, where they are often spatially associated with type 1A deposits. The deposits are characterized by small- to large-tonnage ores (up to hundreds of Mt) with relatively low nickel grades (0.5 to 1.5% Ni). Other komatiite-associated occurrences include: the Beasley prospect on the southern margin of the Pilbara Craton, where the host komatiite flows are thought to be comagmatic with late Archean continental flood basalts; and the Collurabbie prospect in the northeast corner of the Yilgarn Craton, which contains unusually high abundances of Cu (up to 2%) and PGEs (2 to 5 g/t Pt+Pd) for komatiitic-mineralizing systems.

The komatiite-hosted deposits have distinctive Ni to Cu ratios that provide a useful criterion for their classification. Type 1A deposits have Ni/Cu ratios of 7 to 20, type 1B are more Ni-rich, with ratios generally greater than 20, whereas Collurabbie-type deposits have distinctly lower Ni to Cu ratios of <2.

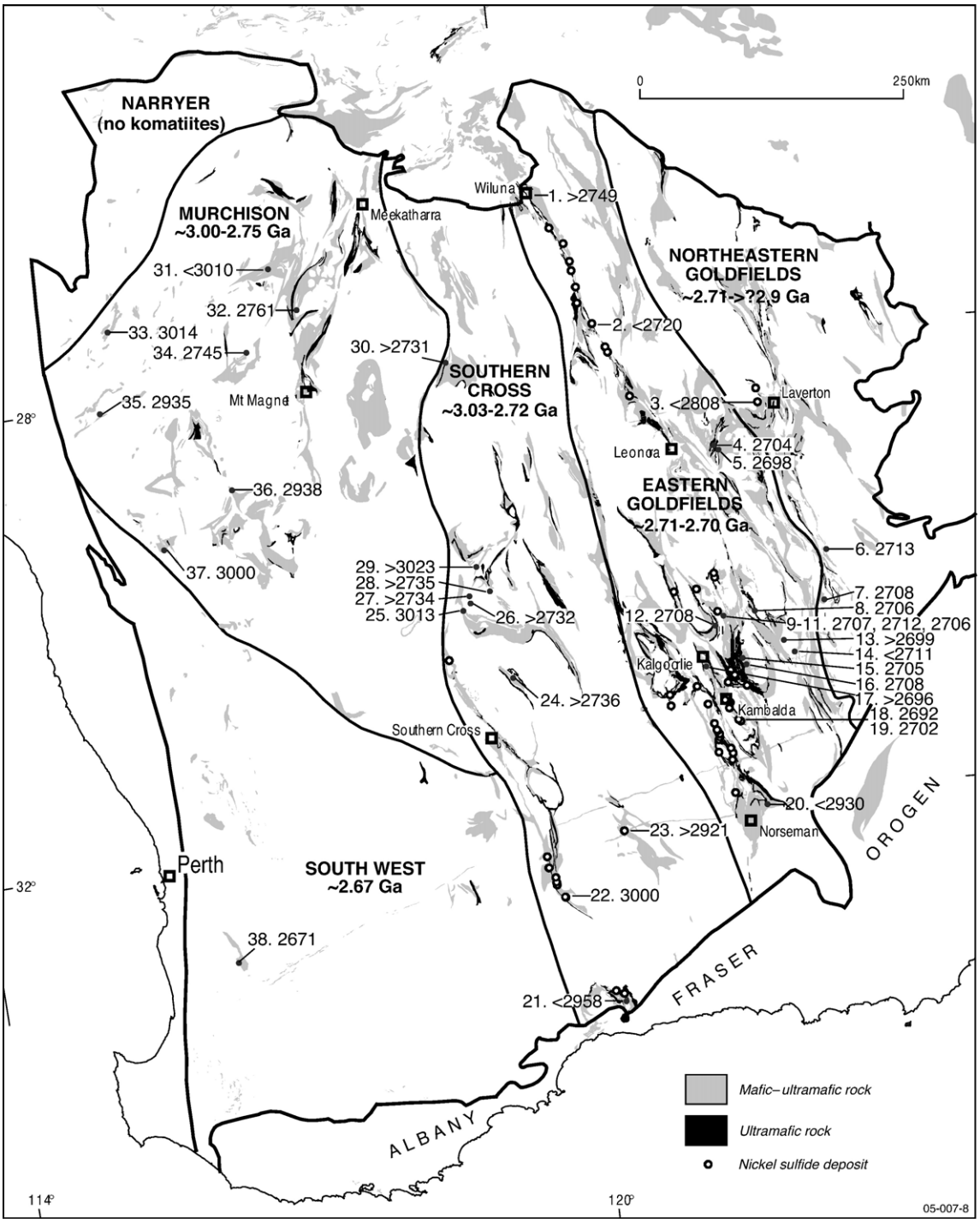

Fig. 10. U–Pb zircon geochronology of Archean komatiitic sequences from different provinces in the Yilgarn Craton, Western Australia. The range of ages for the komatiitic sequences in each province is indicated below the province names. The geochronology data (compiled from the literature and OZCHRON 2005 — Geoscience Australia's national database of geochronological data) includes U–Pb zircon ages of felsic units intercalated with komatiitic sequences (i.e., direct age of komatiites), felsic footwall units (maximum age), felsic hangingwall units (minimum age), and felsic dikes cutting the komatiitic sequences (minimum age). Details of the geochronology samples are in Table 3. The boundaries of the provinces are modified from Tyler and Hocking (2002).

Table 3
U–Pb zircon and U–Pb baddeleyite geochronology of Precambrian komatiites, associated rocks, and mafic–ultramafic intrusions in Australia

No.	Superprovince	Province/terrane	Formation/location	Co-ordinates[a]	Age (Ma)[b]	Description and comments	Reference
Komatiites and associated rocks							
1	Yilgarn Craton	Kalgoorlie	Wiluna West Lode Gold mine	26°8′S 120°15′E	>2749±7	Microdiorite dike cutting volcanics provides possible minimum age for komatiites in Wiluna domain (45 Ma older than ~2705 Ma komatiites in Kambalda Dome region)	Kent and Hagemann (1996)
2	Yilgarn Craton	Kalgoorlie	Perseverance Ni–Cu mine	27°48′S 120°42′E	<2720±14	Deformed felsic volcanic rock from footwall unit of ultramafic sequence at the Rockys Reward–Perseverance Ni–Cu mines	Nelson (1997b)
3	Yilgarn Craton	Laverton	South Windarra Ni–Cu mine	429364 6833977	<2808±8	Feldspathic sandstone unit from Windarra mafic–ultramafic succession	Barley et al. (2003)
4	Yilgarn Craton	Kurnalpie	Murrin Murrin Ni–Co laterite mine	NA[c]	2704±8	Chert in high-Mg basalts underlying Kilkenny layered intrusion; part of komatiites and Murrin Murrin Ni–Co deposit	Claoué-Long in Cassidy et al. (2002)
5	Yilgarn Craton	Kurnalpie	Murrin Murrin ultramafic complex	NA	2698±5	Volcaniclastic dacite intermixed with komatiitic volcanic rocks of the Minerie Sequence	Doyle et al. (in press)
6	Yilgarn Craton	Pinjin	Pinjin North–Northeast	473700 6676800	2713±4	Coeval dacite unit in komatiite flow and banded iron formation sequence	Nelson (1997a)
7	Yilgarn Craton	Edjudina	Liberty Bore East	475750 6637300	2708±6	Coeval dacite unit in basalt and dolerite (associated ultramafic rocks nearby)	Nelson (1997a)
8	Yilgarn Craton	Kurnalpie	North Burton Tank	405500 6628400	2706±3	Coeval dacite unit interlayered with komatiites	Nelson (1997a)
9	Yilgarn Craton	Kalgoorlie	Black Swan Ni–Cu mine	370801 6636858	2707±4	Rhyolite porphyry clast (dacitic lava) interlayered with komatiites of the Kambalda Komatiite Formation	Kositcin et al. (in press)
10	Yilgarn Craton	Kalgoorlie	Black Swan Ni–Cu mine	370801 6636858	2712±6	Volcanogenic rhyolitic conglomerate interlayered with komatiites of the Kambalda Komatiite Formation	Kositcin et al. (in press)
11	Yilgarn Craton	Kalgoorlie	Black Swan Ni–Cu mine	370801 6636858	2706±5	Volcanogenic rhyolitic conglomerate interlayered with komatiites of the Kambalda Komatiite Formation	Kositcin et al. (in press)
12	Yilgarn Craton	Kalgoorlie	Ballarat–Last Chance mine	364500 6614350	2708±7	Coeval dacite unit in komatiite flow	Nelson (1997a)
13	Yilgarn Craton	Kurnalpie	Steeple Hill	436100 6599600	>2699±4	Hangingwall sodic trachyte unit to komatiite flow	Nelson (1997a)
14	Yilgarn Craton	Kurnalpie	Christmas Gift Dam	442300 6594200	<2711±5	Footwall dacite unit to komatiite flow	Nelson (1997a)

Table 3 (*continued*)

No.	Superprovince	Province/terrane	Formation/location	Co-ordinates[a]	Age (Ma)[b]	Description and comments	Reference
Komatiites and associated rocks							
15	Yilgarn Craton	Gindalbie	Bulong townsite	387730 6594360	2705±4	Coeval felsic tuff interlayered with lower ultramafic lava flows of Bulong Complex; correlated with typical ~2705 Ma Kambalda Komatiite Formation	Nelson (1997a)
16	Yilgarn Craton	Gindalbie	Bulong	387814 6594545	2708±5	Silicified feldspathic volcanogenic sandstone intercalated with komatiite	Kositcin et al. (in press)
17	Yilgarn Craton	Kalgoorlie	Williamstown peridotite	357754 6590939	>2696±5	Granophyric quartz gabbro sill cutting Devon Consuls Basalt and Paringa Basalt	Fletcher et al. (2001)
18	Yilgarn Craton	Kalgoorlie	South of Lake Lefroy	NA	2692±4	Tuffaceous shale of Kapai Slate near top of basalt–komatiite sequence	Claoué-Long et al. (1988)
19	Yilgarn Craton	Kalgoorlie	South of Lake Lefroy	NA	2702±4	Shale near base of basalt–komatiite sequence	Unpub data of Claoué-Long et al. (1988)
20	Yilgarn Craton	Norseman	Penneshaw, Norseman	388552 6430238	<2930±4	Rhyolite of Upper Penneshaw Formation with overlying chert, banded iron formation, komatiitic basalt of Woolyeenyer Formation; older basement than basement at Kambalda	Nelson (1997a)
21	Yilgarn Craton	Southern Cross	Bandalup, Ravensthorpe	256400 6271100	<2958±4	Bandalup rhyolite forming older greenstone basement to 2.7 Ga basement sequence in Eastern Goldfields? (no reference to relationship with komatiite)	Nelson (1997a)
22	Yilgarn Craton	Southern Cross	Forrestania	NA — unpublished data	3000	Greenstones (unpublished data; no reference to relationship with komatiite)	Wang et al. (1996)
23	Yilgarn Craton	Southern Cross	Maggie Hays Ni–Cu mine	264680 6430568	>2921±4	Felsic porphyry dike cutting komatiite, not footwall unit as described in Wang et al., 1996 (pers. comm., K. Cassidy, GA, 2003)	Wang et al. (1996)
24	Yilgarn Craton	Southern Cross	Koolyanobbing	30°50′30″S 119°35′E	>2736±10	Felsic volcanic rock from pillow basalt–greenstone sequence (no reference to relationship with komatiite)	Pidgeon and Wilde (1990)
25	Yilgarn Craton	Southern Cross	Jackson Homestead	NA	3013±16	Felsic volcanic unit within greenstones (no reference to relationship with komatiite)	Dalstra (1995)
26	Yilgarn Craton	Southern Cross	Marda Tank	720730 6659080	>2732±3	Felsic ignimbrite of the Marda Complex overlying greenstone (no reference to relationship with komatiite)	Nelson (2001)
27	Yilgarn Craton	Southern Cross	Marda Tank	720500 6664440	>2734±3	Welded tuffaceous rhyolite of the Marda Complex overlying greenstone (no reference to relationship with komatiite)	Nelson (2001)

(continued on next page)

Table 3 (*continued*)

No.	Superprovince	Province/terrane	Formation/location	Co-ordinates[a]	Age (Ma)[b]	Description and comments	Reference
Komatiites and associated rocks							
28	Yilgarn Craton	Southern Cross	Marda Tank	30°7′S 119°10′E	>2735±2	Rhyolite of the Marda Complex overlying greenstone (no reference to relationship with komatiite)	Pidgeon and Wilde (1990)
29	Yilgarn Craton	Southern Cross	Deception Hill	NA	>3023±10	Intrusive quartz–feldspar porphyry associated with high-Mg basalt, tholeiitic basalt, ultramafic rocks, banded iron formation, chert	Greenfield and Chen (1999)
30	Yilgarn Craton	Southern Cross	Bulchina Gold mine	719300 6893100	>2731±14	Porphyritic microgranite intrudes komatiites in the openpit of the Bulchina Gold mine	Chen et al. (2005)
31	Yilgarn Craton	Murchison	Weld Range	27°12′46″S 117°51′49″E	<3010	Felsic volcanic from basal part of Weld Range greenstone belt (no reference to relationship with komatiite)	Pidgeon and Wilde (1990)
32	Yilgarn Craton	Murchison	Emily Well, Cue	582575 6970710	2761±1	Rhyolitic crystal–vitric tuff associated with high-Mg basalt, komatiite, graphitic shale, and felsic volcanics in Meekatharra–Mt Magnet greenstone belt	Pidgeon and Hallberg (2000)
33	Yilgarn Craton	Murchison	Twin Peaks	27°22′S 115°49′15″E	3014	Felsic volcanic rock from greenstone–banded iron formation sequence at Twin Peaks (no reference to relationship with komatiite)	Pidgeon and Wilde (1990)
34	Yilgarn Craton	Murchison	Dalgaranga Homestead	522264 6933866	2745±4	Felsic tuff associated with high-Mg basalt, komatiite, graphitic shale, and felsic volcanics in Dalgaranga greenstone belt	Pidgeon and Hallberg (2000)
35	Yilgarn Craton	Murchison	Tallering	28°08′S 115°37′E	2935±2	Rhyodacite from greenstone sequence in Tallering greenstone belt, Greenough River (no reference to relationship with komatiite)	Pidgeon and Wilde (1990)
36	Yilgarn Craton	Murchison	Golden Grove mine	28°46′S 116°57′E	2938±10	Felsic volcaniclastic rock from greenstone sequence at Gossan Hill, Golden Grove (no reference to relationship with komatiite)	Pidgeon and Wilde (1990)
37	Yilgarn Craton	Murchison	Koolanooka Hills	NA (wrong in reference)	3000	Felsic volcanic rock within volcanic sequence of Koolanooka Hills greenstone belt (no reference to relationship with komatiite)	Pidgeon and Wilde (1990)
38	Yilgarn Craton	South West	George Hill, southwest Boddington	32°55′S 116°22′15″E	2671±6	Tuffaceous pyroclastic from Wells Formation in Mount Saddleback Greenstone sequence (no reference to relationship with komatiite)	Wilde and Pidgeon (1986)
39	Pilbara Craton	Western Pilbara	Ruth Well	NA	2876±38	Re–Os isochron age of three komatiitic samples from the Ruth Well Formation (Roebourne Group)	Meisel et al. (2001)

Table 3 (*continued*)

No.	Superprovince	Province/terrane	Formation/location	Co-ordinates[a]	Age (Ma)[b]	Description and comments	Reference
Komatiites and associated rocks							
40	Pilbara Craton	Western Pilbara	Mount Regal	20°49′58″S 116°46′49″E	>3270±2	Tonalite (Karratha Granodiorite) intrudes peridotite and komatiite of Ruth Well Formation (Roebourne Group) (?conflict with Re/Os age of previous entry)	Nelson (1998)
41	Pilbara Craton	Western Pilbara	Rocky Creek	20°41′59″S 117°00′51″E	>3018±2	Dacite porphyry intrudes peridotitic komatiite, pillow basalt and chert of the Regal Formation (top of Roebourne Group)	Nelson (1998)
42	Pilbara Craton	Western Pilbara	Red Hill	554310 7681970	>3009±4	Vitric tuff and volcaniclastic rocks (Cistern Formation–Whim Creek Group) underlying komatiitic and pillowed tholeiitic basalt of the Louden Volcanics (top of Whim Creek Group)	Nelson (1998)
43	Pilbara Craton	Eastern Pilbara	Panorama Ridge	21°15′55″S 119°23′31″E	<3458±2	Rhyolite of Panorama Formation underlying high-Mg pillowed basalt and komatiitic basalt lava from the Cloisters Member of the Euro Basalt Formation (Warrawoona Group)	Thorpe et al. (1992)
44	Pilbara Craton	Eastern Pilbara	East Pilbara	21.4294°S 119.0734°E	>3240±2	Dacite from Kangaroo Caves Formation overlying pillowed basalt, high-Mg basalt, and komatiitic basalt of the Kunagunarrina Formation (Sulfur Springs Group)	Unpub data: Thorpe in Van Kronendonk (2000)
45	Gawler Craton	Harris Greenstone	Lake Harris	513430 6567151	2520	Banded felsic volcanics interlayered with komatiites of the Lake Harris Komatiite	Hoatson et al. (2005b)
Mafic–ultramafic intrusions							
46	Yilgarn Craton	Kalgoorlie	Kathleen Valley Gabbro	258435 6953159	2736±3	Crystallization age of tonalite (quartz gabbro) from differentiated layered mafic intrusion northwest of old Wiluna–Leinster road in the Cosmos nickel mine area	Liu et al. (2002)
47	Yilgarn Craton	Kalgoorlie	Kathleen Valley Gabbro	NA	2795±38	Crystallization age of granophyre from differentiated layered mafic intrusion in the Perseverance nickel mine, Jones Creek area	Cooper and Dong (1983)
48	Yilgarn Craton	Kalgoorlie	Fraser Dike Swarm, Victory Gold mine	31°19′38″S 121°46′4″E	1212±10	U–Pb baddeleyite age of medium-grained granophyre that forms a central part of a northeast-trending quartz dolerite dike	Wingate et al. (2000)

(continued on next page)

Table 3 (*continued*)

No.	Superprovince	Province/terrane	Formation/location	Co-ordinates[a]	Age (Ma)[b]	Description and comments	Reference
Mafic–ultramafic intrusions							
49	Yilgarn Craton	Kalgoorlie	Jimberlana Dike	32°11′S 121°18′E	2411±55	Sm–Nd age of gabbro from DDH BRDIIA at Bronzite Ridge	Fletcher et al. (1987)
50	Yilgarn Craton	Kalgoorlie	Celebration Dike	NA	2411±52	Rb–Sr rock and mineral separate age of dike (adjusted age)	Fletcher et al. (1987)
51	Yilgarn Craton	Narryer	Dugel gneiss	26°26′S 116°26′E	3730±6	Deformed leucogabbro and meta-anorthosite within Dugel gneiss (formerly part of Manfred layered igneous complex); these samples are the oldest dated rocks in Australia	Kinny et al. (1988)
52	Yilgarn Craton	South West	Binneringie Dike, Airport quarry, Narrogin	32°57′S 117°7′E	2418±3	U–Pb baddeleyite age of granophyric part of 200-m-wide dike interpreted as crystallization age for western part of Binneringie Dike (member of Widgiemooltha dike swarm)	Nemchin and Pidgeon (1998)
53	Yilgarn Craton	South West	Boyagin Dike Swarm, York	31°52′30″S 116°44′40″E	1204±10	Crystallization age of east–west-trending quartz dolerite dike in the township of York	Pidgeon and Nemchin (2001)
54	Yilgarn Craton	South West	Un-named amphibolite dike	NA	2711±7	U–Pb titanite age of possible amphibolite dike cutting sediments in the Jimperding Metamorphic Belt; may represent emplacement age of dike or age of earlier metamorphic event	Bosch et al. (1996)
55	Yilgarn Craton	South West	Un-named mafic granulites, Corrigin	Various	2649±6 to 2640±1	U–Pb zircon age range of granulite facies metamorphism	Nemchin et al. (1994)
56	Yilgarn Craton	South West	Boyagin Dike Swarm, Brigadoon	412548 6482629	1214±5	Crystallization age of quartz dolerite dike (1210 Ma Marnda Moorn Large Igneous Province)	Pidgeon and Cook (2003)
57	Pilbara Craton	Western Pilbara	Radio Hill intrusion	486340 7679240	2892±34	Re–Os isochron age of massive sulfides from basal contact of intrusion	Frick et al. (2001)
58	Pilbara Craton	Western Pilbara	Munni Munni intrusion	483608 7664250	2927±13	Sm–Nd isochron age of mineral separates for samples from PGE-bearing porphyritic websterite layer and gabbroic zone	Hoatson and Sun (2002)
59	Pilbara Craton	Western Pilbara	Munni Munni intrusion	484420 7664930	2925±16	Ferrogabbro pegmatite near contact of ultramafic–gabbroic zone is interpreted to be coeval with layered stratigraphy of intrusion	Arndt et al. (1991)
60	Pilbara Craton	Western Pilbara	Munni Munni intrusion	21°07′11″S 116°51′42″E	2924±5	Granite dike intrudes lower pyroxenite and upper gabbro series of Munni Munnni intrusion	Nelson (1998)
61	Pilbara Craton	Western Pilbara	Sherlock Bay intrusion	20°55′S 117°32′E	2866±66	Model 3 Sm–Nd isochron age	Hoatson and Sun (2002)

Table 3 (*continued*)

No.	Superprovince	Province/terrane	Formation/location	Co-ordinates[a]	Age (Ma)[b]	Description and comments	Reference
Mafic–ultramafic intrusions							
62	Pilbara Craton	Western Pilbara	Mundine Well Dike Swarm	Various	755±3	Crystallization age of olivine gabbro and quartz dolerite dikes	Wingate and Giddings (2000)
63	Pilbara Craton	Central Pilbara	Black Range Dike	NA	2772±2	U–Pb baddeleyite age of gabbroic dolerite dike (Black Range dike) interpreted to be a feeder to basal volcanic units in the Fortescue Group (Mt Roe flood basalts)	Wingate (1999)
64	Pilbara Craton	Eastern Pilbara	Un-named dolerite sill, Marble Bar	21°59′41″S 119°48′49″E	3487±8	Igneous crystallization or xenocrystic age of dolerite sill in the McPhee Formation, Marble Bar region	McNaughton et al. (1993)
65	Pilbara Craton	Eastern Pilbara	Un-named dolerite sill, Marble Bar	21°59′41″S 119°48′ 49″E	3432±6	Igneous crystallization or hydrothermal age of dolerite sill in the McPhee Formation, Marble Bar region	McNaughton et al. (1993)
66	Pilbara Craton	Sylvania Dome	Sylvania dike	NA	2747±4	Quartz dolerite dike interpreted to be a feeder to volcanic units in Fortescue Group (Kylena Formation)	Wingate (1999)
67	Pilbara Craton	Hamersley Basin	Un-named mafic sill	NA	2208±10	U–Pb baddeleyite age of mafic sills that intrude the Turee Creek Group in the Hardey Syncline	Müller et al. (2005)
68	Pilbara Craton	Hamersley Basin	Un-named dolerite dike, Paraburdoo Mine	NA	2008±16	U–Pb baddeleyite age of dolerite dike that cuts the Cheela Springs Basalt in the Hardey Syncline	Müller et al. (2005)
69	Albany–Fraser Orogen	Albany–Fraser Orogen	Fraser Complex Unit 5	NA	1291±21	Sm–Nd isochron age of mineral separates for olivine gabbronorite	Fletcher et al. (1991)
70	Albany–Fraser Orogen	Albany–Fraser Orogen	Fraser Complex, Mt Malcolm	NA	1301±6	Crystallization age of charnockite provides an estimate for the age of intrusion of Fraser Complex gabbroic rocks	Clark et al. (1999)
71	Pinjarra Orogen	Northampton Complex	Woodbine mafic granulite	NA	1079±3	Age of zircon growth during granulite facies metamorphism	Bruguier et al. (1999)
72	Halls Creek Orogen	East Kimberleys	Sally Malay intrusion	396074 8081664	1844±3	Crystallization age of mottled anorthosite from upper fractionated part of gabbroic zone	Page and Hoatson (2000)
73	Halls Creek Orogen	East Kimberleys	Sally Malay intrusion	396074 8081664	1846±5	U–Pb baddeleyite age of mottled anorthosite from upper fractionated part of gabbroic zone	Page and Hoatson (2000)
74	Halls Creek Orogen	East Kimberleys	Panton intrusion	375877 8034974	1856±2	Crystallization age of mottled anorthosite from upper fractionated part of gabbroic zone	Page and Hoatson (2000)
75	Halls Creek Orogen	East Kimberleys	Panton intrusion	375473 8032534	1825±10	Muscovite pegmatite dike cutting mafic–ultramafic stratigraphy of Panton intrusion	Page and Hoatson (2000)
76	Halls Creek Orogen	East Kimberleys	Springvale intrusion	354261 8035097	1857±2	Leucogabbro from upper fractionated part of intrusion	Page and Hoatson (2000)

(continued on next page)

Table 3 (*continued*)

No.	Superprovince	Province/terrane	Formation/location	Co-ordinates[a]	Age (Ma)[b]	Description and comments	Reference
Mafic–ultramafic intrusions							
77	Halls Creek Orogen	East Kimberleys	Toby intrusion	357120 8058510	1855±2	Quartz gabbro from upper fractionated part of intrusion	Page and Hoatson (2000)
78	Kimberley Basin	West Kimberleys	Hart Dolerite	732434 8108060	1790±4	Igneous crystallization age of granophyre form upper part of Hart Dolerite	OZCHRON[d]
79	Musgrave Province	West Musgrave	Giles Complex, Bell Rock intrusion	477572 7091672	1078±3	Granophyric unit from Bell Rock intrusion	Glikson et al. (1996)
80	Musgrave Province	West Musgrave	Giles Complex, Hinckley Range intrusion	473425 7118022	1073±5	Recrystallized ?chilled biotite gabbronorite from Hinckley Range intrusion	Glikson et al. (1996)
81	Musgrave Province	West Musgrave	Western Champ de Mars	491537 7107415	1176±6	Crystallization age of biotite-rich leucogabbro body that is significantly older than that of the Giles Complex	OZCHRON
82	Musgrave Province	West Musgrave	Western Champ de Mars	490141 7103427	1058±14	Leucocratic gabbronorite dike contemporaneous or slightly younger than the Giles Complex	OZCHRON
83	Musgrave Province	West Musgrave	Western Champ de Mars	493039 7101546	824±4	U–Pb baddeleyite age of quartz dolerite dike	Glikson et al. (1996)
84	Arunta Region	Central Arunta	Enbra Granulite, Enbra Hills	383477 7433235	1811±3	Crystallization age of precursor to zirconium-bearing mafic granulite from northern part of mafic granulite intrusion	Claoué-Long and Hoatson (2005)
85	Arunta Region	Central Arunta	Johannsen Metagabbro intrusion, Utnalanama Range	405982 7429714	1805±3	Crystallization age of precursor to zirconium-bearing mafic granulite from stacked sequence of mafic sills cut by Harry Anorthositic Gabbro	Claoué-Long and Hoatson (2005)
86	Arunta Region	Central Arunta	Un-named dolerite dike, Utnalanama Range	404377 7429359	1689±8	Crystallization age of zirconium-bearing dolerite dike that cuts Johannsen Metagabbro and Harry Anorthositic Gabbro	Claoué-Long and Hoatson (2005)
87	Arunta Region	Central Arunta	Mount Hay Granulite, Mount Hay	300975 7407259	1803±5	Crystallization age of precursor to zirconium-bearing mafic granulite from central part of large mafic granulite body	Claoué-Long and Hoatson (2005)
88	Arunta Region	Central Arunta	Mount Chapple Metamorphics, Mount Chapple	273600 7418972	1774±2	Crystallization age of precursor to zirconium-bearing mafic granulite from central part of large mafic–felsic granulite body	Claoué-Long and Hoatson (2005)
89	Arunta Region	East Arunta	Attutra Metagabbro intrusion	635228 7499425	1786±4	Crystallization age of zirconium-bearing gabbro from western margin of intrusion	Claoué-Long and Hoatson (2005)
90	Arunta Region	East Arunta	Mordor intrusion	448651 7408367	1133±5	Crystallization age of zirconium-bearing plagioclase pyroxenite from northeastern margin of intrusion	Claoué-Long and Hoatson (2005)

Table 3 (*continued*)

No.	Superprovince	Province/terrane	Formation/location	Co-ordinates[a]	Age (Ma)[b]	Description and comments	Reference
Mafic–ultramafic intrusions							
91	Arunta Region	West Arunta	Papunya ultramafic intrusion, Papunya	776315 7421751	1639±2	Crystallization age of zirconium-bearing gabbro from eastern margin of intrusion	Claoué-Long and Hoatson (2005)
92	Arunta Region	West Arunta	Papunya gabbro intrusion, Papunya	775879 7423495	1636±2	Crystallization age of zirconium-bearing gabbro from northern margin of intrusion	Claoué-Long and Hoatson (2005)
93	Arunta Region	West Arunta	South Papunya gabbro intrusion, Papunya	789617 7420123	1635±5	Crystallization age of zirconium-bearing gabbro from southeastern margin of intrusion	Claoué-Long and Hoatson (2005)
94	Arunta Region	West Arunta	Andrew Young Hills intrusion, west Papunya	697394 7474000	1633±3	Crystallization age of zirconium-bearing biotite gabbronorite	Claoué-Long and Hoatson (2005)
95	Arunta Region	West Arunta	Ilpili Dolerite	643200 7420990	1633±3	Crystallization age of dolerite dike intruding granodiorite of the Waluwiya Suite	Close (NTGS, personal communication, 2006)
96	Arunta Region	West Arunta	Stuart Pass Dolerite	386593 7474106	976±4	Crystallization age of Neoproterozoic dike that also contains xenocrysts of 1630 Ma country rocks	OZCHRON
97	Tennant Region	Tennant Creek	Un-named gabbro intrusion	430156 7814201	1841±6	Crystallization age of small gabbro intruding Mumbilla Granodiorite	Compston (1994)
98	Tennant Region	Tennant Creek	Un-named dolerite intrusion, Warrego Mine	382511 7864116	1821±7	Igneous crystallization age of a monzodiorite differentiate in dolerite dike intruding Flynn Subgroup north of the Warrego mine	Compston (1994)
99	Tennant Region	Tennant Creek	Un-named dolerite intrusion	385127 7819169	1842±8	Baddeleyite data that provide probable crystallization age of metamorphosed dolerite intruding Wundirgi Formation	OZCHRON
100	Tanami Region	Tanami	Coora Dolerite	597929 7729354	<1882±8	Maximum emplacement age of dolerite intruding sedimentary rocks underlying the Killi Killi Formation at Callie gold mine	Claoué-Long and Hoatson (2005)
101	Pine Creek Region	Pine Creek	Zamu Dolerite	247327 8501164	1870±6	Crystallization age of chloritized dolerite	OZCHRON
102	Pine Creek Region	Pine Creek	Zamu Dolerite	212527 8523464	2100	Maximum age for fractionated dolerite in the Zamu Dolerite as the zircons are xenocrystic; other inheritance at 2500–2700 Ma	OZCHRON
103	Pine Creek Region	Pine Creek	Oenpelli Dolerite	317527 8638662	1723±6	Pooled age of unknown accuracy	OZCHRON
104	Western-central Australia	Several	Various dolerite dikes and sills (Warakurna intrusions)	Various	1070 to 1078	U–Pb and Sm–Nd ages of mafic rocks comprising the Warakurna Igneous Province (Glenayle Dolerite, Bangemall Supergroup sills, Stuart Pass Dolerite, Alcurra sills) of western and central Australia	Wingate et al. (2004)

(continued on next page)

Table 3 (*continued*)

No.	Superprovince	Province/terrane	Formation/location	Co-ordinates[a]	Age (Ma)[b]	Description and comments	Reference
Mafic–ultramafic intrusions							
105	Curnamona Craton	Broken Hill	Un-named gabbro, top of Round Hill	548297 6466953	1683±5	Crystallization age of gabbro from un-named gabbro intrusion of the Cues Formation (Thackaringa Group)	OZCHRON
106	Curnamona Craton	Broken Hill	Little Broken Hill gabbro	32°06′S 141°32′E	827±9	Crystallization age of zirconium-bearing gabbro and associated dikes	Wingate et al. (1998)
107	Curnamona Craton	Broken Hill	Un-named mafic intrusion	516517 6446386	1593±5	Recrystallization age of amphibolite intrusion in the Cues Formation (Thackaringa Group)	OZCHRON
108	Curnamona Craton	Broken Hill	Un-named gabbro intrusion, Broken Hill Synform	549999 6464274	1594±11	Recrystallization age of amphibolite intrusion in the Cues Formation (Thackaringa Group)	OZCHRON
109	Curnamona Craton	Broken Hill	Un-named mafic intrusion, Allendale area	545949 6502803	1594±7	Metamorphic age of amphibolite intrusion in the Parnell Formation	OZCHRON
110	Curnamona Craton	Broken Hill	Un-named mafic intrusion, north of Hores mine	550888 6498718	1676±7	Minimum age of amphibolite intrusion in the Parnell Formation	OZCHRON
111	Coen Region	Yambo	Un-named mafic granulite	815276 8208143	1585±3	Igneous crystallization age of precursor to this mafic granulite (Yambo Metamorphic Group)	OZCHRON
112	Georgetown Block	Etheridge	Cobbold Metadolerite near Ironbark	769800 8007400	1656±2	Crystallization age of leucogabbro (Cobbold Metadolerite–Einasleigh Metamorphics)	Black et al. (1998)
113	Georgetown Block	Etheridge	Turpentine Hill	195300 7950100	1553±3	Age of granulite facies metamorphism for mafic granulite (Cobbold Metadolerite–Einasleigh Metamorphics)	Black et al. (1998)
114	Georgetown Block	Etheridge	Stockmans Creek	812515 7943545	1675±3	Crystallization age of precursor to amphibolite (Cobbold Metadolerite–Einasleigh Metamorphics)	Black et al. (1998)
115	Mount Isa Inlier	Mary Kathleen Syncline	Lunch Creek Gabbro	403420 7704873	1740±20	Olivine–pyroxene–biotite pegmatoidal gabbro	Page (1983)
116	Gawler Craton	Yorke Peninsula	Curramulka Gabbronorite	34.627332°S 137.702675°E	1589±5	Gabbronorite intrudes Aagot Member of the Wandearah Formation, intruded by Arthurton Granite of the Hiltaba Suite, and overlain by Winulta Formation	Zang (2003)
117	Gawler Craton	Olympic	Bills Lookout gabbro, east Olympic Dam	~35 km E of Olympic Dam Mine	1764±12	Age of anorthositic gabbro (from DDH BLD1)	Johnson (1993)
118	Gawler Craton	Olympic	Snake Gully microgabbro dike, northeast Olympic Dam	689940 6634800	1596±4	Intrusive age of unaltered and undeformed microgabbro dike that intrudes Donington Suite granite (from DDH SGD4)	Jagodzinski (2005)
119	Gawler Craton	Mount Woods	Leucogabbro, Peculiar Knob North iron ore prospect	538128 6730169	1587±4	Crystallization age of fine-grained, recrystallized leucogabbro (from DDH PK1)	Jagodzinski (2005)

Table 3 (*continued*)

No.	Superprovince	Province/terrane	Formation/location	Co-ordinates[a]	Age (Ma)[b]	Description and comments	Reference
Mafic–ultramafic intrusions							
120	Gawler Craton	Olympic	Altered dolerite, near Olympic Dam mine	681735 6630758	1725	Possible maximum age of dolerite from xenocrystal zircon (from DDH RD160)	Jagodzinski (2005)
121	Gawler Craton	Olympic	Altered mafic–ultramafic dike, near Olympic Dam mine	681641 6629439	1597±4	Crystallization age of zircon, although not clear if zircons are of magmatic, inherited, or hydrothermal origin (from DDH RD1408)	Jagodzinski (2005)
122	Adelaide Geosyncline	Stuart Shelf	Gairdner Dike Swarm, Reedy Lagoon	30°19′S 136°04′E	827±6	U–Pb baddeleyite age of dolerite dike	Wingate et al. (1998)

[a] Locations for most dated samples are shown as Map Grid of Australia (MGA) coordinates using the Geocentric Datum of Australia (GDA1994), or as longitude and latitude co-ordinates. The locations of the komaite and associated rocks from the Yilgarn Craton are shown in Fig. 10.

[b] All ages are U–Pb zircon or baddeleyite ages (unless otherwise stated).

[c] NA=not available.

[d] OZCHRON is Geoscience Australia's national database of geochronologic data.

4.2. Tholeiitic association

Ni–Cu–Co±PGE sulfide mineralization is associated with mafic-dominated intrusions emplaced in rift zones in Archean cratons or Proterozoic orogens. This category has been previously referred to by Marston (1984) and Pratt (1996) as the gabbroid or gabbroic association. The vast majority of the intrusions are derived from the differentiation of tholeiitic basaltic magmas that have experienced variable amounts of crustal contamination. In contrast to komatiite-hosted deposits, the mineralized tholeiitic intrusions are widely distributed throughout the western half of the continent and do not show any preferred geological time period. They range in age from ~2930 Ma to 2890 Ma in the west Pilbara Craton (Radio Hill, Mt Sholl), ~2800 Ma to 2700 Ma in the Yilgarn Craton (Carr Boyd Rocks), ~1865 Ma to 1840 Ma in the Halls Creek Orogen (Sally Malay, Copernicus, Bow River, Corkwood, Keller Creek), to ~1080 Ma in the Musgrave Province (Nebo–Babel, ?Mt Harcus). Similar examples elsewhere (Fig. 6) extend their temporal distribution into the Phanerozoic. Exploration interest has also focused on stratabound PGE–Ni–Cu±Cr layers in large layered tholeiitic mafic–ultramafic intrusions (Munni Munni, Weld Range, Panton) in the Pilbara, Yilgarn, and Gawler cratons, and Arunta, Musgrave, Albany–Fraser, and Halls Creek orogenic zones (Hoatson, 1998).

Type 2A nickel deposits are generally hosted by small- to medium-sized (<3 km thick) sill-like and lopolithic mafic intrusions that may be layered or massive. Production is currently restricted to the Sally Malay and Radio Hill intrusions, but significant resources have also been defined in the Babel, Mt Sholl, and Copernicus prospects (Fig. 9). Deposits are 1 to 5 Mt in size, with Ni grades ranging from 0.5 to 3% and Cu grades up to 2%. Nickel to copper ratios are typically 0.5 to 7. *Type 2B and 2C nickel deposits* that are associated with relatively large layered tholeiitic mafic–ultramafic intrusions are subeconomic, but contain significant amounts of nickel as a by-product of other commodities (e.g., PGEs, Cu, Cr, and Au). For example, the Munni Munni and Panton mafic–ultramafic intrusions have as much contained nickel metal (~50 000 t) as many of the komatiite nickel deposits mined in Australia (Fig. 5) but at much lower grades. *Type 2D* mineralized breccia pipes that have been mined are restricted to the Carr Boyd Rocks Complex in the Eastern Goldfields Province.

4.3. Hydrothermal-remobilized association

Hydrothermal-remobilized nickel sulfide deposits hosted by a variety of igneous and metasedimentary rocks occur throughout Western Australia and western Tasmania (*Type 3 deposits*). Despite their diverse settings and ages, they have the common characteristic of often being hosted by, or spatially near, altered ultramafic rocks. For many of these deposits, nickel was remobilized from the ultramafic rocks during igneous or metamorphic events and redeposited in favorable structural and/or chemical traps. Deposits

range from the local remobilization and physical dislocation of magmatic sulfides (e.g., faulted-breccia ores), through metamorphic–metasomatic replacement (veins proximal to remobilized massive sulfides), to more distal hydrothermal deposits (vein-type ores in metasedimentary and igneous host rocks) that show no spatial association with, or obvious derivation from, ultramafic–mafic igneous rocks (Hoatson and Glaser, 1989). Deposits which highlight these different settings include Avebury in western Tasmania, Sherlock Bay in the west Pilbara Craton, Corkwood and Bow River in the Halls Creek Orogen, Mt Martin in the Yilgarn Craton, and Elizabeth Hill and Bamboo in the Pilbara Craton (Table 2, Fig. 9). Nickel grades (0.1 to 2% Ni) of hydrothermal-remobilized deposits are typically variable, and they contain a variety of associated metals (base and precious metals) that reflect the different compositions of the source rocks and fluids. Relative to the komatiitic and tholeiitic associations, these deposits are of lesser economic significance, with the largest deposits — Avebury and Sherlock Bay— containing ~118 000 t and ~101 000 t of Ni metal, respectively.

5. Australia's nickel sulfide deposits

The following section summarizes the major geological and mineralization features of the nickel sulfide deposit that is considered the type example (in italics) of the various groups of deposits shown in Table 2. The descriptions below are in part derived from the key references shown in parenthesis after each deposit type and the reader is referred to these publications for further information.

5.1. Komatiitic association

5.1.1. Type 1A: Kambalda (Cowden and Roberts, 1990; Dowling and Hill, 1998; Barnes et al., 1999; Lesher and Keays, 2002; Barnes, 2004b; Beresford and Stone, 2004)

Kambalda, in the southern part of the Norseman–Wiluna greenstone belt of the Eastern Goldfields Province, is the type location for type 1A deposits that contain accumulations of massive sulfide ores (>35% sulfides) at the base of thin (typically meters to tens of meters thick) komatiite flows. The importance of this mining district is indicated by several separate deposits in the Kambalda Dome, St. Ives, and Tramways areas having a collective global nickel resource of ~1.39 Mt (42 Mt @ 3.3% Ni). The deposits are spatially associated with the Kambalda Komatiite Formation — a complex ~2700 Ma volcanic–minor sedimentary sequence — that overlies pillowed tholeiitic basalts of the Lunnon Basalt. The mineralized sequence has been multiply deformed, metamorphosed to lower amphibolite facies, and intruded by felsic dikes.

The Kambalda Komatiite displays considerable lateral continuity and systematic variation in rock types and facies up the sequence. Beresford and Stone (2004) describe three to six high-Mg (up to 45% MgO) komatiite flows (25 to 100 m thick) at the base (Silver Lake Member), which transgress upwards to multiple thin (<10 m thick), less magnesian (15 to 35% MgO) spinifex-textured flows at the top of the sequence (Tripod Hill Member). Intercalated thinly laminated sulfidic sediments are restricted to the basal member which is dominated by olivine ortho- and mesocumulates. Lateral variations of stratigraphic units, flow compositions, and distribution of interflow sediments within the Silver Lake Member define lava channel (ore environment) and sheet flow (non-ore environment) facies (Cowden and Roberts, 1990). The mineralized channel facies, which is interpreted to represent the main locus of flow within an active lava flow, consists of a stacked sequence of thick primitive flows and an absence of interflow sediments. The more distal sheet flow facies is characterized by thinner (10 to 20 m) and more evolved flows and thin interflow sediments are common.

The nickel sulfide orebodies are hosted by specific volcanic facies within long linear and anastomosing lava pathways (section C–D in Fig. 11). Lenticular shoots of massive, matrix, and disseminated ores occur at the base of the flows, commonly confined by shallow embayments or depressions in the basal ultramafic–basalt contact of the channel facies (called contact ore), and, more rarely in the overlying flows (hangingwall ore) and in crosscutting structures (off-set ore). The contact massive ores form continuous ribbon-like ore shoots, up to 2500 m long and 300 m wide, or more rarely as equidimensional pods (Fig. 12). They are by far the most economically important ore type constituting more than 80% of the total nickel resources in these deposits. Major minerals in the massive and disseminated ores are pyrrhotite, pentlandite, pyrite, chalcopyrite, magnetite, and chromite, with rare millerite and heazlewoodite generally confined to disseminated ores. Post-magmatic processes (tectonic, metamorphic, intrusive, and weathering events) have also resulted in a spectrum of mineralization types, ranging from dislocation (faulted ores), and more localized mobilization (stringer sulfides), through metamorphic replacement (interpillow–interbreccia sulfides), hydrothermal dissolution and

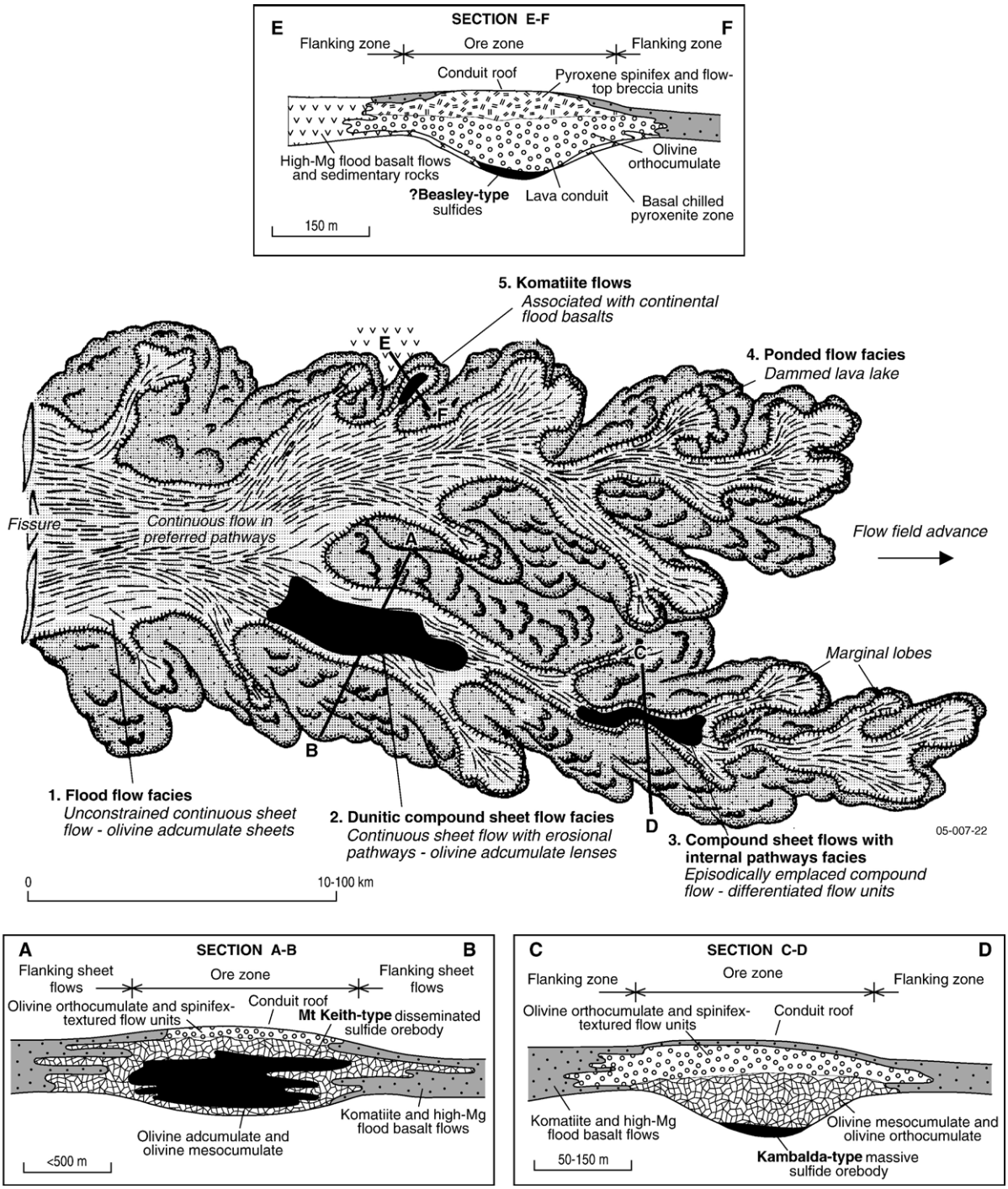

Fig. 11. Schematic section through an inflationary komatiite flow field that developed through sustained eruption of komatiite. The spatial relationships between various komatiite facies and types of nickel mineralization are shown for the Mt Keith — type 1B (section A–B), Kambalda — type 1A (section C–D), and Beasley — type (section E–F) deposits. Modified after Dowling and Hill (1998).

redeposition (vein-type sulfides), to lateritization–oxidation enrichment (supergene sulfides–oxides). The structural controls (e.g., tectonic versus volcanic, assimilation, ground melting) of the Kambalda ores have been reviewed by Stone and Archibald (2004) and Barnes et al. (2004a).

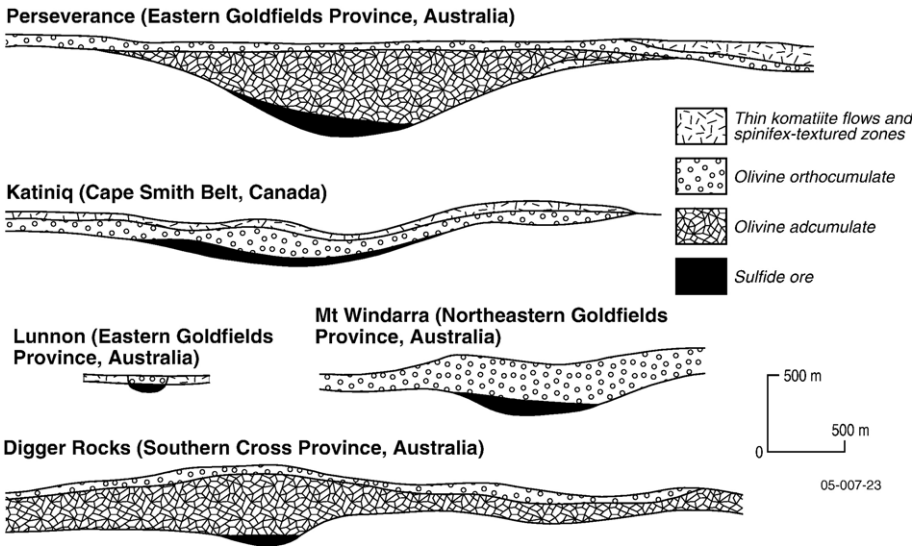

Fig. 12. Distribution of massive sulfide ores along the basal contacts of type 1A komatiitic sequences dominated by olivine cumulates. The sections, drawn to the same scale, also highlight the concentration of sulfides in shallow depressions of the basal contacts, and the different thicknesses of the overlying cumulate units. Modified after Hill et al. (1996).

5.1.2. Type 1B: Mt Keith (Hopf and Head, 1998; Dowling and Hill, 1998; Barnes et al., 1999; Lesher and Keays, 2002; Barnes, 2004b; Beresford and Rosengren, 2004)

The Mt Keith nickel deposit contains one of the largest resources of nickel (600 Mt @ 0.57% Ni; global resource of nickel metal of ~3.4 Mt) that are associated with komatiitic rocks in the world. Located in a narrow section of the Norseman–Wiluna greenstone belt in the northern part of the Eastern Goldfields Province, Mt Keith is the type 1B example of low-grade (0.5–1.5%), large-tonnage disseminated nickel sulfide deposits in the central zones of thick dunitic bodies. These deposits were formerly classified as 'intrusive-dunite associated' (Marston, 1984), 'dunite-hosted deposits' (Donaldson et al., 1986), and 'type 2 deposits' (Dowling and Hill, 1998). Controversy has surrounded their origin for several decades with interpretations ranging from extrusive (i.e., slowly-cooled bodies that are integral parts of the extrusive komatiite stratigraphy: Hill et al., 1996; Barnes et al., 1999), to more intrusive origins involving serpentinized dunite dikes (Burt and Sheppy, 1975), or subvolcanic lava feeder zones or sill-like emplacement into volcanic piles (Rosengren et al., 2005).

The komatiite stratigraphy of the Mt Keith deposit can be correlated for >100 km of strike from the Perseverance deposit in the south to the Honeymoon Well deposit in the north of the greenstone belt (Fig. 9). The 650-m-thick serpentinized host body consists of a basal zone of olivine orthocumulate overlain by a thick zone of barren olivine adcumulate and a thick zone of layered mineralized olivine adcumulate and olivine mesocumulate (MKD5 orebody). This sequence grades laterally and vertically into an upper zone of olivine orthocumulate, spinifex-textured flows, and other minor ultramafic and gabbroic lithologies. The ultramafic host rocks are not depleted in Al and have near-chondritic Al_2O_3/TiO_2 ratios of ~20 and olivine compositions ranging from Fo_{87} to Fo_{94} (S. Barnes, pers. comm.., 2006). Most of the nickel mineralization is confined to the central olivine adcumulate–mesocumulate zone. The sulfides are typically disseminated and layered, with nickel grades ranging from 0.1 to 1.0% and averaging 0.6%. Pyrrhotite, pentlandite, magnetite, pyrite, chalcopyrite, and chromite are the major phases in ores grading more than 1% Ni, whereas millerite, heazlewoodite, godlevskite, and polydymite occur in ores less than 1% Ni. The dominance of pentlandite makes the deposit economically viable, despite the low grades. Supergene minerals commonly include violarite, pyrite, and marcasite. This diverse mineralogy is the result of primary magmatic, secondary hydrothermal, and weathering processes. Nickel enrichment of the sulfides occurred during the re-equilibration of olivine with a residual sulfide-rich melt prior to complete crystallization, and also during the serpentinization of olivine that accompanied greenschist-facies metamorphism.

On the basis of type and distribution of lithologies, igneous textures, and whole-rock geochemistry, Barnes et al. (1999) suggested that the Mt Keith body represents a large lava pathway or lava tube that experienced a

prolonged period of continuous eruption and flow of komatiite lava (section A–B in Fig. 11).

5.2. Other komatiitic deposits

5.2.1. Beasley (AUSQUEST Limited, 2003, 2004)

The Beasley Ni–Cu–PGE prospect, located 50 km west of Tom Price in the Hamersley Basin (Fig. 9), contains mineralized komatiite rocks that are interpreted by company geologists to be comagmatic with late Archean continental flood basalt flows. The ultramafic rocks at the Beasley prospect are intercalated with basaltic and sedimentary rocks of the Late Archean (~2770 Ma) Fortescue Group — an extensive platform sequence on the southern margin of the Pilbara Craton that has been gently folded into broad domal and basinal structures. The mineralized basaltic komatiite sequence is sandwiched between andesitic basalts and gabbroic sills. A typical 150-m-thick flow is shown in section E–F of Fig. 11. Magmatic sulfides are concentrated in serpentinized olivine cumulates within the lowermost komatiite unit. Gossans near the base of an interpreted channel flow facies have unusually low Ni/Cu ratios and elevated PGE concentrations (1.8% Ni, 0.6% Cu, 3.4 g/t Pd, 1 g/t Pt, and 1.1 g/t Au) for komatiitic systems.

5.2.2. Collurabbie (Dundas, 2004; Falcon Minerals Limited, 2004)

In November 2004, WMC Limited (now BHPB) announced a high-grade massive sulfide intersection (5.8 m @ 3% Ni, 2% Cu, 5.3 g/t PGEs) at the Olympia Prospect, Collurabbie (Fig. 9), that highlights the potential of poorly exposed Archean greenstone sequences near the margins of the Yilgarn Craton. This high-value-type of mineralization has not been previously documented in the Yilgarn and it has defined a new metallogenic province in the northern part of the Gerry Well (Duketon) greenstone belt. The Olympia Prospect consists of a parallel series of narrow ribbon-like bands of komatiitic and other ultramafic rocks that steeply dip within a dominantly basaltic sequence. Narrow zones of massive sulfides, often structurally remobilized and containing the highest grades of Ni, Cu, Co, Au, and PGEs, are spatially associated with matrix and disseminated sulfides near the contacts of the ultramafic rocks (Fig. 13). The high abundance of PGEs and low Ni/Cu ratios (<3) are not typical of komatiite-hosted deposits in the Yilgarn Craton, but are features characteristic of the Raglan Ni–PGE komatiite deposit in northern Quebec (average grades 2.7% Ni, 0.8% Cu, and 4 g/t PGEs: Seabrook et al., 2004) and the Kuhmo

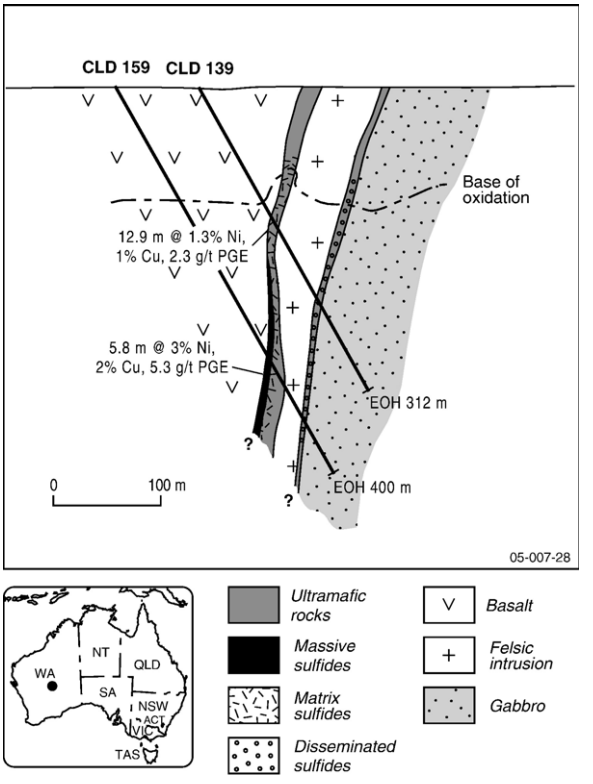

Fig. 13. Diamond drill hole section (looking north) of the Collurabbie Ni–Cu–PGE deposit (Olympia Prospect) in the Northeastern Goldfields Province, Yilgarn Craton. Modified after Falcon Minerals Limited-project presentation, November 2004 (www.falconminerals.com.au).

nickel prospect in eastern Finland (Vulcan Resources Limited, 2005).

High-Mg ultramafic sequences with high metal grades (up to 13.5% Ni, 17.5% Cu, 52 g/t PGEs+Au) occur at the Daltons Ni–Cu–PGE prospect in the southeast Pilbara Craton (Giralia Resources NL, 2004). A narrow basal layer of massive and disseminated sulfides in peridotite and remobilized sulfides in a footwall chert unit have elevated PGEs and low Ni/Cu ratios (<4) similar to the Beasley and Collurabbie–Olympia prospects.

5.3. Tholeiitic association

5.3.1. Type 2A: Radio Hill mafic–ultramafic intrusion (De Angelis et al., 1987, 1988; Hoatson et al., 1992; Frick et al., 2001; Hoatson and Sun, 2002)

The 2892±34 Ma Radio Hill intrusion (Fig. 14) is a small mafic–ultramafic body that contains the most significant known Ni–Cu–Co sulfide resource in the Pilbara Craton. Intermittent phases of exploration since its discovery in the mid-1980s have defined a global

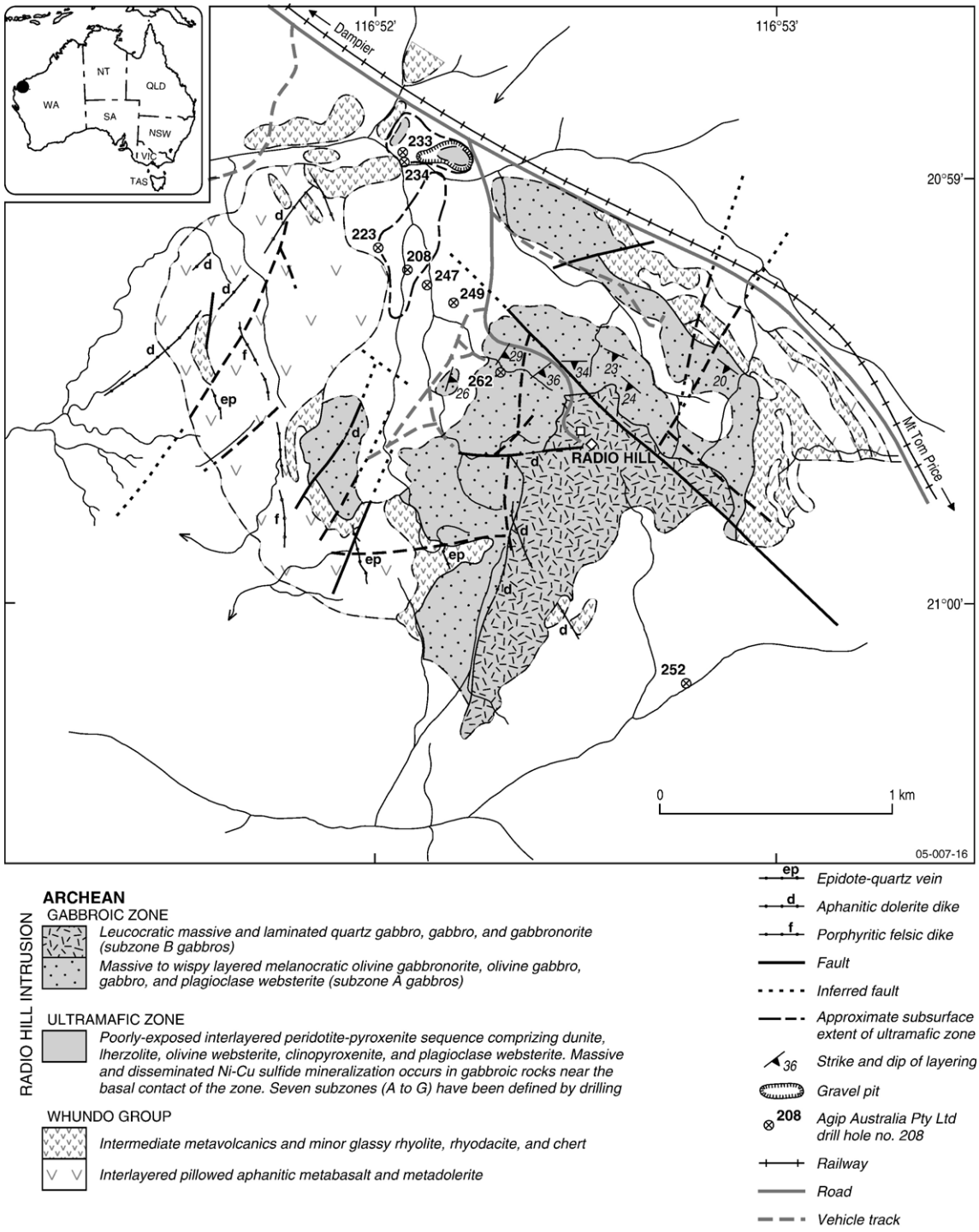

Fig. 14. Geology of the Radio Hill mafic–ultramafic intrusion, west Pilbara Craton. Modified after Hoatson et al. (1992).

nickel metal resource of ~42 000 tonnes (2.8 Mt of ore grading 1.53% Ni). Covering an area of 3.6 km^2, this moderately dipping sheet-like body comprises a 330-m-thick basal ultramafic cumulate zone that is overlain by a 440-m-thick sequence of olivine gabbro, which in turn is truncated by a steeply dipping 430-m-thick quartz gabbro sequence. The poorly-exposed ultramafic zone along the northwestern margin of the

intrusion is dominated by lherzolite, dunite, olivine websterite, clinopyroxenite, and websterite. The overlying gabbroic zone comprises a homogeneous mafic sequence of olivine gabbro and olivine gabbronorite, with the highest exposed stratigraphic level of the intrusion comprising quartz-bearing gabbro and gabbronorite.

Sulfides are largely hosted by thin gabbroic and plagioclase pyroxenite units that persist along the basal contact of the intrusion between the overlying ultramafic cumulates and hornfelsed metavolcanic country rocks. Most mineralization occurs in structural depressions along the basal contact and in a feeder conduit. The confluence of this moderately plunging conduit with the basal contact defines the thickest section of the mineralized host rocks (Fig. 15). Massive, disseminated, and stringer vein pyrrhotite–chalcopyrite–pentlandite–magnetite ores form discrete lenses within the structural depressions, and massive chalcopyrite ores enriched in Au, Pd, Pt, Cu, and Ag are prominent in the feeder conduit. Ultramafic and mafic cumulates throughout the intrusion have sulfur contents ranging up to 2000 ppm indicating that the Radio Hill body formed from magmas that were sulfur saturated.

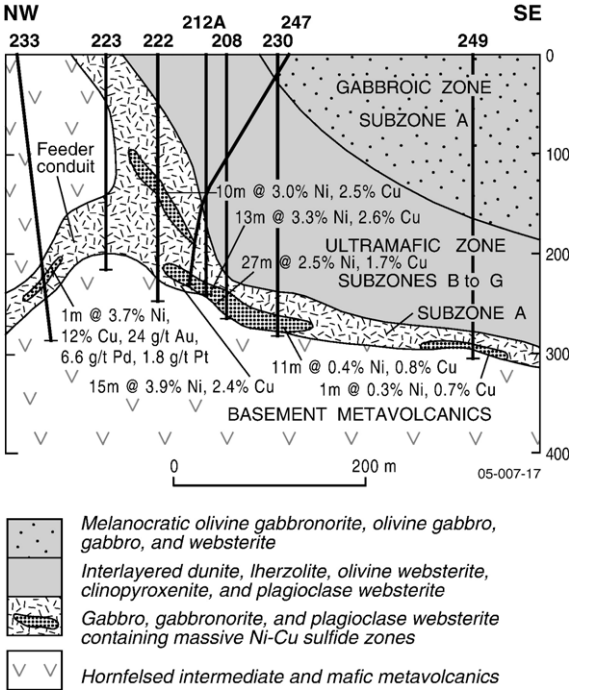

Fig. 15. Diamond drill hole section (looking northeast) of the mineralized basal contact and interpreted feeder conduit of the Radio Hill intrusion. The locations of the drill holes in the section are indicated on Fig. 14. Drill hole data from De Angelis et al. (1987). Modified after Hoatson et al. (1992).

The Radio Hill and nearby Mt Sholl intrusions have very similar mineralization features, namely the mineralized host rocks are predominantly gabbroic units that form thin marginal envelopes to the overlying ultramafic cumulates, and the massive sulfides are concentrated in feeder conduits and in depressions along the basal intrusive contacts beneath the thickest sequence of mafic–ultramafic cumulates. The localization of massive sulfides near the entry point of the feeder conduit to the chamber (analogous to Voisey's Bay, Canada) indicates that the dynamics of magma flow (e.g., rate and turbulence of magma), feeder-chamber geometry (e.g., changes from narrow vertical conduits to broad open magma chambers) and physical traps were important for the accumulation of the sulfides. Very similar spatial relationships of massive ores to feeder conduits are also seen in the Sally Malay (Hoatson et al., 1997) and Nebo–Babel (Figs. 16 and 17; Dundas, 2004; Seat et al., 2005) deposits.

In contrast to the single-chambered Radio Hill intrusion, the Sally Malay intrusion in the Halls Creek Orogen consists of an array of ovoid-shaped chambers that are detached or interconnected by narrow feeder zones and dikes. The Nebo–Babel Ni–Cu–Co–PGE prospects south of the Jameson Range intrusion in the west Musgrave Province contains the largest nickel resource hosted by a mafic intrusion in Australia. Dundas (2004) indicated a preliminary contained metal inventory at Babel of ~1 Mt Ni, ~1 Mt Cu, @ ~0.47% Ni equivalent, with additional PGE and Co credits. High-grade mineralization at Nebo appears not to be continuous and a formal resource estimate is not yet available. The two prospects, which are part of the same mineralizing system, are offset ~1.5 km from each other by an east–west trending fault. Massive sulfides (Nebo) and disseminated sulfides (Babel) occur in a gabbronorite-dominated tube-like feeder conduit that intruded granulite facies granitic gneiss and mafic country rocks. The moderately plunging conduit has a cross-section size of 0.5 by 1 km. Breccia zones near the upper contact of the conduit contain sulfide-bearing fragments, country rock fragments, and variably-textured gabbronorite (Seat et al., 2005; Pirajno et al., in press).

5.4. Other tholeiitic deposits

5.4.1. Type 2B: Munni Munni mafic–ultramafic intrusion (Donaldson, 1974; Hoatson and Keays, 1989; Barnes et al., 1992; Hoatson et al., 1992; Barnes and Hoatson, 1994; Hoatson and Sun, 2002)

The 2925 Ma Munni Munni intrusion (Fig. 18) in the west Pilbara Craton contains the largest resource of PGEs

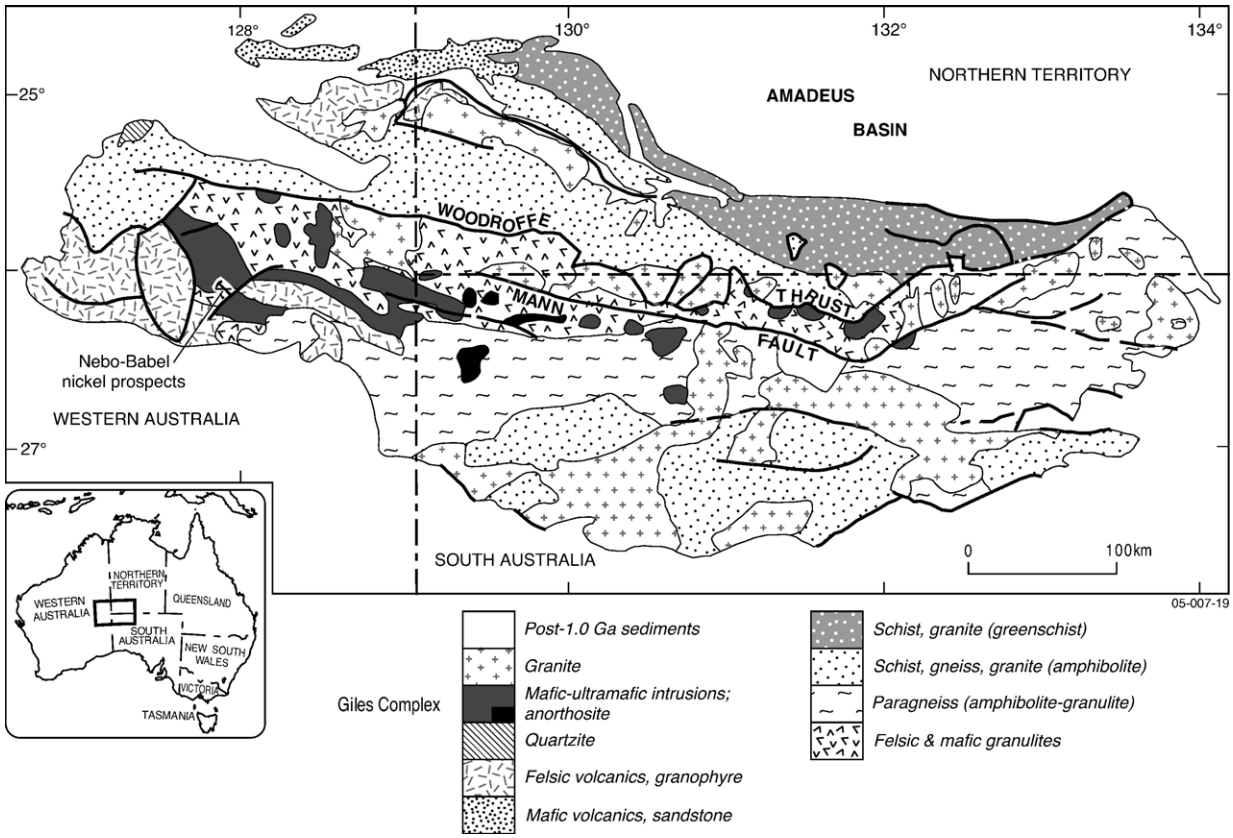

Fig. 16. Generalized regional geology of the Musgrave Province, central Australia. The Proterozoic mafic–ultramafic intrusions of the Giles Complex (highlighted) represent one of the largest intrusive igneous associations in Australia. The location of the Nebo–Babel Ni–Cu prospect is shown south of the large Jameson Range intrusion in the west Musgraves. Modifed after Glikson et al. (1996).

and a small nickel resource (24 Mt @ 2.9 g/t Pt+Pd+Au, 0.3% Cu, and 0.2% Ni: Helix Resources Ltd, 2004) associated with a layered intrusion in Australia. The large size of the intrusion, its Precambrian age, tholeiitic fractionation trends, and the presence of a distinctive porphyritic plagioclase websterite layer at the contact between the ultramafic and overlying gabbroic zones indicated there was considerable potential for stratabound PGE–Cu–Ni mineralization of Merensky Reef-type (Hoatson, 1984). The intrusion is a 5.5-km-thick elongated body interpreted to be a slightly asymmetric boat-like structure plunging moderately to the south–southwest (Fig. 18). The lower 1.85-km-thick ultramafic zone comprises macrorhythmic cycles of olivine and olivine–clinopyroxene mesocumulates and adcumulates, and the overlying 3.6-km-thick gabbroic zone consists largely of intergranular gabbronorite, magnetite gabbro, and granophyric gabbro. The upper part of the ultramafic zone contains a distinctive 30- to 80-m-thick orthocumulate layer referred to as the porphyritic websterite layer (PWL: Figs. 18 and 19). Persistent PGE mineralization associated with disseminated chalcopyrite, pentlandite, and pyrrhotite (up to 2 vol.%) occurs along the exposed 22 km strike extent of the PWL. Hoatson and Keays (1989) proposed that the PGE mineralization resulted from the combined processes of crystal fractionation, and mixing of sulfur-undersaturated, PGE-bearing magnesian magma with more evolved sulfur-saturated tholeiitic mafic magma.

5.4.2. Type 2C: Panton mafic–ultramafic intrusion (Hamlyn and Keays, 1979; Hamlyn, 1980; Perring and Vogt, 1991; Hoatson and Blake, 2000)

The 1856±2 Ma Panton mafic–ultramafic intrusion (Fig. 20) in the Halls Creek Orogen is one of the most intensively explored intrusions in Australia. Platinum Australia Limited (2005) have defined a resource of 14.3 Mt @ 2.19 g/t Pt, 2.39 g/t Pd, 0.27% Ni, 0.31 g/t Au, and 0.07% Cu (with a nickel resource of 33.6 Mt @ 0.16% Ni, i.e., 54 000 t) in PGE–Ni–bearing stratabound chromitite layers. The well layered intrusion forms a steep-sided asymmetric syncline, 10.5 km long by

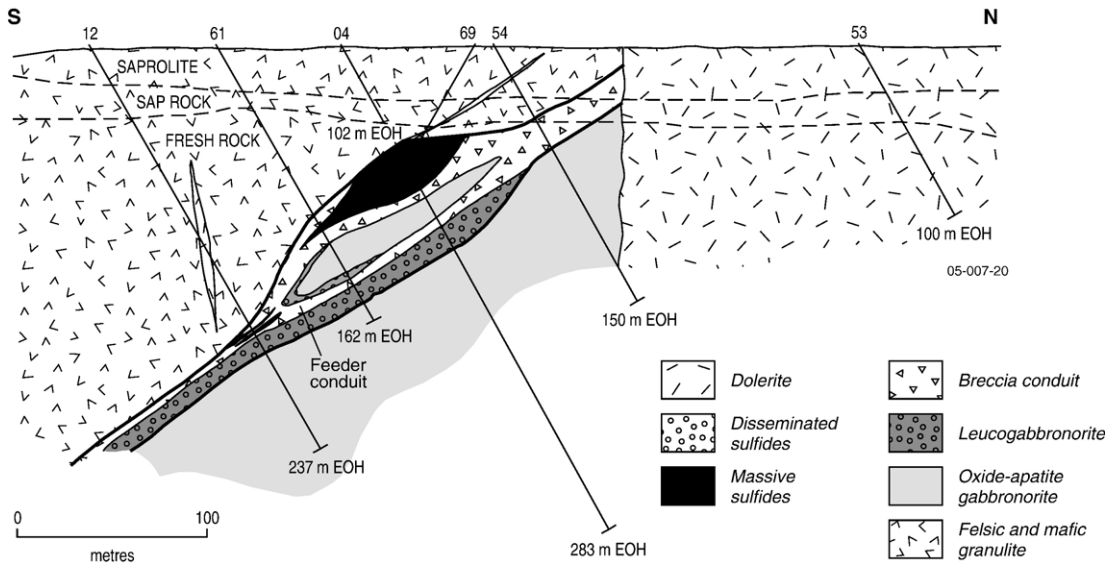

Fig. 17. Diamond drill hole section (looking west) of the interpreted mineralized feeder conduit at the Nebo deposit. Reproduced with permission from J. Hronsky (previously WMC Resources Ltd) from a presentation (Geological setting of Ni–Cu–PGE mineralization at the west Musgrave) at Mining and Exploration Group of Western Australia Meeting, Perth, January 2003 (unpublished).

2.5 km wide, which plunges moderately towards the southwest. Cyclic units of dunite, lherzolite, and chromitite characterize the lower 650-m-thick Ultramafic Series, and gabbro, gabbronorite, norite, ferrogabbro, and anorthosite are the dominant rock types of the 900-m-thick Gabbroic Series. Chromitite layers occur at three major stratigraphic levels in the intrusion, notably: (1) as thin (<10 cm) lenses in harzburgite and dunite in the basal part of the Ultramafic Series; (2) as economically important dunite-hosted PGE-enriched layers up to 2.4 m thick, 120 to 150 m below the contact of the Ultramafic and Gabbroic Series; and (3) as thin (0.3 m) fractured layers in dunite lenses in the Gabbroic Series. The PGE-enriched chromitites contain sperrylite, palladium sulfides, tellurides, bismuthinides, pyrite, pyrrhotite, chalcopyrite, bornite, covellite, and the main nickel mineral is pentlandite. High sulfur contents of most ultramafic (300 to 1750 ppm) and gabbroic (340 to 920 ppm) cumulates testify to sulfur-saturated conditions which were probably induced by repeated mixing events between the slightly evolved resident magma and influxes of hotter more primitive magma.

5.4.3. Type 2D: Carr Boyd Rocks (Purvis et al., 1972; Marston, 1984; Ahmat, 1993; Groenewald et al., 2000)

The Carr Boyd Rocks intrusion is the only layered tholeiitic mafic body in the Eastern Goldfields Province known to host significant Ni–Cu mineralization (~1 Mt @ 1.2% Ni, 0.6% Cu). The lobate-shaped intrusion is composed of magmatic cycles of basal dunite, peridotite, harzburgite, troctolite, olivine norite, olivine anorthosite, norite, and gabbro, with the layered cyclic sequence forming a broad concentric belt parallel to the margins of the complex. Ni–Cu sulfide ores occur in steep, west-plunging bronzite pegmatoids and sulfide-bearing pegmatoids that are discordant to the mafic–ultramafic stratigraphy and are interpreted as intrusive breccia pipes developed late in the crystallization history of the complex. Remobilized sulfides also occur along the basal contact of the intrusion. The mineralized pipes occur in an 800-m-wide ENE-trending zone within the upper mafic unit of the intrusion. Individual pipes are 20 to 60 m across and at least 300 m long. They contain massive and disseminated sulfides (up to 30% pyrrhotite, pentlandite, chalcopyrite, pyrite) and have a bulk Ni/Cu ratio of 3, which is similar to other tholeiitic-associated nickel deposits shown in Table 2. Purvis et al. (1972) interpreted the orebodies and bronzitite pipes to have formed from liquids derived from the mafic–ultramafic stratigraphy. The pipes also have potential for PGE-sulfide and/or Pt–Fe alloy mineralization similar to the high-grade pegmatoidal dunite pipes of the Bushveld Complex (Scoon and Mitchell, 2004).

5.5. Hydrothermal-remobilized association

5.5.1. Type 3A: Avebury (Newnham, 2003; Morrison et al., 2003; Howland-Rose, 2005)

The Avebury nickel deposit (Fig. 21), discovered in 1998 near Zeehan, western Tasmania, is an unusual style

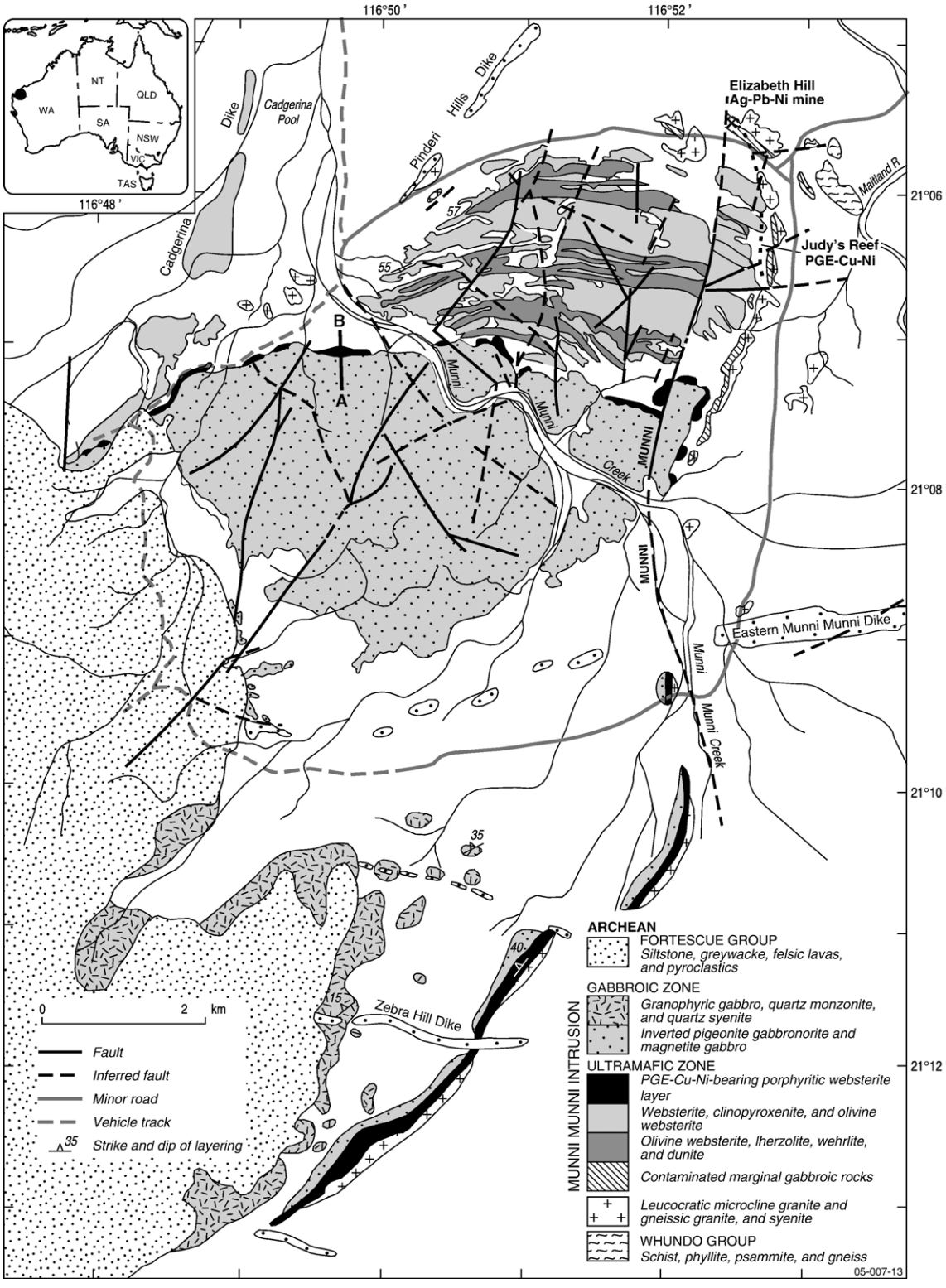

Fig. 18. Geology of the Munni Munni intrusion, west Pilbara Craton. The locations of the PGE-enriched porphyritic websterite layer at the contact between the ultramafic and gabbroic zones, Judy's Reef (PGE–Cu–Ni) on the northeastern margin of the intrusion, and nearby Elizabeth Hill Ag–Pb–Ni mine are shown. The drill hole section A–B is shown on Fig. 19. Modified after Hoatson and Sun (2002).

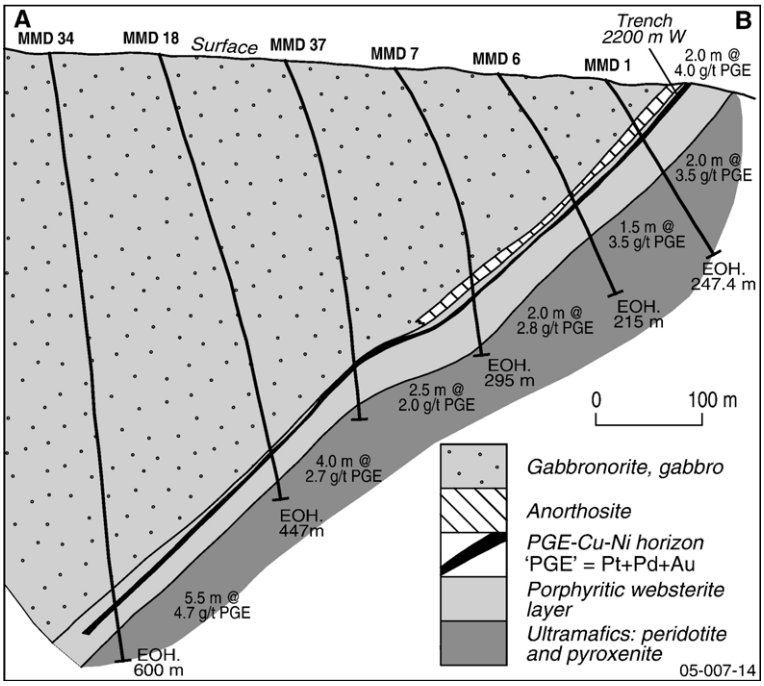

Fig. 19. Diamond drill hole section (looking west) of the PGE-enriched porphyritic websterite layer and associated rocks at the ultramafic–gabbroic zone contact in the Munni Munni intrusion. The location of the drill hole section A–B is shown on Fig. 18.

of nickel sulfide mineralization in a new nickel metallogenic province. Drilling has defined some of the thickest mineralized sections (48 m true width @ 1.7% Ni: Allegiance Mining NL, 2005) reported in Australia in recent years. The current resource of 11.59 Mt @ 1.02% Ni has considerable potential for expansion with production planned to commence in 2007.

The Avebury deposit occurs in a Cambrian sequence of sediments, mafic volcanics, and ultramafic flows or intrusives that were intensely altered during the intrusion of the 360 Ma (Black et al., 2005) Heemskirk Granite. This large granite body appears to have provided the heat and/or fluids for the remobilization of nickel, which was subsequently redeposited in structural trap sites around the margins of an intensely serpentinized 'anticlinal' ultramafic body. The sulfur-poor and iron-rich mineralizing system produced a coarse-grained assemblage of pentlandite and magnetite, with minor pyrrhotite, pyrite, and nickel arsenides. A distinctive feature of the deposit is that it is devoid of Cu, Au, and PGEs.

The Avebury deposit has not been properly characterized yet, but it displays similarities to a hydrothermally modified magmatic sulfide deposit spatially associated with serpentinized ultramafic rocks. Detailed mineralogical studies are required to assess the true origin (magmatic, hydrothermal, skarn) of this unusual deposit.

Other prospects associated with mafic–ultramafic rocks near Avebury contain different metal associations (e.g., Burbank Ni–Zn, Melba Flats Ni–Cu–Co–Pt–Pd–Au) that highlight the diversity of nickel mineralization in the Zeehan region.

5.5.2. Type 3B: Sherlock Bay (Miller and Smith, 1975; Marston, 1984; Ruddock, 1999; Hoatson and Sun, 2002; Sherlock Bay Nickel Corporation Limited, 2005)

The Sherlock Bay Ni–Cu deposit is located on the Sholl Shear Zone — a major regional strike-slip fault that traverses the northwestern margin of the Caines Well Granitoid Complex in the west Pilbara Craton. This unusual covered deposit consists of remobilized base-metal sulfides spatially associated with mafic to felsic volcanics, metasedimentary rocks, and mafic–ultramafic intrusives. The mineralized horizon is a steeply-dipping banded quartz–magnetite–amphibole schist (also referred to as a siliceous banded iron formation or amphibole-bearing chert). Several small elongated bodies of serpentinized peridotite and talc–chlorite–calcite rock are spatially associated with the mineralized schist adjacent to the Caines Well Granitoid Complex. The deposit is at least 1.6 km long, has an average width of 24 m, and contains an estimated

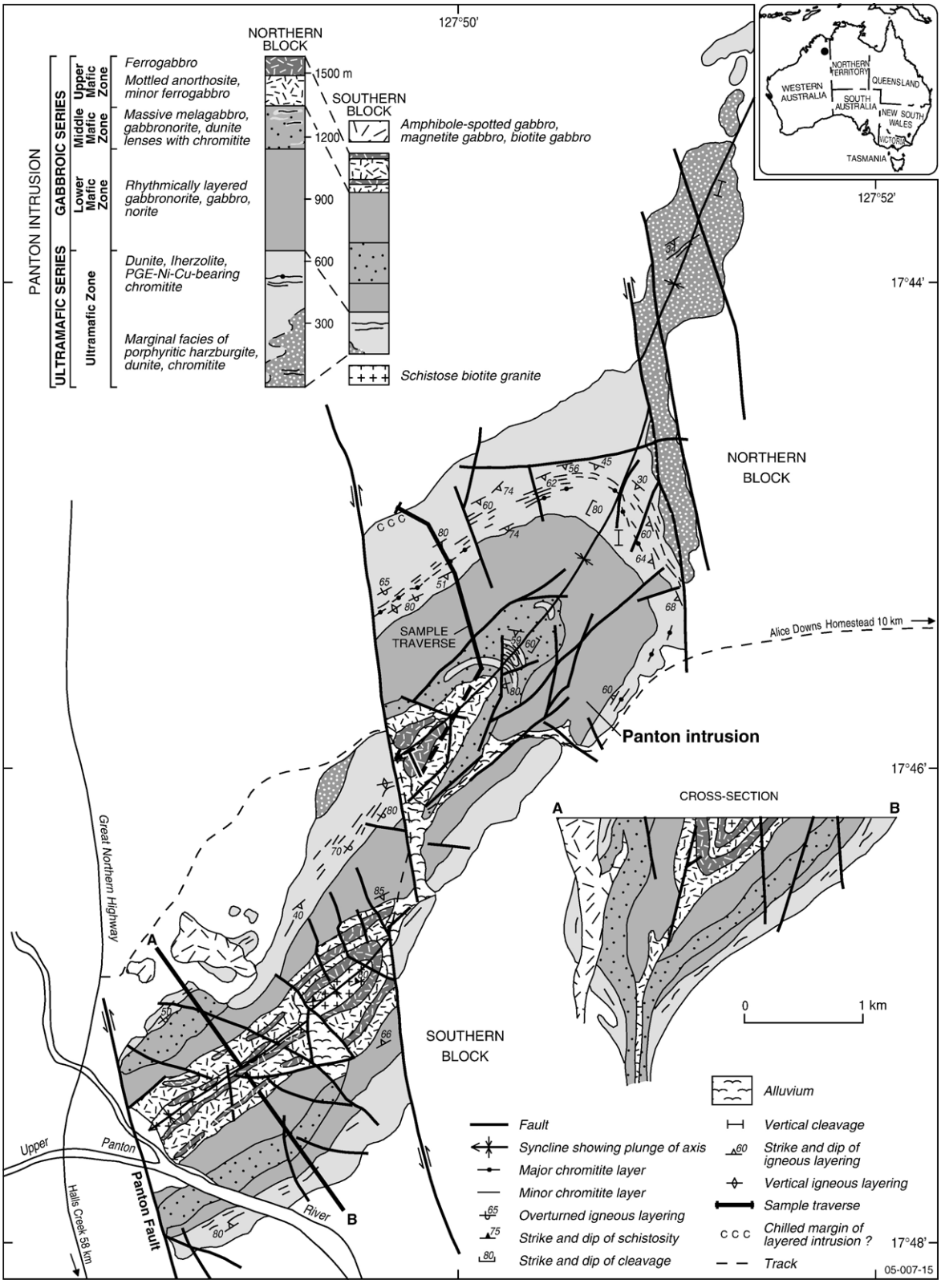

Fig. 20. Geological map and schematic cross section of the Panton mafic–ultramafic intrusion, Halls Creek Orogen, East Kimberleys. Modified after Hoatson and Blake (2000).

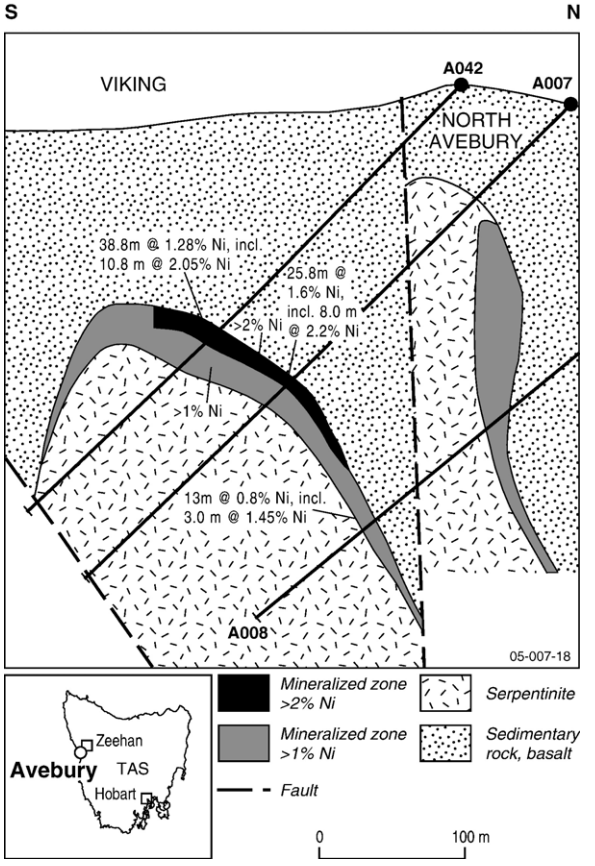

Fig. 21. Diamond drill hole section (looking west) of the Avebury deposit, Dundas Trough, west Tasmania. Modified from Allegiance Mining NL (2002).

resource of 25.4 Mt @ 0.40% Ni and 0.1% Cu (Sherlock Bay Nickel Corporation Limited, 2005). Miller and Smith (1975) documented nickel depletion and erratic Ni/Cu ratios in some of the ultramafic bodies associated with the mineralized schist. They interpreted the mineralization to be fracture-controlled vein-filling with the Ni and Cu derived from the nearby altered ultramafic rocks. However, Marston (1984) proposed a hydrothermal volcanic–exhalative origin for the deposit.

5.6. Other hydrothermal-remobilized deposits

5.6.1. Elizabeth Hill (De Angelis et al., 1988; Barnes, 1995; Marshall, 2000; Hoatson and Sun, 2002)

The abandoned Elizabeth Hill Ag–Pb–Ni mine is a small high-grade, structurally controlled hydrothermal vein deposit in the west Pilbara Craton that was briefly mined from 1999 to 2000. The polymetallic deposit occurs on the northern basal contact of the Munni Munni intrusion where the north-trending Munni Munni Fault cuts ultramafic rocks of the intrusion and granitic rocks (Fig. 18). Mineralized calcite–quartz breccia veins contain spectacular Ag grades (up to 16% Ag) and anomalous concentrations of Pb, Ni, Pd, Cu, Au, Ti, Ba, and Mo.

5.6.2. Corkwood (Barnes, 1994; Sanders, 1999; Hoatson and Blake, 2000)

The Corkwood Ni–Cu prospect is a small metagabbro-hosted deposit (~0.2 Mt @ 0.65% Ni, 0.24% Cu, 0.03% Co) located in a narrow north–northeast-striking zone of high-grade Tickalara Metamorphics in the Halls Creek Orogen, East Kimberleys. The 200-m-thick metagabbroic body forms a steeply dipping lenticular mafic body that is concordant with the country rocks. Recrystallization and mineralogical features are indicative of transitional amphibolite to granulite facies metamorphism, similar to other mineralized granulite intrusions in the Tickalara Metamorphics (Bow River, Norton, Keller Creek). The distribution of narrow bands of sulfides distant from the intrusive margins of the host body and their preference for the less deformed rocks implies metamorphic remobilization of the sulfides into low-strain regions.

5.6.3. Mt Martin (Marston, 1984; Harrison, 1990)

Hydrothermal nickel mineralization is associated with anomalous gold grades at Mt Martin, north of Kambalda (Fig. 9). The vein-type deposit (72 000 t @ 2% Ni) occurs in a strongly deformed and sheared zone containing intercalated layered and foliated pelitic to siliceous metasediments and lenticular ultramafic units. The mineralized quartz–carbonate–arsenide veins contain pyrite, pyrrhotite, pentlandite, chalcopyrite, arsenopyrite, gersdorffite, niccolite, ullmanite, minor tellurides, and rare free gold. Marston (1984) considered the deposit to be of late metamorphic–hydrothermal origin as carbonate metasomatism, which is associated with the mineralizing event, apparently followed the peak of regional metamorphism.

6. Discussion and exploration implications

6.1. Metal endowment of komatiitic– and tholeiitic–magmatic systems: fertile versus barren

World-class Ni–Cu±PGE sulfide deposits are rare and many recent studies have examined the question ‘what gives magma ore potential?’ Naldrett (2002) proposed that the essential ingredients for the formation of world-class Ni–Cu±PGE sulfide deposits are: large magmatic systems involving nickel-bearing magma(s), source of sulfur in rocks traversed by the magma close to its point of

final emplacement, reaction with country rocks, and focused magma flow in feeder conduits. Similarly, Arndt et al. (2005) suggested that some of the most important petrogenetic controls include (1) the abundance of ore metals in the magma, (2) the sulfide saturation status of the magma, and (3) the capacity of the magma to interact with other rocks (e.g., temperature, viscosity, volatile content, dynamics of magma emplacement, nature of wall rocks). In this respect, hot, low-viscosity primitive komatiite and tholeiitic picrite have more potential for forming Ni–Cu±PGE sulfide deposits than relative colder, volatile-rich alkali picrite and basalt.

The following discussion examines some of the more important parameters that are thought to influence the fertility of komatiitic– and tholeiitic–magmatic systems.

6.1.1. Komatiitic–magmatic systems

A comparison of global resources of nickel in the major komatiite provinces of the world reveals significant differences in nickel endowment (Fig. 8c and Table 4). For example, the Eastern Goldfields Province accounts for approximately 63% of the world's total nickel sulfide resources (see Tables 1 and 4), which is almost twice the collective nickel resources of the Abitibi, Thompson, Cape Smith, Southern Cross, and Zimbabwe greenstone provinces. It is not clear if these differences in nickel endowment are due to processes at a global (mantle), regional (geodynamic setting), or more local (volcanic architecture, magma composition or volume, type of country rocks) scale, or a combination of these factors. Despite controversy surrounding the genesis of komatiite-associated nickel sulfide deposits (see Lesher and Keays, 2002), there is some consensus about two significant petrogenetic aspects of these deposits: firstly, komatiitic magmas are derived from high-degrees of partial melting of mantle material and arrive at the eruptive site undersaturated in sulfur; and secondly, physical and chemical assimilation of sulfur-bearing substrate (ground melting or substrate erosion) initiates sulfur saturation and the precipitation of nickel sulfides (see Barnes et al., 2004a).

Lithogeochemistry of komatiites has been found to be useful in distinguishing between fertile and barren sequences by helping to identify favorable volcanic environments, and more directly through the geochemical characterization of crustal contamination and sulfur-saturation processes (Barnes et al., 2004a). According to these authors, favorable volcanic environments, such as those containing large-volume lava pathways, can be identified on the basis of the distribution and ratios of whole-rock Mg, Fe, Ni, Cr, and Ti abundances. Crustal contamination can be indicated by enriched abundances and abundance ratios of strongly to weakly incompatible lithophile elements in fractionated lavas, but the effects of metamorphism and alteration on the sequences are often significant and may be misleading. Lesher et al. (2001) have also discriminated between komatiites generated from normal igneous crystallization processes (barren) and those that were formed during ore-forming processes (fertile) by identifying geochemical and isotopic signatures typical of crustal contamination (e.g., Th–U–LREE enrichment, negative Nb–Ta–Ti anomalies) and/or sulfide segregation (e.g., Ni–Cu–Co–PGE depletion).

Recent studies have shown relationships between the fertility, the age of emplacement and the geochemical type of the komatiites (Perring et al., 1996; Arndt et al., 1997; Lesher et al., 2001; Ferreira Filho and Lesher, 2001; Lesher and Keays, 2002; Barnes et al., 2004a; Maier, 2004; this study). It has been suggested that fertile komatiites were emplaced in the late Archean (~2700 Ma) as part of a global metallogenic event (Fig. 6 and Table 4; see Section 6.2). The relatively older komatiites (>~2900 Ma) in the Yilgarn (Southern Cross Province), Pilbara, and Aldan (Siberia) cratons, and in the Barberton Belt are less fertile or even barren. It is possible that this increase in the fertility of the late Archean komatiites is related to changes in the composition or physical characteristics of the mantle source, but the evidence (e.g., Nd isotopes) for this is ambiguous (Arndt et al., 1997). According to Maier (2004), the apparent infertility of the older (~3500 to 3200 Ma) South African komatiite sequences may be due to the lower sulfide content of the older Archean (meta) sedimentary substrate.

Table 4 shows that fertile komatiitic provinces are dominated by late Archean, Al-undepleted komatiites (AUDK) or 'Munro-type' komatiites. Their Al_2O_3/TiO_2 ratios vary between 15 and 25 and they are typically depleted in incompatible trace elements. The less fertile and older (>~2900 Ma) komatiites in the Yilgarn (Southern Cross Province), Pilbara and Aldan cratons, and in the Barberton and Crixás (Brazil) belts are dominated by Al-depleted komatiites (ADK) or 'Barberton-types', with Al_2O_3/TiO_2 ratios of <15 and enrichment of the more incompatible elements.

Based on the Sm/Nd ratios and the concentrations of the incompatible elements, Arndt et al. (1997) suggested that the 'Barberton-type' komatiitic magmas were probably generated from relatively low degrees of partial melting at greater depths and higher temperatures. The fertile 'Munro-type' magmas, on the other hand, were either formed from higher degrees of partial melting at shallower depths and lower temperatures, or from dynamic melting

Table 4
Significant features of fertile and barren komatiitic provinces

Feature	Eastern Goldfields Province, Australia	Thompson Belt, Canada	Abitibi Belt, Canada	Cape Smith Belt, Canada	Zimbabwe Craton, Zimbabwe	Southern Cross Province, Australia	Crixás Belt, Brazil	Pilbara Craton, Australia	Barberton Belt, South Africa	Gawler Craton, Australia
Global resources of nickel metal (Mt)	11.89 (63%)	4.22 (22%)	1.09 (6%)	0.73 (4%)	0.51 (3%)	0.44 (2%)	No significant resources	No significant resources	No significant resources	No known resources
Classification of deposits (see Table 2)	1A, 1B	?1A	1A, 1B	1A, 1B	1A, 1B	1A, 1B	?1A	?1A	?1A/3B	No known deposits
Type deposit(s)/ prospect(s)	Kambalda, Mt Keith	Thompson, Bowden	Dumont, Shebandowan	Raglan, Expo-Ungava	Hunter's Road, Shangani	Maggie Hays, Emily Ann	Boa Vista	Ruth Well, Beasley	Bon Accord	Lake Harris, ?Mt Hope
Approximate age (Ma)	2700	1880	2710	1920	2700	2900–3000	2800	2880 to < 3460	3500	2520
Geodynamic setting	Plume-related extensional basin, rift (possibly back-arc)	Plume-related rifted continental margin	Plume-related extension with adjacent volcanic arc, rift	?Plume-related continental margin, rift	Plume-related rifting (possibly back-arc)	Plume-related extensional basin, rift	Plume-related extensional basin, rift	Plume-related extension, rift	Plume-related oceanic plateau/ ridge, rift	Plume-related extension, rift
Magma composition (AUDK or ADK) [a]	AUDK, ADK	AUDK	AUDK, ADK	AUDK	AUDK	ADK, AUDK	ADK	ADK	ADK	ADK
Dominant volcanic facies [b]	CSF, DCFS	?	CSF	?CSF, LLLS	TDF, ?CSF	TDF, CSF	?	?LLLS	TDF	LLLS, TDF
Basement rocks	Felsic and mafic volcanics, sulfidic shale, chert	Graphitic units, sulfide- and silicate-facies iron formation, pillowed basalt	Felsic volcanics, sulfide-facies iron formation	Gabbro, shale, slate, high-Mg basalt	Sulfide-bearing felsic units, silicate-facies iron formation	Volcaniclastics, oxide-facies iron formation	Iron formation, mafic units	Felsic volcanics; sulfide-facies iron formation	Silicified volcaniclastic, chert, schist, conglomerate, serpentinite	Granite, orthogneiss, paragneiss, iron formation
Intensity of deformation and/or remobilization	Moderate to high	High	Moderate	Moderate	Moderate to high	Moderate	Moderate	Moderate	Moderate	Moderate
					Increasing metal endowment (fertility) of provinces					

Data from: Anhaeusser and Maske (1986); Naldrett (1989, 1997, 2002); Parrish (1989); Eckstrand (1995); Eckstrand et al. (2003); Ernst and Buchan (2001); Ferreira Filho and Lesher (2001); Meisel et al. (2001); Ayer et al. (2002); Lesher and Keays (2002); Barnes et al. (2004a,b); Hoatson et al. (2005b); Hulbert et al. (2005); this study; and references cited within these publications.

[a] AUDK ($Al_2O_3/TiO_2 = 15–25$): aluminium-undepleted komatiite (Munro-type); ADK ($Al_2O_3/TiO_2 < 15$): aluminium-depleted komatiite (Barberton-type). Where both types are present, the dominant chemical type is shown first.

[b] TDF: thin differentiated flows; CSF: compound sheet flows with internal pathways; DCSF: dunitic compound sheet flows; LLLS: layered lava lakes and/or sills (Barnes et al. 2004a,b).

processes in which low-degree partial melts were progressively extracted leaving an ever more refractory material. This could mean that the 'Barberton-type' magmas were initially sulfur saturated and hence reached the site of eruption depleted in the chalcophilic elements Ni, Cu, and the PGEs. In contrast, the fertile 'Munro-type' magmas would be progressively sulfur undersaturated because of batch melting processes and arrive at the site of eruption with enriched metal abundances. However, nickel concentrations of the two major types of komatiitic magmas do not show any significant differences that could indicate saturation levels with respect to sulfur in the initial magmas (Arndt et al., 1997).

Cassidy et al. (2005) have described similar scenarios for the petrogenesis of komatiites from the Yilgarn Craton to that of the 'Barberton-' and 'Munro-type' komatiites. They suggest that the Al-depleted komatiites of the Yilgarn Craton reflect high-pressure melting of undepleted mantle, possibly during the rise and stalling of a mantle plume against the base of a thick continental lithosphere mantle. In contrast, the more prospective Al-undepleted komatiites, typical of the Eastern Goldfields Province, may indicate limited or thinned lithospheric mantle as they are sourced from high degrees of melting of depleted mantle at moderate pressures.

Another critical factor that may control the fertility of komatiitic magmas at the site of eruption is the composition of the substrate that may be assimilated through thermal erosion. Such assimilation would lead to cooling of the magma, an increase in silica concentration, and the crystallization of olivine causing a decrease in the solubility of sulfur in the magma leading to sulfur saturation. A major difference between the contrasting nickel endowments of the Southern Cross and Eastern Goldfields provinces may be related to the chemical composition of the substrate (Table 4). According to Groves and Batt (1984), the relatively less-fertile komatiites in the Southern Cross Province belong to the so-called platform-type greenstones, formed in a shallow-water environment under conditions of low-crustal extension dominated by shallow-water volcaniclastics and/or oxide-facies iron formations. The more fertile komatiites of the Eastern Goldfields Provinces, on the other hand, are suggested to represent rift-phase greenstones formed in relatively deep-water environments under conditions of high-crustal extension. Such environments contain abundant sulfidic shales and/or cherts (Perring et al., 1996), the assimilation of which would facilitate rapid sulfur saturation. The fertile komatiites in the Abitibi Belt have been interpreted as part of rift-phase greenstones, and those in the Proterozoic Thompson Belt inferred to have formed on a rifted-continental margin that contained abundant graphitic-sulfide-bearing units and silicate-facies iron formations (Bleeker and Macek, 1996).

Most komatiite-associated deposits have undergone variable degrees of deformation, metamorphism, and remobilization of nickel sulfides. In some cases massive sulfides are remobilized on a scale from centimeters to several tens of meters (Lesher, 1989; Prendergast, 2003). Apart from causing modification of original textures, deformation and metamorphism can lead to stress-induced diffusion of Cu, PGEs and S (Lesher, 1989). The remobilization of sulfides related to partitioning of strain in deformed mafic–ultramafic bodies can have important implications (e.g., upgrading of metal contents/ratios, thickening of orebodies) for the economics of a deposit. Intensive remobilization of sulfides also characterizes the Paleoproterozoic nickel deposits of the Thompson Belt, Canada. The Thompson, Birchtree, and Pipe II deposits formed when ultramafic sills intruded various graphitic units and sulfide-facies iron formations. Most of the remobilization of massive sulfide ores occurred during deformation and metamorphism of the original host horizon and within some veins that filled late faults and tension gashes (Bleeker and Macek, 1996). However, in the large Thompson deposit, the massive sulfides are accompanied by significant amounts of Ni-enriched sedimentary sulfides. These sulfides formed through extensive redistribution (by fluids) of nickel (and PGEs) during high-grade metamorphism of the massive sulfides and also during serpentinization of the ultramafic rocks (Bleeker and Macek, 1996). Formation of nickel sulfide deposits by aqueous solution migration of nickel during upper amphibolite facies metamorphism of serpentinite bodies has also been proposed (Juhas, 1995).

The presence of relatively larger deposits (in terms of global resources of nickel metal) in the Thompson Nickel Belt compared to the more nickel-endowed Eastern Goldfields Province is reflected in the cumulative frequency diagram (Fig. 22). The curves show that, although the total nickel endowment of the Thompson Nickel Belt is less than half (and has fewer deposits) than that of the Eastern Goldfields Province, the former province contains relatively larger deposits, thereby shifting the curve to higher nickel-resource values. A possible mechanism for this distribution of deposits is that intense deformation resulted in the generation of larger (and fewer) deposits by tectonic-fluid remobilization of the smaller deposits in the belt. The contrasting endowment curves may also reflect differences between those deposits which are mainly intrusion-related (Thompson) from those which form in a volcanic environment (Eastern Goldfields). The curves for the Abitibi

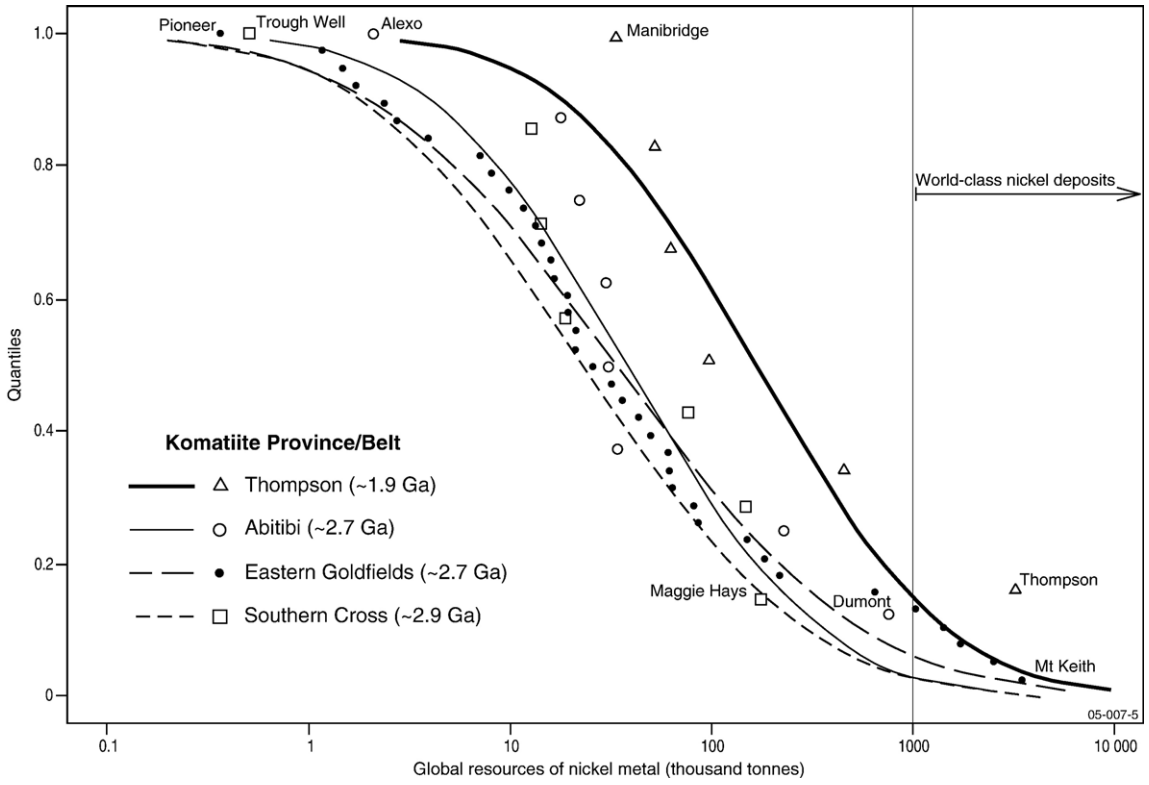

Fig. 22. Cumulative frequency distribution of global resources of nickel metal (production plus reserves and resources) for the major nickel-bearing komatiite belts and provinces of the world (source of data indicated in Table 1).

Belt and the Eastern Goldfields Province are very similar suggesting similar nickel endowment. On the other hand, the curve for the Southern Cross Province has the same general character, but is shifted to relatively smaller nickel-resource values, relative to the more mineralized Abitibi Belt and the Eastern Goldfields Province. The similar cumulative frequency trends for the smaller-sized deposits in both the Eastern Goldfields and Southern Cross provinces also implies that the latter province may host yet to be discovered (under cover?) larger deposits than presently known.

A comparison of significant features of fertile and non-fertile komatiite belts (Table 4) shows that various criteria can be used as regional indicators of fertility. Al-undepleted and Al-depleted komatiitic sequences sometimes occur together in the same fertile province, where the most significant mineralization is invariably associated with the former sequences (Sproule et al., 2002; Barnes et al., 2004a). The most endowed provinces (Eastern Goldfields, Thompson, Abitibi, Cape Smith, and Zimbabwe) are all dominated by Al-undepleted komatiites. Therefore, the predominance of Al-undepleted komatiites in a greenstone belt could be used as a broad regional indicator of fertility. There also appears to be a correlation between the age of the komatiite and nickel endowment. Table 4 highlights that ~2700 Ma and ~1900 Ma komatiites contain substantially more resources than komatiites of other ages. Within individual greenstone belts, the type of volcanic facies or flow environment appears to be important in determining fertility. Empirical data for fertile and non-fertile komatiitic sequences suggest that thin differentiated flows and layered lava lakes and/or sills are not as prospective as compound sheet flows with internal pathways or dunitic compound sheet flows, although these latter facies are not always mineralized (Barnes et al., 2004a). The compound sheet flow and dunitic compound sheet flow sequences are not only more likely to have well-insulated lava channels, but they will also contain larger volumes of primitive ultramafic magma in more dynamic environments (i.e., unlike a passive lava lake or pond facies). Thermal erosion of any substrate will help saturate the magma with sulfur and the presence of sulfidic sediments in the substrate that can be readily assimilated will substantially accelerate and enhance mineralizing processes.

In summary, the following factors are considered significant in defining the fertility of komatiitic sequences:

1. *Age*: Most fertile komatiite sequences are either of late Archean (~2700 Ma) or Paleoproterozoic (~1900 Ma to 1800 Ma) age. Komatiitic sequences outside these ages appear to be either weakly mineralized or barren.
2. *Chemical affinity*: Many provinces contain both Al-undepleted ($Al_2O_3/TiO_2 = 15–25$) and Al-depleted ($Al_2O_3/TiO_2 < 15$) komatiite sequences. However, the most significant mineralization is associated with the Al-undepleted komatiites. Al-depleted komatiitic sequences are generally not well mineralized, particularly if they are spatially associated with Al-undepleted sequences.
3. *Volcanic facies*: Mineralization is predominantly associated with two major facies: compound sheet flows with internal pathways, or dunitic compound sheet flows. In contrast, such passive facies as thin differentiated flows, lava lakes, and sill-like ponded flows are generally unmineralized. Well-insulated dynamic lava pathways that help focus large volumes (i.e., high-magma flux) of magma flow and facilitate chemical interaction of the magma with the substrate are more likely to occur in the prospective compound sheet flow facies.
4. *Thermal erosion of sulfide-bearing substrate*: With a few exceptions, examples of thermal erosion and/or assimilation of substrate have been demonstrated in fertile komatiite sequences. The assimilation of sulfide-bearing substrate can dramatically accelerate the sulfur saturation of a primitive ultramafic magma and deposition of sulfides.
5. *Intensity of deformation, metamorphism, and post-mineralization remobilization*: Most mineralized komatiite sequences show evidence of variable degrees of post-mineralization deformation, metamorphism, and remobilization of sulfides. In some instances this has resulted in upgrading of deposits.

6.1.2. Tholeiitic–magmatic systems

In contrast to komatiitic sequences (Table 4) where a number of criteria (factors 1 to 5 above) appear to be useful for broadly assessing their nickel prospectivity, the situation for tholeiitic mafic–ultramafic intrusions (Table 5) is less clear. Metal endowment for the 'typical tholeiitic layered intrusions' shown in Table 5 is dominated by the 2060 Ma Merensky Reef and Platreef deposits of the Bushveld Complex, South Africa, with the other significantly mineralized intrusions showing a wide range of ages extending from the Archean to the Phanerozoic. Intracontinental rifts are the most important geodynamic settings in Archean terranes whereas multiply deformed orogenic belts characterize both Archean and Proterozoic terranes. Most Ni-bearing intrusions are mafic in bulk composition, although a number of ultramafic-dominated intrusions are also mineralized. Parent magmas are generally of (evolved) basaltic parentage, with compositions generally ranging from high-Mg basalt (15% MgO), magnesian basalt (12% MgO), tholeiitic basalt (7% MgO), to more silica-rich variants such as boninite and siliceous high-Mg basalt. Some deposits (e.g., Pechenga: Barnes et al., 2001) that have more primitive ferropicritic parent magmas (17% MgO) also show some similarities with komatiitic–magmatic systems. There is no obvious correlation between mineralization and composition of basement rock lithologies, or between mineralization and metamorphic grade of basement lithologies. Low-grade pelitic sedimentary rocks, chemical sediments, and mafic–felsic volcanics are equally represented with the more high-grade migmatitic, gneissic, and granitic country rocks. This is not surprising since what may be more important in regard to the sulfur evolution of the mineralized intrusions are the rocks the magma(s) interacted with during their ascent through the crust rather than those rocks at the final crustal level of emplacement (i.e., the importance of the third dimension).

The timing of the sulfur-saturation event (e.g., through crustal contamination, magma mixing, temperature gradients) and the mechanism of magma emplacement are critical elements for the concentration of massive sulfides in such deposits as Voisey's Bay (Naldrett, 1997). These deposits are favored by dynamic feeder systems, physical and chemical interaction with sulfur-bearing country rocks, and a structural framework that facilitates the rapid emplacement of voluminous amounts of hot primitive nickel-bearing magmas (Scoates and Mitchell, 2000). The dynamics of a focused magma flow (e.g., fast, slow, turbulent, passive, changes from narrow vertical conduits to broad sub-horizontal open magma chambers) are important for the deposition of the economically significant massive sulfides.

Evans-Lamswood et al. (2000) highlighted the importance of geometric and morphologic changes in the magmatic feeder conduit for mineralization at Voisey's Bay. Sulfides are preferentially concentrated in traps where physical irregularities and changes in conduit morphology favor the precipitation, capture, and preservation of sulfides as a result of changes in the velocity and viscosity of the ascending magma. Therefore, sulfide deposition at Voisey's Bay is ultimately related to the complex interplay of dike geometry (i.e., changes in dike

Table 5
Significant features of fertile tholeiitic mafic–ultramafic intrusion[a] provinces

Feature	Kaapvaal Craton, South Africa	Sino–Korean Craton, China	Zimbabwe Craton, Zimbabwe	Baltic Shield, Russia	Torngat Orogen, Canada	Limpopo Orogenic Belt, Botswana	Kibaran Orogenic Belt, Tanzania	Svecokarelian Orogenic Belt, Finland	Halls Creek Orogen, Australia	Pilbara Craton, Australia	Yilgarn Craton, Australia
Global resources of nickel metal (Mt)	12.86 (41%)	5.46 (17%)	5.41 (17%)	4.33 (14%)	2.17 (7%)	0.51 (2%)	0.20 (0.6%)	0.16 (0.5%)	0.12 (0.4%)	0.11 (0.4%)	0.01 (0.1%)
Classification of deposits (see Table 2)	2A, 2B	2A	2B	2A	2A	2A	?2A	2A	2A, 2C	2A, 2B	2D
Type deposit(s)	Merensky Reef[b], Platreef[b]	Jinchuan	Great Dike of Zimbabwe[b]	Pechenga, Monchegorsk	Voisey's Bay	Selebi–Phikwe	Kabanga	Kotalahti	Sally Malay, Panton[b]	Radio Hill, Munni Munni[b]	Carr Boyd Rocks
Approximate age (Ma)	2060	830	2590	1980, 2490	1330[c]	>2500	1275	1880	1850	2925	?2700
Geodynamic setting	Intracontinental rift	Rifted continental margin	Intracontinental rift	Rifted continental margin	Proterozoic orogenic belts	Archean orogenic belt	Mesoproterozoic orogenic belt	Paleoproterozoic orogenic belt	Paleoproterozoic orogenic belt	Intracontinental rift	Intracontinental rift
Bulk composition	Mafic>ultramafic	Ultramafic	Ultramafic>mafic	Ultramafic>mafic, mafic>ultramafic	Mafic	Mafic	Ultramafic>mafic	Mafic>ultramafic	Mafic>ultramafic, ultramafic>mafic, mafic	Mafic>ultramafic	Mafic>ultramafic
Parent magma composition(s)	Tholeiitic basalt, high-Mg basalt (~7%–14% MgO) Ultramafic–boninite (~9%–17% MgO)	High-Mg basalt (~11%–13% MgO)	High-Mg tholeiitic basalt (~15% MgO)	Ferropicrite (~17% MgO)	High-Al basalt (~8%–9% MgO)	?Tholeiitic basalt	Siliceous high-Mg basalt (~13% MgO)	Tholeiitic basalt, ?high-Mg basalt	Olivine tholeiitic basalt, quartz tholeiitic basalt (~4%–9% MgO)	Siliceous high-Mg basalt (~9%–12% MgO)	Tholeiitic basalt (<12% MgO)
Mineralization setting (s)	Stratabound reef, basal contact	Basal contact, remobilized veins	Stratabound reef	Basal contact, wall-rock contact, fold axes, fault breccia, veins	Feeder conduit, basal contact	Basal contact, wall-rock contact, fold axes, veins	Basal contact	Basal contact, wall-rock contact, veins	Basal contact, feeder conduit, stratabound reef	Basal contact, feeder conduit, stratabound reef	Discordant pipe
Basement rocks	Shale, dolomite, quartzite, banded iron formation, conglomerate, felsic volcanics, granite,	Migmatite, biotite gneiss, schist, marble	Granite, gneiss, mafic volcanics, banded iron formation, greenstone	Gabbro, shale, tuff, sulfur-bearing graphitic sediments, gneiss, schist	Biotite orthogneiss, pelitic and psammitic paragneiss, sulfur-bearing paragneiss	Hornblende gneiss, biotite schist	Schist, quartzite, granite	Granite gneiss, gneiss, graphitic schist, amphibolite, quartzite, calc-silicate rocks	Migmatitic gneiss, schist, granite, mafic granulite	Granite, mafic and felsic metavolcanics	Mafic and felsic metavolcanics, clastic and chemical sediments

Increasing metal endowment (fertility) of provinces ←

Data from: Purvis et al. (1972); Papunen and Gorbunov (1985); Anhaeusser and Maske (1986); Naldrett (1989, 1997, 2002); Prendergast and Jones (1989); Hoatson et al. (1992); Eckstrand (1995); Eckstrand et al. (2003); Amelin et al. (1999); Hoatson and Blake (2000); Li et al. (2004); Lesher (2004); this study; and references cited within these publications.

[a] Deposits/camps such as Sudbury (astrobleme-associated), Noril'sk (sub-volcanic sills associated with flood basalts), and Duluth (flood basalt associated) are not included in this table since they are of different origin to 'typical' tholeiitic mafic–ultramafic intrusions. The Pechenga deposit has been included in this table, but it does have chemical affinities with both primitive tholeiitic– and komatiitic (Table 4)–magmatic systems.

[b] These deposits contain significant global resources of nickel despite their low grades (<0.4% Ni).

[c] Mineralized intrusions from other Canadian provinces have approximate ages of 100 Ma, 230 Ma, 400 Ma, 1110 Ma, and 2700 Ma (see Table 1).

orientation and thickness) and the fluid dynamics of the magma within the conduit system. Evans-Lamswood et al. (2000) also state that the Voisey's Bay deposit does not conform to the traditional model of magmatic sulfide generation within a mafic intrusion (e.g., Sudbury), where sulfides largely accumulate by gravitational settling within a chamber following S-saturation of the magma through crustal contamination. In fact, they proposed that little gravitational settling took place at Voisey's Bay, and that the distribution of sulfides was controlled by magma emplacement through multiple braids of a dynamic, channel-like conduit dike system. An assessment of the critical mineralizing elements at Voisey's Bay can be found in a Special Issue of *Economic Geology* (2000, Volume 95, Number 4).

6.2. Global-scale nickel-metallogenic events

A compilation of mineralization ages of magmatic nickel sulfide deposits indicates that there are at least three major global-scale nickel-metallogenic events during which different types of deposits formed in different locations at about the same time (Fig. 6). The three most prominent global nickel-metallogenic events occurred at ~3000 Ma, ~2700 Ma, and ~1900 Ma. Although some important individual deposits fall outside these metallogenic events, more than 60% of the world's nickel sulfide resources are related to events occurring in the late Archean and early Proterozoic. The most economically important metallogenic periods are the late Archean event (~2705 Ma to 2690 Ma) of dominantly komatiite-associated deposits, and a Paleoproterozoic event (~1920 Ma to 1840 Ma, and possibly extending to 2060 Ma) comprising komatiite-, mafic–ultramafic intrusion- and astrobleme-associated deposits. The oldest event (~3000 Ma to 2875 Ma) is represented by small-tonnage deposits associated with komatiites and layered intrusions in Australia. Another, major global metallogenic event during the Permian–Triassic (~270 Ma to 230 Ma) led to the formation of mineralized mafic±ultramafic intrusions associated with comagmatic flood basalts in Siberia (Noril'sk), and much smaller deposits in Canada (Wellgreen), China (Emeishan), and possibly with komatiites in Vietnam (Song Da: Hanski et al., 2004).

Recent studies on the temporal distribution of mineral deposits have underlined the role of mantle-lithosphere-scale processes in the formation and preservation of different types of mineral deposits, thus determining the metallogenic specialization of large regions and geological periods (Barley and Groves, 1990; Groves et al., 2005). The late Archean (~2705 Ma to 2690 Ma) and Paleoproterozoic (~1920 Ma to 1840 Ma) nickel-metallogenic events identified above correspond with two major periods of juvenile crustal growth, interpreted to be caused by mantle overturn events associated with mantle plumes (Condie, 1997; Abbott and Isley, 2002; Groves et al., 2005). Of the 36 mantle-plume events recognized in the last 3800 million years of the earth's evolution, two major events at ~2700 Ma and ~1900 Ma, that correlate with the global nickel events identified in this study, are called superplume events (Pirajno, 2004) or catastrophic mantle-plume events (Groves et al., 2005). These superplume events are characterized by the development of large volumes of primitive komatiitic and tholeiitic magmas that may form fragments of plume-related oceanic plateaus (Pirajno, 2004). The other less significant Archean nickel event (~3000 Ma to 2875 Ma) recognized in this study also correlates with a relatively smaller event that involved the growth of the juvenile crust (Groves et al., 2005). Studies of mantle plume events over Earth's history by Abbott and Isley (2002) have shown that over 66% of superplume events last less than 8 million years and that the average duration of Archean and Phanerozoic superplume events varies between 13±7 and 12±3 million years, respectively. However, they state that the largest Precambrian superplume events erupted at least ten times more lava than the largest Phanerozoic superplume event. Between 2900 and 1700 million years ago there were enough superplume events to completely resurface the planet. The higher nickel endowment of the Precambrian could thus reflect the greater volumes of mafic and ultramafic magmas during this period.

The secular change in the nickel metallogeny from Archean to the Phanerozoic (Fig. 6) may be a response to the temporal evolution of the subcontinental lithosphere from strongly plume-influenced Archean tectonics to Phanerozoic-styled plate tectonics. This evolution may not only have controlled the formation of different styles of mineral deposits, but also played a significant role in the preservation of mineralized mafic–ultramafic intrusions (Groves et al., 2005).

6.3. Potential of nickel-mineralizing systems and exploration strategies in Australia

6.3.1. Komatiitic association

Economically the most important komatiite-associated deposits in Australia can be classified into two end-members: accumulations of massive sulfides at the base of compound komatiite sheet flows that occupy preferred lava pathways (Kambalda — type 1A), and large disseminated sulfide zones in thick channel-like lenses of olivine cumulates (Mt Keith — type 1B). An analysis of the major komatiite provinces of the world (Table 4)

reveals that the most fertile komatiite sequences are generally of late Archean (~2700 Ma) or Paleoproterozoic (~1900 Ma to 1800 Ma) age, and have dominantly Al-undepleted (Al_2O_3/TiO_2=15–25) chemical affinities. Compound sheet flows with internal pathways and dunitic compound sheet flows are considered more favorable facies for hosting massive sulfides than thin differentiated flow, lava lake, and sill-like pond facies. Well-insulated lava pathways that focus large volumes of magma flow and facilitate dynamic interaction of the magma with a sulfur-bearing substrate are more likely to occur in the compound sheet flow facies. The assimilation of such a substrate can accelerate the sulfur saturation of a primitive ultramafic magma and initiate the deposition of sulfides.

Suggested exploration strategies for type 1A and type 1B komatiite deposits based on Australian examples are summarized in Table 6.

In addition to the more typical komatiite-associated nickel deposits of the Yilgarn Craton (Types 1A and 1B), recent exploration at greater depths and in less traditional environments has defined an increasing number of deposits and prospects that have unusual settings and metal signatures. These include those komatiite deposits and prospects with exceptionally high Ni grades (e.g., Cosmos, Long, Flying Fox-T5), with normal Ni/Cu ratios and high PGE grades (Waterloo), with low Ni/Cu ratios and high PGE grades (Collurabbie, Collurabbie South, Daltons). This diversity of mineralization styles, which enhances the prospectivity of this magmatic association, is likely to expand in the future with the increasing emphasis of exploration away from the more traditionally explored parts of the greenstone belts.

Proterozoic sedimentary rocks of the Yerrida and Earaheedy basins unconformably overlie Archean greenstone sequences on the northern margins of the Yilgarn Craton. Geophysical studies (aeromagnetics and gravity) have shown that narrow, high-amplitude magnetic signatures typical of komatiitic sequences and/or banded iron formations can be traced northwards under these sedimentary sequences for several tens of km strike extent. The greenstone sequences between Leinster and Wiluna (Fig. 23) represent the richest nickel-bearing komatiite belt in the world, with four world-class deposits, five of the six largest nickel sulfide deposits in Australia, and a collective global nickel resource of at least 9.2 Mt, equivalent to more than 70% of Australia's known total nickel sulfide resources. The interpreted extensions of the ultramafic sequences beneath the Proterozoic rocks north of Wiluna have considerable potential for nickel mineralization, especially in view of the significant metal endowment of the greenstones immediately to the south of Wiluna and the recent discovery of massive sulfides (0.3 m @ 6.6% Ni: Agincourt Resources Limited, 2005) at Bodkin north of Wiluna (inset of Fig. 23). This is the first time massive nickel sulfides have been reported from the northern part of the Perseverance–Wiluna greenstone belt. The presence of thick MgO-rich komatiite channel sequences, massive sulfides in embayment structures, and sulfidic footwall rocks in this part of the belt indicate favorable environments conducive to economic concentrations of nickel sulfides. Recent significant drill intersections, such as at Collurabbie, highlight the potential of poorly exposed greenstone sequences near the margins of the craton that have experienced little exploration. Similarly, extensions of potentially mineralized komatiitic sequences may also exist under cover for other sections of the Eastern Goldfields, Northeastern Goldfields, and Southern Cross provinces (see Fig. 23). The Eastern Goldfields and Southern Cross provinces have similar cumulative frequency endowment trends (Fig. 22), except for the apparent absence of world-class deposits in the latter province. These similar grade-tonnage trends suggest that large deposits may remain to be found under cover in the Southern Cross Province.

Komatiitic rocks in Australia have previously been considered to be confined to the older Archean components of the West Australian Craton (Myers et al., 1996), namely the Yilgarn and Pilbara cratons. However, the recent documentation of primitive komatiitic rocks near Lake Harris and Mt Hope in the Gawler Craton (Hoatson et al., 2005b) now extend their regional distribution much further east on the Australian continent. The wider distribution of the komatiites has implications for further discoveries of nickel deposits and the geodynamic reconstruction of Australia's Precambrian crustal architecture (see Betts and Giles, 2006).

6.3.2. Tholeiitic association

Differentiated sulfur-saturated tholeiitic mafic intrusions (type 2A) are favorable bodies for hosting Ni–Cu–Co±PGE sulfide ores that need to be concentrated in restricted environments to attain economic status (Fig. 24). Such environments include shallow depressions and structural embayments in basal contacts beneath the thickest sequence of mafic–ultramafic cumulates, or the confluence regions of feeder conduits and magma chambers. Therefore, the major exploration challenges for finding these deposits in poorly exposed Precambrian provinces are to determine the

Table 6
Exploration guidelines for nickel sulfide deposits (based on Australian examples)

(1) Komatiite-associated Ni–Cu ± PGEs sulfides (e.g., Types 1A and 1B: Kambalda, Mt Keith, Cosmos, Flying Fox)

Regional geological criteria:

1. Komatiitic magmas emplaced in rift zones in granite–greenstone belts in Archean cratons (Yilgarn, Pilbara, Gawler).
2. Granite–greenstone belts: sub-parallel linear and sinuous greenstone sequences; elongate, ovoid, and domal granitic bodies; coeval komatiitic, basaltic (tholeiitic), and felsic volcanics; metasedimentary rocks; province-wide shear systems; and linear tectonic patterns.
3. Intracratonic–extensional rift environments (Groves and Batt, 1984): (a) rift-phase greenstone sequences formed in deep-water under conditions of high-crustal extension; abundant sulfidic shale and chert (e.g., Kambalda and Mt Keith districts); or (b) platform-phase greenstone sequences formed in relatively shallow-water under conditions of low-crustal extension; volcaniclastic rocks and oxide-facies iron formation (e.g., Forrestania district).
4. Regionally extensive (10s to 100s km strike extent) komatiite sequences containing thick olivine cumulate units. Cumulates proportionally thicker relative to more evolved komatiitic rocks from upper parts of sequences.
5. Emplacement ages: ~2700 Ma, and ~2900 to ~3000 Ma in the Yilgarn (Kambalda, Mt Keith, Maggie Hays); ~2880 to ~3460 Ma in the Pilbara (Ruth Well, East Pilbara); and ~2520 Ma in the Gawler (Lake Harris, Mt Hope) cratons.
6. Although most mineralized provinces contain both Al-undepleted ($Al_2O_3/TiO_2 = 15–25$) and Al-depleted ($Al_2O_3/TiO_2 < 15$) komatiitic sequences, the most significant mineralization is generally associated with the former type. Provinces with only Al-depleted sequences are generally poorly mineralized or barren.

Local geological criteria:

1. Presence of outcropping gossans and primitive komatiitic rocks: spinifex, quench, breccia, and aphyric textures for komatiitic basalts and low- to high-Mg komatiites (15 to 32% MgO whole-rock compositions), and cumulus (orthocumulate, mesocumulate, adcumulate) textures for more primitive (32 to 50% MgO whole-rock and $>Fo_{85}$ olivine compositions) sequences.
2. Massive and matrix ores concentrated in basal part of stacked sequence of relatively thin (few meters up to tens of meters) compound sheet flows with internal pathways (Kambalda-type), or disseminated ores within thick (up to 800 m) olivine cumulate dunite lenses with transgressive basal contacts (Mt Keith-type).
3. Preserved lava pathways or lava tubes (i.e., focussed flow) within thick inflated flows.
4. Presence of sulfide-bearing substrate lithologies (chemical–exhalative sediments, volcanics) that have relatively low melting points to facilitate thermal erosion.
5. Presence of transgressive embayments and structural traps along footwall contacts of channel facies to concentrate massive sulfides.
6. Evidence of sulfur saturation (e.g., presence of Ni-enriched magmatic sulfides, nickel depletion trends in olivine compositions, depletion of PGEs).

Exploration methods:

1. Geophysics: regional aerial magnetic and gravity surveys to define potential host komatiitic rocks (generally, but not always strongly magnetic) and lava pathways, and ground magnetics to identify lithological contacts and small-scale structures; airborne–surface electromagnetics to delineate electrically conductive Fe–Ni–Cu sulfides (can be hampered by barren sulfide-bearing sediments and saline groundwaters). Downhole electromagnetics are becoming more effective due to greater depth of penetration and they avoid problems related to conductive regolith. New 'Geoferret' electromagnetic technology has the ability now to detect orebodies up to 500 m below the surface.
2. Identify physical or chemical haloes which are much larger than the orebodies themselves. Gossans of massive sulfides defined by coincident high Ni, Cu, and PGEs; most deposits are covered by alluvium, laterite, or lacustrine sediments thus regolith and geobotanical mapping to interpret subsurface geology and supergene geochemistry (Sheard and Robertson, 2002).
3. Determine magmatic environments (volcanic, subvolcanic, intrusive) and facies (flood sheet flows, compound flows, ponded lakes: Dowling and Hill, 1998).
4. Chemical evidence of substrate erosion and crustal contamination (enrichment in Zr, La, Th, U, Y, Nd, Ti, Al, Fe, negative Nb–Ta–Ti anomalies: Barnes et al., 1999; Lesher, 2004); depletion trends in chalcophile trace element ratios (Pd/S, Cu/Pd) along basal flows to indicate location of sulfur saturation and mineralization.
5. Close-spaced core drilling of most primitive parts of komatiite sequences.

(2) Basal Ni–Cu–Co ± PGEs sulfides (e.g., Type 2A: Sally Malay, Radio Hill, Mt Sholl, Nebo–Babel)

Regional geological criteria:

1. Tholeiitic mafic dominated intrusions emplaced in rift zones in Archean–Proterozoic cratons (Pilbara, Yilgarn) or in Proterozoic orogenic belts (Halls Creek, Albany–Fraser).
2. Cratonic settings: postorogenic intrusions associated with sinuous greenstone sequences of coeval komatiitic–basaltic–felsic volcanics, metasediments, elongate to ovoid granitic bodies; anastomosing to linear tectonic patterns. Orogenic settings: tectonized orogenic to post-orogenic bodies associated with fault-bounded linear belts of metasediments and metavolcanics, elongate granitic bodies; linear tectonic patterns.
3. Emplacement ages: ~2925 to ~2700 Ma in the Pilbara and Yilgarn (Radio Hill, Mt Sholl, Windimurra), ~1865 Ma to ~1850 Ma in the East Kimberleys (Sally Malay, Corkwood, Keller Creek, Bow River, Norton), ~1080 Ma in the Musgraves (Nebo–Babel).
4. Small- to medium-sized (<3 km thick) differentiated mafic ± ultramafic intrusions. Intrusions are sometimes associated with comagmatic volcanic sequences and sub-volcanic feeder conduits that may have been removed through erosion. Deposits are generally not hosted in thick large intrusions that have had protracted and passive evolutions.
5. Ni-bearing magmas (Ni not depleted by early-crystallizing olivine or early sulfur-saturation events) that achieve rapid sulfur saturation by contamination and/or turbulent mixing in a crustal environment.

Local geological criteria:

1. Mafic-dominated tholeiitic intrusions with ultramafic rocks generally forming thin sequences in lower parts of stratigraphy.
2. Massive or layered bodies consisting of cumulus (adcumulate, mesocumulate, orthocumulate)-, equigranular-, intergranular-, subophitic-textured rocks.
3. Presence of massive, matrix, and disseminated Fe–Ni–Cu–Co sulfides in lower parts of stratigraphy, and remobilized and fractionated Cu–Pd–Pt–Au–Ag-enriched sulfides in country rocks.

Table 6 (*continued*)

Local geological criteria:

4. Massive sulfides — critical to the economic status of deposit — are confined to structural embayments and depressions in basal contacts below the thickest sequence of cumulates, or in feeder conduits (see Fig. 24A,B).

5. Preservation of basal contacts and feeder conduits (not sheared out or overprinted by younger intrusions).

6. Massive sulfides are generally hosted by thin (meters to tens of meters thick) basal 'veneers' of evolved gabbroic rocks located between the country rocks, and an overlying, more primitive ultramafic–mafic cumulate sequence (Sally Malay, Radio Hill).

7. Dynamic, open-magmatic systems (periodically replenished magma chambers, subvolcanic feeder sills and dikes, volcanic vents, extensive interaction of hot primitive magma(s) with sulfur-bearing country rocks, brecciation, turbulent magma mixing) rather than passive, slowly evolving magmatic systems. Dynamics of focussed magma flow and conduit geometry (slow, fast, or turbulent flow; changes from narrow vertical conduits to subhorizontal broad magma chambers; physical traps) are important considerations for the precipitation and capture of massive sulfides.

Exploration methods:

1. Geophysics: regional aerial magnetic and gravity surveys to determine total extent, pre-deformational geometries, and fractionation (younging) directions of intrusions, and locate favorable mineralized environments (basal contacts, feeder conduits); ground magnetics to define lithological contacts and small-scale mineralized structures (embayments); airborne–ground electromagnetics and induced polarization to delineate conductive sulfides.

2. Geochemical profiling (S, Cu, Ni, PGEs, Cu/Pd, mg number) along type stratigraphic sections to determine stratigraphic level and effectiveness of sulfur-saturation event(s).

3. Evidence for thermal–chemical interaction of magma(s) with sulfur-bearing country rocks (fractionated compositions of marginal rocks, xenoliths of country rock, xenocrysts, hybrid rocks, association of sulfides and alkalies, elevated Zr, Y, Ti, Al, Fe, Nd contents).

4. Composition of olivine (Ni content versus mg number) is a useful indicator of nickel depletion in the magma from which the olivine has crystallized.

5. Gossans of massive sulfides defined by coincident high Ni, Cu, and PGE contents; regolith and geobotanical mapping since many deposits are covered by alluvium, laterite, or lacustrine sediments.

6. Close-spaced core drilling of basal contact and feeder conduit (especially entry point region into magma chamber).

(3) Stratabound PGE–Ni–Cu (e.g., Type 2B: Munni Munni, Weld Range, Windimurra) and stratabound PGE–Ni–Cu–Cr (e.g., Type 2C: Panton, Eastmans Bore, Mt Davies) layers

Regional geological criteria:

1. Tholeiitic-dominated intrusions emplaced in rift zones in Archean–Proterozoic cratons (Pilbara, Yilgarn, Gawler) or in Proterozoic orogenic belts (Halls Creek, Albany–Fraser).

2. Cratonic settings: dominantly postorogenic intrusions associated with sinuous greenstone sequences of coeval komatiitic–basaltic–felsic volcanics, metasediments, elongate to ovoid granitic bodies; anastomosing to linear tectonic patterns. Orogenic settings: tectonized orogenic to postorogenic bodies associated with fault-bounded linear belts of metasediments and metavolcanics, elongate granitic bodies; linear tectonic patterns.

Table 6 (*continued*)

Regional geological criteria:

3. Emplacement ages: ~2925 to ~2700 Ma in the Pilbara and Yilgarn (Munni Munni, Weld Range, Windimurra), ~1850 Ma in the East Kimberleys (Panton, Eastmans Bore, Lamboo, Big Ben), ~1080 Ma in the Musgraves (Mt Davies).

4. Large and thick (>3 km) differentiated layered mafic–ultramafic and ultramafic intrusions that display open fractionation systems involving large pulses of primitive sulfur-undersaturated magma (source of PGEs) and younger, more evolved sulfur-saturated mafic magma (source of sulfur).

5. Fertile PGE-bearing magmas (not depleted by early sulfur-saturation events) that achieve late sulfur saturation (in the magma chamber) through magma mixing, crystal fractionation, crustal contamination, and/or movement of fluids.

Local geological criteria:

1. Macrorhythmic cycles of ultramafic (ol–opx–cpx–chr) and mafic (pl–cpx–opx–ol–mt–ap) rocks that show considerable lateral continuity; most mineralized layers are stratabound, although some may be discordant to the underlying stratigraphy (Munni Munni); the mineralized layers need to maintain uniform thicknesses and constant metal grades over considerable strike distance (km's) to be economic.

2. The most PGE-enriched mineralized layers generally occur at, or near, major compositional interfaces in the intrusion that involved the cumulus crystallization of plagioclase (i.e., near major contacts between ultramafic and mafic sequences). Exploration should initially focus on the stratigraphic interval from 150 m below the contact between ultramafic and mafic sequences up to 500 m above this contact (see Fig. 24A).

3. PGE-enriched layers either show no spatial relationship with cyclic units (Munni Munni), or occur at the base or within cyclic units (Panton) that are tens to hundreds of meters thick.

4. High tenor PGEs are associated with either minor (2–3 vol.%) disseminated magmatic Fe–Ni–Cu sulfides (chalcopyrite–pentlandite–pyrrhotite±magnetite) and/or with chromite, at some appreciable height above the base of the intrusion. Ores are often associated with reappearance in stratigraphy of high-temperature, primitive cumulus minerals (olivine, chromite, orthopyroxene); orthopyroxene and/or olivine cumulates are more favorable than clinopyroxene cumulates for hosting stratabound chromitite layers because of the relative high partitioning of Cr into clinopyroxene (inhibits precipitation of chromite).

5. Textures of ultramafic rocks: cumulus (adcumulate, mesocumulate, orthocumulate), foliated, massive; textures of gabbroic rocks: intergranular, subophitic, laminated.

6. Textures of sulfide ore layers: porphyritic, pegmatoidal, coarse-grained (host rocks: plagioclase-bearing pyroxenite, gabbro); textures of chromitite ore layers: disseminated, massive, cumulus (host rocks: dunite, troctolite, orthopyroxenite).

7. Wide-scale turbulent and efficient mixing of resident with new primitive magma in the chamber and/or rapid turbulent flow through a narrow conduit is required so that sulfides equilibrate with a large volume of magma to achieve significant PGE enrichment.

Exploration methods:

1. Geophysics: aerial magnetic and gravity surveys to determine regional extent, geometries, major compositional interfaces (ultramafic versus mafic), and major structures of poorly exposed bodies; ground magnetics to define lithological contacts, magmatic unconformities, and magnetite-bearing reefs; electromagnetic and

(continued on next page)

Table 6 (*continued*)

Exploration methods:

induced polarization methods to delineate large concentrations of disseminated sulfides. Satellite hyperspectral imagery and gamma-ray spectrometry are useful for discriminating broad packages of ultramafic, mafic, and felsic rock types.

2. Detailed geological mapping and close-spaced rock sampling (10–20-m intervals) through the entire stratigraphic succession to assess stratigraphic level of sulfur saturation.

3. Marked discontinuities in lithogeochemical profiles of S, Cu, Zr, Rb, Sr, Cs, Cu/Pd, Pd/Zr, Pd/Ir, Cu/Zr, and mg number indicate stratigraphic levels of new magma pulses and sulfur saturation, and mineralized layers formed by magma mixing. For example, the stratigraphic level of a stratabound PGE layer/reef may be indicated by a sharp increase in Cu/Pd up the stratigraphy. If the intrusion is sulfur saturated throughout the stratigraphy, Ni–Cu–Co±PGE sulfides along the basal contact or in the feeder conduit (Type 2A) should be investigated.

4. Important mineralizing processes, such as mixing of primitive magma with more fractionated magma, are indicated by: rapid changes in compositions of cumulus minerals and the volume of intercumulus melt; presence of sulfides, chromite, graphite, and halogen-bearing minerals (apatite, biotite, amphibole); transitions from Fe-rich to Cu-rich sulfide assemblages; development of porphyritic, pegmatoidal, and orthocumulus textures; presence of hybrid rocks, xenoliths in slump deposits, lateral variations of rock types; and unconformities that indicate magmatic erosion/disruption of footwall units.

5. High Mg, high-Cl primitive 'basaltic' parent magmas (e.g., contaminated komatiitic, picritic, siliceous high-magnesian, boninitic types) with Pt and Pd concentrations of greater than 10 ppb are favored for the formation of PGE-sulfide deposits.

6. Stratabound PGE-sulfide layers are difficult targets to explore because they are generally narrow (~1–2-m-thick layers in up to 10-km-thick sequences), and they have weak geophysical (only 2–3 vol. % disseminated sulfides) and geochemical signatures; in contrast, chromitite layers often crop out, are readily identified, and are defined by elevated contents of pathfinder elements Cr, Pt, Pd, Ni, Cu, Co, Au, Mg, As, and Hg.

ap=apatite, chr=chromite, cpx=clinopyroxene, hb=hornblende, mt=magnetite, ol=olivine, opx=orthopyroxene, pl=plagioclase.
Sources of information: Lesher (1989); Naldrett (1989, 2002); Groves and Hudson (1990); Dowling and Hill (1998); Hoatson (1998, 2001); Hoatson and Keays (1989); Hoatson and Blake (2000); Hoatson and Sun (2002); Perring and Barnes (2002); Hronsky, pers. commun. (2004); Hoatson et al. (2005a,b); and this study.

pre-deformational geometries and younging directions of the intrusions, and from this information locate structural irregularities in the basal contacts and feeder conduits under shallow cover (Table 6).

Some important nickel sulfide discoveries have highlighted the potential and under-explored status of many Precambrian provinces in Australia. The discoveries in 1993 of the world-class Voisey's Bay Ni–Cu deposit (2.2 Mt) in Labrador, Canada, and in 2000 of the Nebo–Babel (~1 Mt) prospect in the Musgrave Province stimulated the exploration of mafic intrusions throughout Australia. The Halls Creek Orogen, Musgrave Province, Arunta Block, Albany–Fraser Orogen, and western parts of the Yilgarn, Pilbara, and Gawler cratons are considered the more prospective regions for Ni–Cu–Co sulfide deposits associated with tholeiitic mafic intrusions (type 2A). Typically these deposits do not appear to be age-specific with economic examples occurring in both Archean and Proterozoic provinces. The regional distribution of the post-orogenic mineralized mafic–ultramafic intrusions in the Halls Creek Orogen defines two parallel northeast-trending corridors, which has focused exploration for Cr–PGEs–Ni–Cu±Au (chromite association) and Ni–Cu–Co± PGEs (sulfide association) mineralization (Hoatson and Blake, 2000). These intrusions represent one of the most extensively mineralized igneous associations of their type in Australia. The Sally Malay deposit shows many similarities (e.g., regional orogenic setting, stratigraphy, fractionated mafic host rocks, mineralized feeder conduit linked to overlying ovoid magma chambers) to that of the Voisey's Bay deposit in Canada (Hoatson et al., 1997). The Mesoproterozoic basement rocks of the Musgrave Province in central Australia have been intruded by the ~1080 Ma mafic–ultramafic intrusions of the Giles Complex. The layered intrusions consist of at least twenty sheet-like bodies that cover an area of at least 100 km north–south by 500 km east–west. The Giles Complex is interpreted to be part of the coeval Warakurna large igneous province that has a total west to east distance across western and central Australia of at least 2400 km (Wingate et al., 2004; Pirajno et al., in press). Many of the Giles Complex intrusions and other dolerite sills and dikes belonging to the extensive Warakurna igneous province further west have not been drilled for basal accumulations of massive sulfides. Hoatson et al. (1997) suggested that the large troctolitic–gabbroic intrusions in the Musgrave Province (e.g., Jameson Range, Cavenagh Range, Blackstone Range, Bell Rock Range) had high potential to host Voisey's Bay-type mineralization. The announcement, in 2000, of significant Ni–Cu–PGE mineralization (26.5 m @ 2.4% Ni, 1.8% Cu, 0.1% Co, 0.7 g/t PGEs+Au: Seat et al., 2005; Baker and Waugh, 2005) at the Nebo deposit south of the Jameson Range intrusion was a catalyst to aggressive tenement acquisition and company exploration in the Musgrave Province. The massive sulfides at Nebo are hosted by a gabbroic feeder conduit similar to the mined Radio Hill, Sally Malay, and Voisey' Bay deposits.

Proterozoic mafic–ultramafic intrusions in the Arunta Region of central Australia are widespread and have substantial extensions under alluvial cover (Meixner and

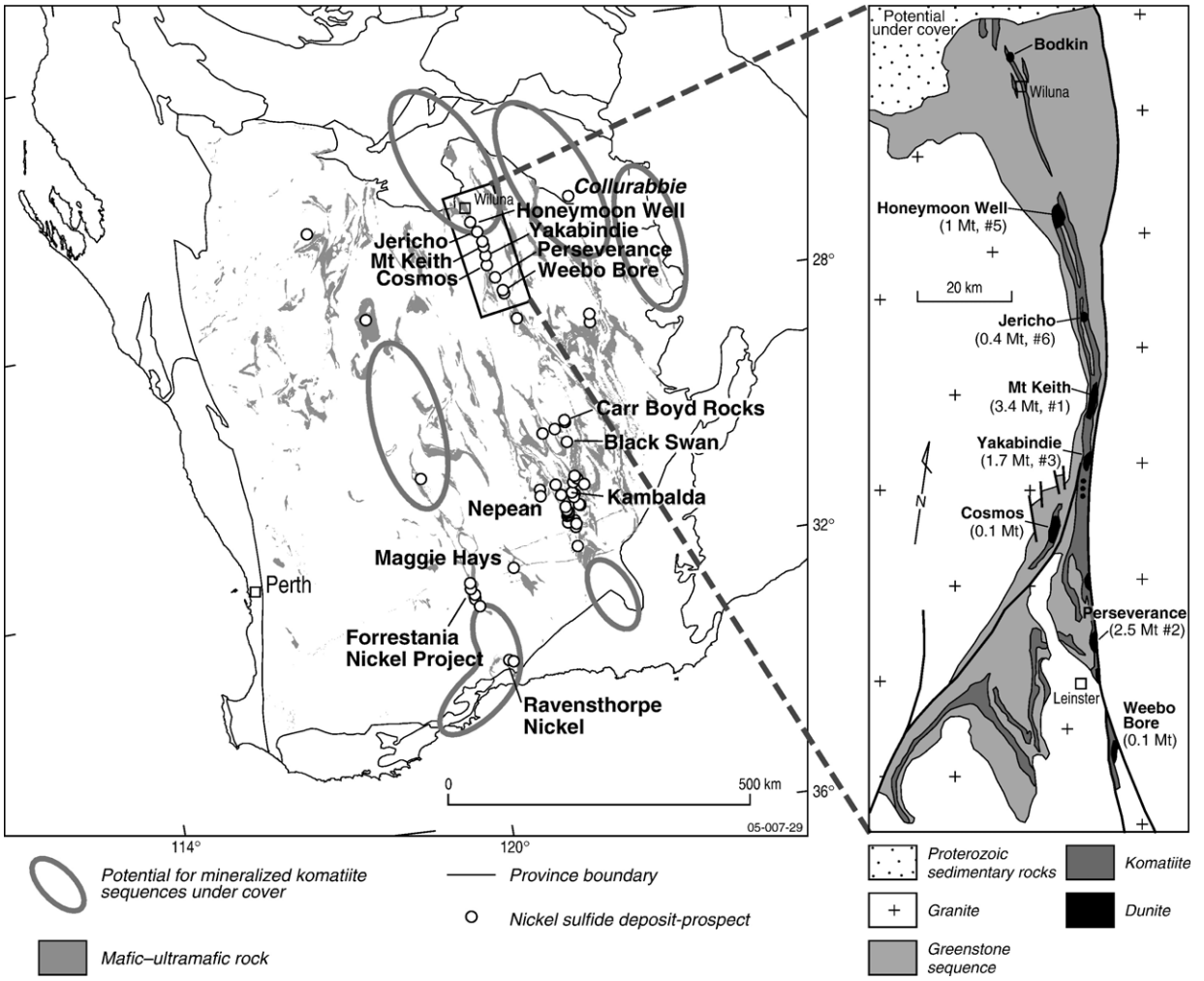

Fig. 23. Interpreted extensions of potentially mineralized komatiite sequences under alluvial cover and sedimentary rocks of Proterozoic basins overlying the Yilgarn Craton. Inset map shows the major komatiite-associated nickel sulfide deposits in the northern part of the Norseman–Wiluna greenstone belt and their global resources of nickel metal and ranking in size relative to other Australian deposits. This particular section of the greenstones contains more than 9 Mt of nickel metal and represents the richest komatiite-hosted nickel belt in the world.

Hoatson, 2004; Hoatson et al., 2005a). Incompatible trace-element trends show that the Arunta intrusions fall into two major geochemical groups that highlight geographical differences in mineral prospectivity: a sulfur-rich group (300 to ~1200 ppm S: Andrew Young Hills intrusion, Mount Hay Granulite, Mount Chapple Metamorphics, Papunya ultramafic) from the western and central Arunta that has potential for basal Ni–Cu–Co sulfide associations (Voisey's Bay-type); and (2) a relatively sulfur-poor (<300 ppm S), slightly more primitive group (Attutra Metagabbro, Mordor Complex) from the eastern Arunta that has greater potential for stratabound PGE-sulfide associations (Merensky Reef-type: Hoatson, 2001; Hoatson et al., 2005a). The large S-saturated mafic magmatic systems also show evidence of extensive crustal contamination and magma mixing processes which are important for initiating sulfur saturation and mineralization. Such an example is the 1630 Ma Andrew Young Hills intrusion (Fig. 25) in the west Arunta Region, which also highlights the challenges confronting many companies exploring poorly-exposed Precambrian intrusions in Australia. Outcrop coverage for this prospective sulfur-saturated mafic body is less than 10% of the total intrusion. Meixner and Hoatson (2004) used aeromagnetic and gravity datasets to show that the overall size and geometry of the body to be a large (13 by 22 km) south–southwest plunging synform. Interpreted structural embayments in a preserved intrusive basal contact and a feeder conduit on the northern side of the body (see inset to Fig. 25) are considered favorable potential mineralized

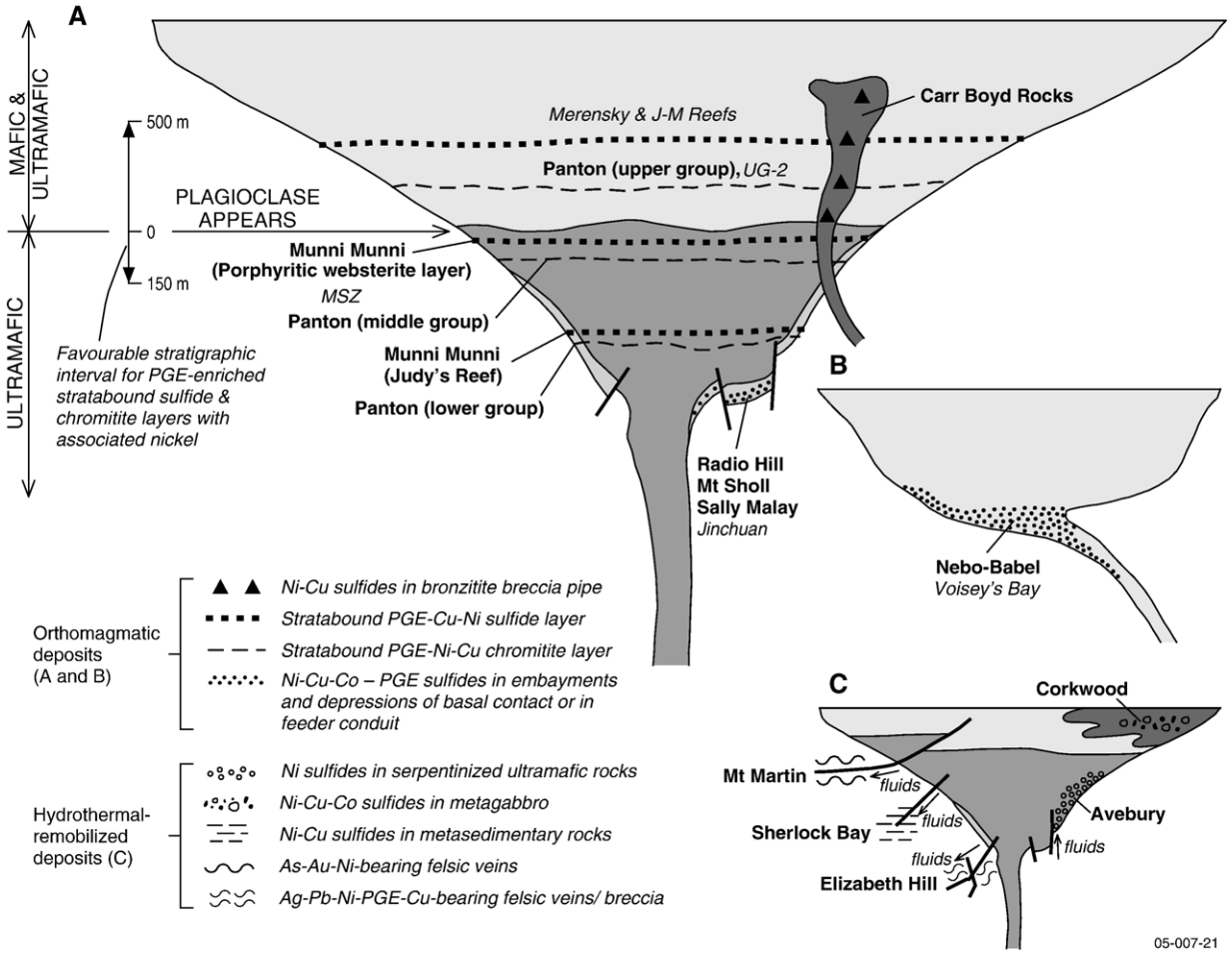

Fig. 24. Schematic distribution of orthomagmatic and hydrothermal-remobilized nickel sulfide deposits associated with mafic–ultramafic and mafic intrusions. A. Idealized tholeiitic mafic–ultramafic intrusion. Distribution of Australian deposits (normal type) include Munni Munni, Radio Hill, and Mt Sholl from the west Pilbara Craton (Hoatson et al., 1992; Hoatson and Sun, 2002), Carr Boyd Rocks from the Yilgarn Craton (Purvis et al., 1972), and Panton and Sally Malay from the Halls Creek Orogen, East Kimberleys (Hoatson and Blake, 2000). Foreign deposits (in italics: after Naldrett, 1993) include the Merensky Reef, UG-2 (Upper Group-2 Chromitite) of the Bushveld Complex, South Africa; the J-M Reef of the Stillwater Complex, Montana, USA; the MSZ (Main Sulfide Zone) of the Great Dike, Zimbabwe; and the Jinchuan Intrusion, China. B. Idealized tholeiitic mafic intrusion. Distribution of massive Ni–Cu–Co sulfide deposits in the feeder conduit of an idealized mafic-dominated tholeiitic intrusion at Nebo–Babel, Musgrave Province, Western Australia; and Voisey's Bay, Canada (after Naldrett, 1997). C. Idealized mafic–ultramafic intrusion with metagabbro component (top right corner). Hydrothermal-remobilized deposits hosted by serpentinized ultramafic (Avebury), deformed mafic (Corkwood), metasedimentary (Sherlock Bay, Mt Martin), and igneous (Elizabeth Hill) rocks.

environments for the accumulation of massive sulfides (Voisey's Bay-type). Poorly exposed Proterozoic intrusions (Plumridge, Salt Creek, Shell Lakes, Loongana, Cooper Hills, Barton, Yumbarra, Streaky Bay) in the Albany–Fraser Orogen, western Gawler Craton, Coompana Block, and other near-by provinces of southern Australia have also recently generated considerable exploration interest.

6.3.3. Hydrothermal-remobilized association

Hydrothermal-remobilized nickel sulfide deposits (type 3) have diverse geological settings and metal associations that reflect the different compositions of the source rocks and fluids. A common feature of these deposits is the close spatial association of altered ultramafic sequences that are interpreted to be the source rocks of the nickel. Deposits related to hydrothermal-remobilizing mineralizing systems cover a wide spectrum, ranging from those which are largely derived from a primary magmatic process and have a minor hydrothermal overprint (e.g., physical dislocation of magmatic sulfides, faulted-breccia ores), through those involving late-stage hydrothermal remobilization of nickel (metamorphic–metasomatic replacement), to other deposits which are

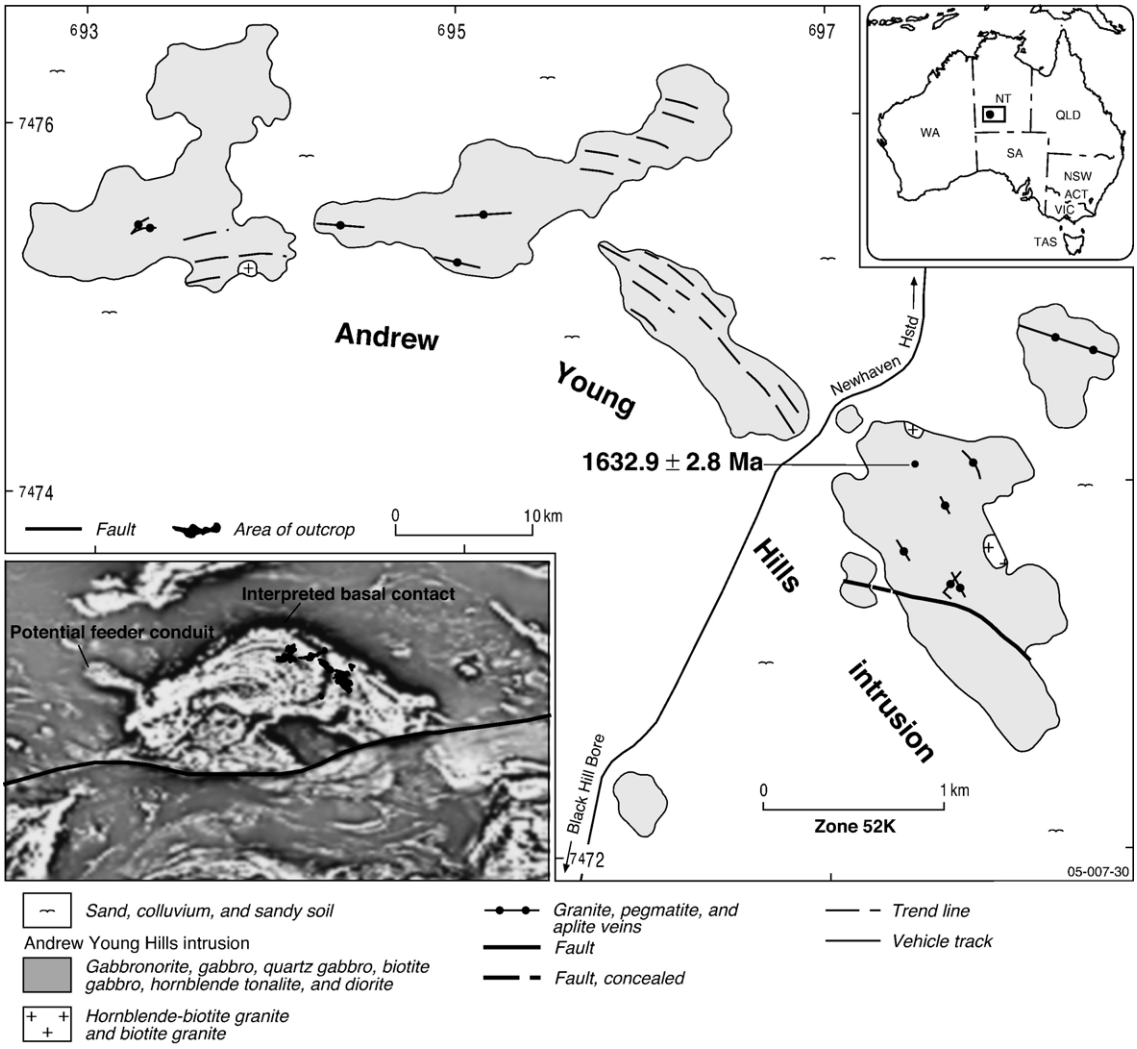

Fig. 25. Geological map of the Andrew Young Hills intrusion, western Arunta Region, central Australia. The poorly exposed gabbroic intrusion has a primary U–Pb zircon crystallization age of 1632.9±2.8 Ma. The vertical gradient of total magnetic intensity image (reduced to pole: processed by T. Meixner, Geoscience Australia) in the bottom left corner shows that outcrop is restricted to the northeastern part of the intrusion and that most of the intrusion extends under shallow alluvial cover. Modified after Hoatson et al. (2005a).

strictly hydrothermal in origin (nickel and associated metals show no spatial association or obvious derivation from ultramafic rocks and fluid movement was the dominant mechanism for metal transport). Relative to the komatiitic and tholeiitic nickel associations, these deposits typically have small-tonnage status and low exploration significance. An exception is Avebury in western Tasmania, which is an unusual nickel deposit that has highlighted the potential of nickel-mineralizing systems in Phanerozoic terranes.

There is also potential in Australia for 'Noril'sk-type' Ni–Cu–PGE deposits associated with large mafic igneous provinces. Hoatson (1984) highlighted the potential of extensive mafic magmatic systems that involved basaltic lava, dike, and sill complexes (e.g., Cooya Pooya Dolerite and Fortescue Group volcanics in the west Pilbara, Antrim Plateau Volcanics, Carson Volcanics, Hart and Woodward Dolerites in the Kimberleys, Oenpelli and Zamu Dolerites in the Pine Creek region, Eastern Creek Volcanics in the Mount Isa Inlier, and younger basaltic provinces in south-eastern Australia) for Noril'sk-type mineralization. More recent geochemical–geochronology studies (Hanley and Wingate, 2000; Glass et al., 2004; Wingate et al., 2004; Pirajno and Morris, 2005; Morris and Pirajno, 2005) have shown that some of the largest igneous provinces, such as the Fortescue Group volcanics, Warakurna igneous province, Bangemall Supergroup,

and Kalkarindji Flood Basalts, formed at about 2800, 1465, 1080, and 500 million years and covered vast areas ($\sim 1.5 \times 10^6$ km^2) of northern and central Australia. These regions represent some of the world's most voluminous flood basalt provinces, similar in size to the Phanerozoic Siberian Traps, and are characterized by the emplacement of huge quantities of mantle-plume derived mafic magma from rift environments. Exploration criteria used by companies investigating the Kalkarindji Flood Basalt Province for Noril'sk-style mineralization include the identification of: major controlling faults as potential feeder zones to prospective magmatic systems; depletion trends of Ni, Cu, and PGEs that indicate sulfur-saturated magmatic systems; and geochemical signatures highlighting the contamination of primitive magma(s) by basinal sedimentary successions.

7. Conclusions

Australia's nickel sulfide industry grew rapidly after the discovery in 1966 of the first significant nickel-sulfide ores at Kambalda, Western Australia. Many other komatiite-hosted deposits in the Yilgarn Craton commenced production within the first two years of their discovery and more than 90% of the nation's known global resources of nickel metal (~12.9 Mt) from sulfide deposits were discovered during the relative short period of 1966 to 1973. Australia is particularly well endowed with world-class (Mt Keith — 3.4 Mt, Perseverance — 2.5 Mt, Yakabindie — 1.7 Mt, Honeymoon Well-1 Mt, Kambalda camp — 1.4 Mt) and smaller high-grade (5 to 9%: Cosmos, Prospero, Long, Silver Swan, Victor) komatiite-associated deposits. However, the known global nickel resources of deposits hosted by tholeiitic mafic–ultramafic intrusions are substantially smaller than the major foreign deposits.

Australia's nickel sulfide deposits are associated with ultramafic and/or mafic igneous rocks in three major geotectonic settings: (1) Archean komatiites emplaced in rift zones of granite–greenstone belts; (2) Precambrian tholeiitic mafic–ultramafic intrusions emplaced in rift zones of Archean cratons or Proterozoic orogens; and (3) hydrothermal-remobilized occurrences with no apparent age or tectonic constraints. Most deposits can be classified into two orthomagmatic associations that reflect the dominant chemical affinities of the host magma (komatiitic or tholeiitic) and a third association that encompasses hydrothermal-remobilized mineralizing systems (Table 2). The largest, and economically the most important deposits, are associated with ~2700 Ma komatiitic rocks in the greenstone belts of the Yilgarn Craton of Western Australia. The ages of the major komatiitic- and tholeiitic-hosted deposits in Australia correlate with at least three major global-scale nickel-metallogenic events at ~3000 Ma, ~2700 Ma, and ~1900 Ma. These events correspond with major periods of juvenile crustal growth and the development of large volumes of primitive komatiitic and tholeiitic magmas interpreted to be caused by mantle overturn events associated with mantle plumes or larger superplumes.

Analysis of the major komatiite provinces of the world reveals that the most fertile komatiite sequences are generally of late Archean (~2700 Ma) or Paleoproterozoic (~1900 Ma to ~1800 Ma) age, have dominantly Al-undepleted ($Al_2O_3/TiO_2 = 15$ to 25) chemical affinities, and form compound sheet flows with internal pathways and dunitic compound sheet flow facies. The lava pathways assist in focusing large volumes of primitive magma flow and facilitate interaction of the magma with a potential sulfur-bearing substrate.

In contrast to komatiitic-mineralizing systems, the broad criteria for assessing the nickel prospectivity of tholeiitic mafic ± ultramafic intrusions and their provinces are less clear. However, a significant exploration advantage for investigating basal Ni–Cu–Co sulfide deposits (Sally Malay, Radio Hill, Nebo–Babel) is that they can occur in small- to medium-sized, sulfur-saturated mafic bodies, of various ages that may be layered or massive. Most Precambrian provinces in Australia and, in particular, Proterozoic orogenic belts, contain an abundance of these intrusions that have not been fully investigated. The Musgrave Province, Halls Creek Orogen, Albany–Fraser Orogen, Arunta Block, and western parts of the Yilgarn, Pilbara, and Gawler cratons are considered the more prospective provinces. The major exploration challenges for finding basal Ni–Cu–Co sulfide deposits are to determine the pre-deformational geometries and younging directions of the intrusions, and to locate structural irregularities and depressions in the basal contacts and feeder conduits under cover. Strata-bound PGE–Ni–Cu deposits in large Archean–Proterozoic layered mafic–ultramafic intrusions (Munni Munni, Panton) of tholeiitic affinity have similar global resources of nickel to most komatiite deposits in the Yilgarn Craton, but significantly lower grades (<0.2% Ni).

Hydrothermal-remobilized nickel sulfide deposits have diverse geological settings and metal associations that reflect the different compositions of the source rocks and fluids. Typically they are of small-tonnage status and of low economic importance. The unusual Avebury deposit in western Tasmania has increased the awareness of hydrothermal-type targets in Phanerozoic provinces that were previously considered to have low prospectivity. There is also potential for 'Noril'sk-type'

Ni–Cu–PGE deposits associated with major basaltic lava provinces of western and central Australia (e.g., late Archean Fortescue and Mesoproterozoic Warakurna igneous provinces, and Cambrian Kalkarindji Flood Basalts).

Acknowledgements

This manuscript draws on many informative discussions with the late Shen-su Sun, Yanis Miezitis, Mike Huleatt, Roy Towner, Tony Meixner, Jonathan Claoué-Long, Mitch Ratajkoski (all GA), and with many colleagues from the Northern Territory Geological Survey, Geological Survey of Western Australia, and the Department of Primary Industries and Resources, South Australia. Alan Whitaker (GA) provided valuable information regarding the distribution of komatiite belts under cover in the Yilgarn Craton. Neal Evans and Roy Towner (both GA) are acknowledged for their assistance in compiling the nickel resource data from OZMIN. Dorothy Close (NTGS) provided geochronology data for Table 3. Neale Jeffery and Chris Fitzgerald (both GA) drafted the line figures. The manuscript benefited from the constructive reviews of Michael Huleatt, Yanis Miezitis, and David Huston (all GA), and Journal reviewers Steve Barnes (CSIRO) and Franco Pirajno (GSWA). The authors publish with the permission of the Chief Executive Officer of Geoscience Australia.

References

ABARE, 2006a. Australian Mineral Statistics. Australian Bureau of Agricultural and Resource Economics, Canberra. December Quarter 2005, 15 March, 31 pp.

ABARE, 2006b. Australian Mineral Statistics. Australian Bureau of Agricultural and Resource Economics, Canberra. June Quarter 2006, pp. 339–341.

Abbott, D.H., Isley, A.E., 2002. The intensity, occurrence, and duration of superplume events and eras over geological time. Journal of Geodynamics 34, 265–307.

Abeysinghe, P.B., Flint, D.J., 2005. Nickel–cobalt in Western Australia: commodity review for 2004–05. Western Australia Geological Survey Annual Review 2004–05, pp. 20–26.

Agincourt Resources Limited, 2005. Agincourt Resources Limited Annual Report, 84 pp.

Ahmat, A.L., 1993. Mafic/ultramafic rocks of the Gindalbie Terrane: a review of the Bulong and Carr Boyd Complexes. An International Conference on Crustal Evolution, Metallogeny and Exploration of the Eastern Goldfields. Extended Abstracts. AGSO Record 1993/54, pp. 23–27.

Allegiance Mining NL, 2002. Allegiance Mining NL Annual Report 2002, p. 6.

Allegiance Mining NL, 2005. Allegiance Mining NL Australian Stock Exchange Announcement 20/5/2005, 2 pp.

Amelin, Y., Li, C., Naldrett, A.J., 1999. Geochronology of the Voisey's Bay intrusion, Labrador, Canada by precise U–Pb dating of coexisting baddeleyite, zircon, and apatite. Lithos 47, 33–51.

Anhaeusser, C.R., Maske, S. (Eds.), 1986. Mineral Deposits of Southern Africa, Volumes I and II. Geological Society of South Africa, 2376 pp.

Arndt, N.T., Nelson, D.R., Compston, W., Trendall, A.F., Thorne, A.M., 1991. The age of the Fortescue Group, Hamersley Basin, Western Australia, from ion microprobe zircon U–Pb results. Australian Journal of Earth Sciences 38, 261–281.

Arndt, N.T., Naldrett, A.J., Hunter, D.R., 1997. Ore deposits associated with mafic magmas in the Kaapvaal craton. Mineralium Deposita 32, 323–334.

Arndt, N.T., Lesher, C.M., Czamanske, G.K., 2005. Mantle-derived Magmas and Magmatic Ni–Cu–(PGE) Deposits, Economic Geology 100th Anniversary Volume, pp. 5–23.

AUSQUEST Limited, 2003. AUSQUEST Prospectus 2003. 63 pp.

AUSQUEST Limited, 2004. Quarterly Report for Period Ended 30 June 2004. AUSQUEST Limited, 6 pp.

Australian Bureau of Statistics, 2006. Mineral and Petroleum Exploration Australia 8412.0, December Quarter 2005 (Reissue). 16 March 2006, 18 pp.

Ayer, J.A., Amelin, Y., Corfu, F., Kamo, S., Ketchum, J., Kwok, K., Trowell, N., 2002. Evolution of the southern Abitibi greenstone belt based on U–Pb geochronology: autochthonous volcanic construction followed by plutonism, regional deformation and sedimentation. Precambrian Research 115, 63–95.

Baker, P.M., Waugh, R.S., 2005. The role of surface geochemistry in the discovery of the Babel and Nebo magmatic nickel–copper–PGE deposits. Geochemistry: Exploration, Environment, Analysis 5, 195–200.

Barley, M.E., Groves, D.I., 1990. Deciphering the tectonic evolution of Archaean greenstone belts: the importance of contrasting histories to the distribution of mineralization in the Yilgarn Craton, Western Australia. Precambrian Research 46, 3–20.

Barley, M.E., Brown, S.J.A., Cas, R.A.F., Cassidy, K.F., Champion, D. C., Gardoll, J., Krapez, B., 2003. An integrated geological and metallogenic framework for the eastern Yilgarn Craton: developing geodynamic models of highly mineralised Archean granite–greenstone terranes. AMIRA Project P624 Final Report, April 2003.

Barnes, G.J., 1994. Surrender report E80/1450—Corkwood Project. Poseidon Group Trading Ltd internal report number 6490 for the Department of Minerals and Energy, Western Australia, Item 7511, AN40093 (unpublished).

Barnes, G.B., 1995. Silver mineralisation at Elizabeth Hill, Munni Munni Complex, Western Australia. In: Ho, S.E., Amann, W.J. (Eds.), Recent Developments in Base Metal Geology and Exploration. Australian Institute of Geoscientists, Bulletin, vol. 16, pp. 89–94.

Barnes, S.J., 2004a. How nickel took off. Earthmatters. CSIRO Exploration, Mining Quarterly Magazine 4, 16–19.

Barnes, S.J., 2004b. Introduction to nickel sulfide orebodies and komatiites of the Black Swan area, Yilgarn Craton, Western Australia. Mineralium Deposita 39, 679–683.

Barnes, S.J., Hoatson, D.M., 1994. The Munni Munni Complex, Western Australia: stratigraphy, structure and petrogenesis. Journal of Petrology 35, 715–751.

Barnes, S.-J., Lightfoot, P.C., 2005. Formation of magmatic nickel sulfide deposits and processes affecting their copper and platinum group element contents. Economic Geology 100th Anniversary Volume, pp. 179–213.

Barnes, S.J., Keays, R.R., Hoatson, D.M., 1992. Distribution of sulphides and PGE within the porphyritic websterite zone of the Munni Munni Complex, Western Australia. Australian Journal of Earth Sciences 39, 289–302.

Barnes, S.-J., Couture, J.-F., Sawyer, E.W., Bouchaib, C., 1993. Nickel–copper occurrences in the Belleterre–Angliers Belt of the Pontiac Subprovince and the use of Cu–Pd Ratios in interpreting platinum-group element distributions. Economic Geology 88, 1402–1418.

Barnes, S.J., Hill, R.E.T., Perring, C.S., Dowling, S.E., 1999. Komatiite flow fields and associated Ni-sulphide mineralisation with examples from the Yilgarn Block, Western Australia. In: Keays, R.R., Lesher, C.M., Lightfoot, P.C. (Eds.), Dynamic Processes in Magmatic Ore Deposits and their Applications in Mineral Exploration. Geological Association of Canada Short Course, vol. 13, pp. 159–194.

Barnes, S.-J., Melezhik, V.A., Sokolov, S.V., 2001. The composition and mode of formation of the Pechenga nickel deposits, Kola Peninsula, northwestern Russia. Canadian Mineralogist 39, 447–471.

Barnes, S.J., Hill, R.E.T., Perring, C.S., Dowling, S.E., 2004a. Lithogeochemical exploration for komatiite-associated Ni-sulfide deposits: strategies and limitations. Mineralogy and Petrology 82, 259–293.

Barnes, S.J., Smith, T., Anderson, J., Kavanagh, M., 2004b. PGE mineralisation related to cyclic layering in the Mordor Complex, Northern Territory: an unusual association of PGE-enriched magmatic sulfides with cumulates from an ultrapotassic hydrous magma. 17th Australian Geological Convention. Dynamic Earth: Past, present and future, 8–13 February 2004, Hobart, Tasmania. Abstracts, vol. 73, p. 51.

Barrie, C.T., Naldrett, A.J., 1989. Geology and tectonic setting of the Montcalm Gabbroic Complex and Ni–Cu deposit, Western Abitibi Subprovince, Ontario, Canada. In: Prendergast, M.D., Jones, M.J. (Eds.), Magmatic Sulphides—The Zimbabwe Volume. The Institution of Mining and Metallurgy, London, pp. 151–163.

Barrie, C.T., Corfu, F., Davis, P., Coutts, A.C., MacEachern, D., 1999. Geochemistry of the Dundonald Komatiite–Basalt Suite and genesis of Dundeal Ni Deposit, Abitibi Subprovince, Canada. Economic Geology 94, 845–866.

Beresford, S.W., Rosengren, N.M., 2004. Komatiite-hosted Ni-Cu-PGE deposits of the Agnew-Wiluna greenstone belt–an overview. In: Neumayr, P., Harris, M., Beresford. S.W. (Compilers), Gold and Nickel Deposits in the Archaean Norseman-Wiluna Greenstone Belt, Yilgarn Craton, Western Australia; A Field Guide. SEG 2004: Predictive Mineral Discovery under Cover, Western Australia. Geological Survey of Western Australia, Record 2004/16, p. 87–91.

Beresford, S.W., Stone, W.E., 2004. Komatiite-hosted Ni-Cu-PGE deposits of the Kambalda nickel camp–an overview. In: Neumayr, P., Harris, M., Beresford. S.W. (Compilers), Gold and Nickel Deposits in the Archaean Norseman-Wiluna Greenstone Belt, Yilgarn Craton, Western Australia; A Field Guide: Predictive Mineral Discovery under Cover, Western Australia. Geological Survey of Western Australia, Record 2004/16, Geological Survey of Western Australia, Perth, Western Australia. Society of Economic Geologists (SEG) 2004, pp. 5–8.

Berkman, D.A., Mackenzie, D.H. (Eds.), 1998. Geology of Australian and Papua New Guinean Mineral Deposits. Monograph, vol. 22. The Australasian Institute of Mining and Metallurgy, Melbourne. 894 pp.

Betts, P.G., Giles, D., 2006. The 1800–1100 Ma tectonic evolution of Australia. Precambrian Research 144, 92–125.

Black, L.P., Gregory, P., Withnall, I.W., Bain, J.H.C., 1998. U–Pb zircon age for the Etheridge Group, Georgetown region, north Queensland: implications for relationship with the Broken Hill and Mt Isa sequences. Australian Journal of Earth Sciences 45, 925–935.

Black, L.P., McClenaghan, M.P., Korsch, R.J., Everard, J.L., Foudoulis, C., 2005. Significance of Devonian–Carboniferous igneous activity in Tasmania as derived from U–Pb SHRIMP dating of zircon. Australian Journal of Earth Sciences 52, 807–829.

Bleeker, W., Macek, J., 1996. Evolution of the Thompson Nickel Belt, Manitoba. Setting of the Ni–Cu Deposits in the Western Part of the Circular Superior Boundary Zone — Field Trip Guidebook A1, Geological Association of Canada/Mineralogical Association of Canada Annual Meeting. Winnipeg, Manitoba, May 27–19, 1996. 44 pp.

Bosch, D., Bruguier, O., Pidgeon, R.T., 1996. Evolution of an Archean Metamorphic Belt: A conventional and SHRIMP U–Pb study of accessory minerals from the Jimperding Metamorphic Belt, Yilgarn Craton, Western Australia. Journal of Geology 104, 695–711.

Brand, N.W., Butt, C.R.M., Elias, M., 1998. Nickel laterites: classification and features. AGSO Journal of Australian Geology and Geophysics 17, 81–88.

Brenner, T.L., Teixeira, N.A., Oliveira, J.A.L., Franke, N.D., Thompson, J.F.H., 1990. The O'Toole nickel deposit, Morro do Ferro Greenstone Belt, Brazil. Economic Geology 85, 904–920.

Bruguier, O., Bosch, D., Pidgeon, R.T., Byrne, D.I., Harris, L.B., 1999. U–Pb chronology of the Northampton Complex, Western Australia-evidence for Grenvillian sedimentation, metamorphism and deformation and geodynamic implications. Contributions to Mineralogy and Petrology 136, 258–272.

Burt, D.R.L., Sheppy, N.R., 1975. Mount Keith nickel sulphide deposit. In: Knight, C.L. (Ed.), Economic Geology of Australia and Papua New Guinea. 1. Metals. Australasian Institute of Mining and Metallurgy. Melbourne, Victoria, Australia. Monograph, vol. 5, pp. 159–168.

Cassidy, K.F., Champion, D.C., Fletcher, I.R., Dunphy, J.M., Black, L.P., Claoué-Long, J.C., 2002. Geochronological constraints on the Leonora–Laverton transect area, northeastern Yilgarn Craton. In: Cassidy, K.F. (Ed.), North Eastern Yilgarn Workshop. 20 June 2002, ARRC Auditorium, CSIRO, Kensington, Western Australia. Geoscience Australia, Workshop Notes, pp. 31–50.

Cassidy, K.F., Champion, D.C., Huston, D.L., 2005. Crustal evolution constraints on the metallogeny of the Yilgarn Craton. In: Mao, J., Bierlein, F.P. (Eds.), Mineral Deposit Research: Meeting the Global Challenge. Springer, pp. 901–904.

Chen, S.F., Morris, P.A., Pirajno, F., 2005. Occurrence of komatiites in the Sandstone greenstone belt, north-central Yilgarn Craton. Australian Journal of Earth Sciences 52, 959–963.

Claoué-Long, J.C., Hoatson, D.M., 2005. Proterozoic mafic–ultramafic intrusions in the Arunta Region, central Australia. Part 2. Event chronology and regional correlations. Precambrian Research 142, 134–158.

Claoué-Long, J.C., Compston, W., Cowden, A., 1988. The age of the Kambalda greenstones resolved by ion-microprobe: implications for Archaean dating methods. Earth and Planetary Science Letters 89, 239–259.

Clark, D.J., Kinny, P.D., Post, N.J., Hensen, B.J., 1999. Relationships between magmatism, metamorphism and deformation in the Fraser Complex, Western Australia: constraints from new SHRIMP U–Pb zircon geochronology. Australian Journal of Earth Sciences 46, 923–932.

Compston, D.M., 1994. The geochronology of the Tennant Creek Inlier and its ore deposits, Northern Territory, PhD thesis, Australian National University, Canberra (unpublished).

Condie, K.C., 1997. Plate Tectonics and Crustal Evolution, 4th edition. Butterworth-Heinemann, Oxford, United Kingdom. 282 pp.

Cooper, J.A., Dong, Y.B., 1983. Zircon age data from a greenstone of the Archaean Yilgarn Block, Australia: Mid-Proterozoic heating or uplift? Contributions to Mineralogy and Petrology 82, 397–402.

Cowden, A., Roberts, D.E., 1990. Komatiite hosted nickel sulphide deposits, Kambalda. In: Hughes, F.E. (Ed.), Geology of the Mineral Deposits of Australia and Papua New Guinea. Monograph, vol. 14. Australasian Institute of Mining and Metallurgy, Melbourne, pp. 567–581.

Cumming, G.L., Krstic, D., 1991. Geochronology at the Namew Lake Ni–Cu deposit, Flin Flon area, Manitoba, Canada: a Pb/Pb study of whole rocks and ore minerals. Canadian Journal of Earth Sciences 28, 1328–1339.

Dalstra, H.J., 1995. Metamorphic and structural evolution of greenstone belts of the Southern Cross–Diemals region of the Yilgarn Block, Western Australia, and its relationship to gold mineralisation. Unpublished PhD thesis, University of Western Australia, Perth.

Davies, D.W., Sutcliffe, R.H., 1985. U–Pb Ages from the Nipigon Plate and Northern Lake Superior. Geological Society of America Bulletin 96, 1572–1579.

De Angelis, M., Hoyle, M.W.H., Peters, W.S., Wightman, D., 1987. The nickel–copper deposit at Radio Hill, Karratha, Western Australia. Australasian Institute of Mining and Metallurgy Bulletin and Proceedings 292, 61–74.

De Angelis, M., Hoyle, M.W.H., Voermans, F.M., 1988. The Radio Hill Ni–Cu deposit and the Mount Sholl–Munni Munni mafic–ultramafic metallogenic province: a case of integrated exploration technique. Second International Conference on Prospecting in Arid Terrain, April 1988, Perth, Western Australia. Australasian Institute of Mining and Metallurgy, pp. 51–58.

Deblond, A., Tack, L., 1999. Main characteristics and review of mineral resources of the Kabanga–Musongati mafic–ultramafic alignment in Burundi. Journal of African Earth Sciences 29, 313–328.

Donaldson, M.J., 1974. Petrology of the Munni Munni Complex, Roebourne, Western Australia. Journal of the Geological Society of Australia 21, 1–16.

Donaldson, M.J., Lesher, C.M., Groves, D.I., Gresham, J.J., 1986. Comparison of Archean dunites and komatiites associated with nickel mineralisation in Western Australia. Mineralium Deposita 21, 266–305.

Dowling, S.E., Hill, R.E.T., 1998. Komatiite-hosted nickel sulphide deposits, Australia. Special Jubilee Issue of Australian Geological Survey Organisation Journal 17 (4), 121–127.

Doyle, M.G., Groenewald, B., Barley, M.E., Krapez, B., in press. Volcanic facies architecture of a basaltic seamount: the Late Archaean Minerie Sequence in the Kurnalpie Terrane, Eastern Goldfields Superterrane, Western Australia. Precambrian Research.

Dundas, A., 2004. WMC Nickel, Business development potential. WMC Resources Limited world wide web report, 28 October 2004, 31 p. (unpublished).

Eckstrand, O.R., 1995. Magmatic nickel–copper–platinum group elements. In: Eckstrand, O.R., Sinclair, W.D., Thorpe, R.I. (Eds.), Geology of Canadian Mineral Deposit Types. The Geology of North America Series, Geological Society of America, vol. P-1. Geological Survey of Canada, Geology of Canada, vol. 8, pp. 583–605.

Eckstrand, O.R., Yakubchuk, A., Good, D.J., Gall, Q., 2003. World Minerals Geoscience Database Project Beta Release 3.5 on 2003-06-20 (see references in: http://www4.geology.utoronto.ca/faculty/mungall/Website/DatabaseHome.htm).

Elias, M., 2002. Nickel laterite deposits—geological overview, resources and exploitation. In: Cooke, D.R., Pongratz, J. (Eds.), Giant Ore Deposits: Characteristics, Genesis, and Exploration. Centre for Ore Deposit Research Special Publication, vol. 4. University of Tasmania, Hobart, pp. 205–220.

Ernst, R.E., Buchan, K.L., 2001. Large mafic magmatic events through time and links to mantle-plume heads. In: Ernst, R.E., Buchan, K.L. (Eds.), Mantle Plumes: Their Identification Through Time. Geological Society of America Special Paper, vol. 352, pp. 483–575.

Evans-Lamswood, D.M., Butt, D.P., Jackson, R.S., Lee, D.V., Muggridge, M.G., Wheeler, R.I., 2000. Physical controls associated with the distribution of sulfides in the Voisey's Bay Ni–Cu–Co deposit, Labrador. Economic Geology 95, 749–769.

Falcon Minerals Limited, 2004. Falcon Minerals Limited Project Summary. . November 2004: www.falconminerals.com.au.

Ferreira Filho, C.F., Lesher, C.M., 2001. The komatiite-associated Ni-sulfide deposit of Boa Vista, Brazil. In: Cassidy, K.F., Dunphy, J.M., Van Kranendonk, M.J. (Eds.), 4th International Archaean Symposium 2001, Extended Abstracts. AGSO-Geoscience Australia, Record 2001/37, pp. 429–431.

Fletcher, I.R., Libby, W.G., Rosman, K.J.R., 1987. Sm–Nd dating of the 2411 Ma Jimberlana Dyke, Yilgarn Block, Western Australia. Geological Note. Australian Journal of Earth Sciences 34, 523–525.

Fletcher, I.R., Myers, J.S., Ahmat, A.L., 1991. Isotope evidence on the age and origin of the Fraser Complex, Western Australia: a sample of Mid-Proterozoic lower crust. Chemical Geology 87, 197–216.

Fletcher, I.R., Dunphy, J.M., Cassidy, K.F., Champion, D.C., 2001. Compilation of SHRIMP U–Pb geochronological data, Yilgarn Craton, Western Australia, 2000–2001. Geoscience Australia Record 2001/47, pp. 44–47.

Flint, D.J., Searston, S.M., Cooper, R.W., Abeysinghe, P.B., 2005. Nickel–cobalt in Western Australia commodity review for 2003. Western Australia Geological Survey Record 2005/3, 38 pp.

Freyssinet, Ph., Butt, C.R.M., Morris, R.C., Piantone, P., 2005. Ore-forming processes related to lateritic weathering. Economic Geology 100th Anniversary Volume, pp. 681–722.

Frick, L.R., Lambert, D.D., Hoatson, D.M., 2001. Re–Os dating of the Radio Hill Ni–Cu deposit, west Pilbara Craton, Western Australia. Australian Journal of Earth Sciences 48, 43–47.

Geoscience Australia, in press. Geoscience Australia 2006. Australia's Identified Mineral Resources 2006. Geoscience Australia, Canberra, Australia.

Giblin, P.E., 1984. History of exploration and development, of geological studies and development of geological concepts. In: Pye, E.G., Naldrett, A.G., Giblin, P.E. (Eds.), The Geology and Ore Deposits of the Sudbury Structure. Ontario Geological Survey Special Volume 1, pp. 3–23.

Giralia Resources NL, 2004. Giralia Resources NL Annual General Meeting presentation 25 November 2004 (unpublished).

Glass, L.M., Bennett, V.C., Philips, D., 2004. A new flood basalt province from northern Australia: geochronology and petrogenesis of the Cambrian Kalkarindji low-Ti basalts. 2004 Goldschmidt Conference, Abstracts. Geochimica et Cosmochimica Acta 68 (11), A585 (Supplement 1).

Glikson, A.Y., Stewart, A.J., Ballhaus, C.G., Clarke, G.L., Feeken, E.H.J., Leven, J.H., Sheraton, J.W., Sun, S.-S., 1996. Geology of the western Musgrave Block, central Australia, with particular reference to the mafic–ultramafic Giles Complex. Australian Geological Survey Organisation Bulletin 239, 206 pp.

Greenfield, J.E., Chen, S.F., 1999. Structural evolution of the Merda–Diemals area, Southern Cross Province. Western Australia Geological Survey, Annual Review 1998–99, pp. 68–73.

Gresham, J.J., 1990. Nickel sulphide deposits of Western Australia — the discovery of the Kambalda nickel deposits. In: Glasson, K.R., Rattigan, J.H. (Eds.), Geological Aspects of the Discovery of Some Important Mineral Deposits in Australia. Monograph, vol. 17. Australasian Institute of Mining and Metallurgy, pp. 395–396.

Groenewald, P.B., Painter, M.G.M., Roberts, F.I., McCabe, M., Fox, A., 2000. East Yilgarn Geoscience Database, 1 : 100 000 geology Menzies to Norseman—An Explanatory Note. Western Australia Geological Survey, Report 78, 53 pp.

Groves, D.I., Batt, W.D., 1984. Spatial and temporal variations of Archaean metallogenic associations in terms of evolution of granitoid–greenstone terrains with particular emphasis on the Western Australian Shield. In: Kroner, A., Hanson, G.N., Goodwin, A.M. (Eds.), Archean Geochemistry. Springer-Verlag, Berlin, pp. 73–98.

Groves, D.I., Hudson, D.R., 1990. Nickel sulphide deposits of Western Australia — exploration for nickel sulphide ores. In: Glasson, K.R., Rattigan, J.H. (Eds.), Geological Aspects of the Discovery of some Important Mineral Deposits in Australia. Monograph, vol. 17. Australasian Institute of Mining and Metallurgy, pp. 421–428.

Groves, D.I., Condie, K.C., Goldfarb, R.J., Hronsky, J.M.A., Vielreicher, R.M., 2005. Secular changes in global tectonic processes and their influence on the temporal distribution of gold-bearing mineral deposits. Economic Geology 100, 203–224.

Hamlyn, P.R., 1980. Equilibration history and phase chemistry of the Panton Sill, Western Australia. American Journal of Science 280, 631–668.

Hamlyn, P.R., Keays, R.R., 1979. Origin of chromite compositional variation in the Panton Sill, Western Australia. Contributions to Mineralogy and Petrology 69, 75–82.

Hanley, L.M., Wingate, M.T.D., 2000. SHRIMP zircon age for an Early Cambrian dolerite dyke: an intrusive phase of the Antrim Plateau Volcanics of northern Australia. Australian Journal of Earth Sciences 47, 1029–1040.

Hanski, E., Huhma, H., Smolkin, V.F., Vaasjoki, M., 1990. The age of the ferropicritic volcanics and comagmatic Ni-bearing intrusions at Pechenga, Kola Peninsula, USSR. Bulletin of the Geological Society of Finland 62, 123–133.

Hanski, E., Walker, R.J., Huhma, H., Polyakov, G.V., Balykin, P.A., Hoa, T.T., Phuong, N.T., 2004. Origin of the Permian–Triassic komatiites, northwestern Vietnam. Contributions to Mineralogy and Petrology 147, 453–469.

Harrison, P.H., 1990. Nickel. Geology and mineral resources of Western Australia. Western Australia Geological Survey Memoir, vol. 3, pp. 702–709.

Helix Resources Limited, 2004. Helix Resources Limited Annual Report 2004, 57 pp.

Hill, R.E.T., Gole, M.J., Barnes, S.J., 1987. Physical volcanology of komatiites. Excursion Guidebook Number 1. Geological Society of Australia, Western Australia. 74 pp.

Hill, R.E.T., Barnes, S.J., Perring, C.S., 1996. Komatiite volcanology and the volcanogenic setting of associated magmatic nickel deposits. In: Grimsey, E.J., Neuss, I. (Eds.), Nickel '96 Mineral to Market. Kalgoorlie, 27–29 November 1996. Australasian Institute of Mining and Metallurgy, Publication Series, vol. 6/96, pp. 91–95.

Hoatson, D.M., 1984. Potential for platinum group mineralisation in Australia. A review. Bureau of Mineral Resources Australia, Record 1984/1, 84 pp.

Hoatson, D.M., 1998. Platinum-group element mineralisation in Australian Precambrian layered mafic–ultramafic intrusions. AGSO Journal of Australian Geology, Geophysics 17 (4), 139–151.

Hoatson, D.M., 2001. Metallogenic potential of mafic–ultramafic intrusions in the Arunta Province, central Australia: some new insights. AGSO Research Newsletter 34, 29–33.

Hoatson, D.M., Blake, D.H. (Eds.), 2000. Geology and economic potential of the Palaeoproterozoic layered mafic–ultramafic intrusions in the East Kimberley, Western Australia. Australian Geological Survey Organisation Bulletin, vol. 246, 476 pp.

Hoatson, D.M., Glaser, L.M., 1989. Geology and economics of platinum-group metals in Australia. Bureau of Mineral Resources, Australia, Resource Report, vol. 5, 81 pp.

Hoatson, D.M., Keays, R.R., 1989. Formation of platiniferous sulfide horizons by crystal fractionation and magma mixing in the Munni Munni layered intrusion, west Pilbara Block, Western Australia. Economic Geology 84, 1775–1804.

Hoatson, D.M., Sun, S.-S., 2002. Archean layered mafic–ultramafic intrusions in the west Pilbara Craton, Western Australia: a synthesis of some of the oldest orthomagmatic mineralizing systems in the world. Economic Geology 97, 847–872.

Hoatson, D.M., Wallace, D.A., Sun, S.-S., Macias, L.F., Simpson, C.J., Keays, R.R., 1992. Petrology and platinum-group-element geochemistry of Archaean layered mafic–ultramafic intrusions, west Pilbara Block, Western Australia. Australian Geological Survey Organisation Bulletin 242, 320 pp.

Hoatson, D.M., Sproule, R.A., Lambert, D.D., 1997. Are there Voisey's Bay-type Ni–Cu–Co sulphide deposits in the East Kimberley of Western Australia? AGSO Research Newsletter 27, 17–19.

Hoatson, D.M., Sun, S.-S., Claoué-Long, J.C., 2005a. Proterozoic mafic–ultramafic intrusions in the Arunta Region, central Australia. Part 1: geological setting and mineral potential. Precambrian Research 142, 93–133.

Hoatson, D.M., Sun, S.-S., Duggan, M.B., Davies, M.B., Daly, S.J., Purvis, A.C., 2005b. Late Archean Lake Harris Komatiite, central Gawler Craton, South Australia: geologic setting and geochemistry. Economic Geology 100, 349–374.

Hopf, S., Head, D.L., 1998. Mount Keith nickel deposit. In: Berkman, D.A., Mackenzie, D.H. (Eds.), Geology of Australian and Papua New Guinean Mineral Deposits. . Monograph, vol. 22. Australasian Institute of Mining and Metallurgy, Melbourne, pp. 307–314.

Howland-Rose, A.W., 2005. Avebury, Tasmania: a unique nickel deposit type. Prospectors and Developers Association of Canada Convention 2005, Toronto, Canada, March 6–9, 2005. C-D ROM.

Hudson, D.R., 1990. Nickel sulphide deposits of Western Australia — evolution of geological concepts. In: Glasson, K.R., Rattigan, J.H. (Eds.), Geological Aspects of the Discovery of Some Important Mineral Deposits in Australia. . Monograph, vol. 17. Australasian Institute of Mining and Metallurgy, Melbourne, pp. 397–420.

Hughes, F.E. (Ed.), 1990. Geology of the mineral deposits of Australia and Papua New Guinea, Monograph, vol. 14, Volume 1. The Australasian Institute of Mining and Metallurgy, Melbourne, 982 pp.

Hulbert, L.J., 1997. Geology and metallogeny of the Kluane Mafic–Ultramafic Belt, Yukon Territory, Canada: Eastern Wrangellia — a new Ni–Cu–PGE metallogenic terrane. Bulletin 506, Geological Survey of Canada, Canada Communications Group, Publication code M42-506E, 265 pp.

Hulbert, L.J., Eckstrand, R., 2005. Magmatic nickel–copper–platinum group element deposits. Abstract. Prospectors and Developers Association of Canada Convention 2005, Toronto, Canada, March 6–9, 2005. CD-ROM.

Hulbert, L.J., Hamilton, M.A., Horan, M.F., Scoates, R.F.J., 2005. U–Pb zircon and Re–Os isotope geochronology of mineralized ultramafic intrusions and associated nickel ores from the Thompson nickel belt, Manitoba, Canada. Economic Geology 100, 29–41.

Jagodzinski, E.J., 2005. Compilation of SHRIMP U–Pb geochronological data, Olympic Domain, Gawler Craton, South Australia, 2001–2003. Geoscience Australia Record 2005/20. 197 pp.

Jaques, A.L., Jaireth, S., Walshe, J.L., 2002. Mineral systems of Australia: an overview of resources, settings and processes. Australian Journal of Earth Sciences 49, 623–660.

Jaques, A.L., Huleatt, M.B., Ratajkoski, M., Towner, R.R., 2005. Exploration and discovery of Australia's copper, nickel, lead, and zinc resources 1976–2005. Resources Policy 30, 168–185.

Johnson, J.P., 1993. The geochronology and radiogenic isotope systematics of the Olympic Dam copper–uranium–gold–silver deposit, South Australia. Unpublished PhD thesis, Australian National University, Canberra.

Juhas, A.P., 1995. Metamorphic dehydration of serpentinite as a source of nickel in nickel–copper (±zinc) sulphide iron formations. In: Pašava, J., Køíbek, B., ák, K. (Eds.), Mineral Deposits: From Their Origin to Their Environmental Impacts. Balkema, Rotterdam, pp. 873–876.

Kamo, S.L., Czamanske, G.K., Amelin, Y., Fedorenko, V.A., Davis, D.W., Trofimov, V.R., 2003. Rapid eruption of Siberian flood-volcanic rocks and evidence for coincidence with the Permian–Triassic boundary and mass extinction at 251 Ma. Earth and Planetary Science Letters 214, 75–91.

Kent, A.J.R., Hagemann, S.G., 1996. Constraints on the timing of lode-gold mineralisation in the Wiluna greenstone belt, Yilgarn Craton, Western Australia. Australian Journal of Earth Sciences 43, 573–588.

Kinny, P.D., Williams, I.S., Froude, D.O., Ireland, T.R., Compston, W., 1988. Early Archaean zircon ages from orthogneisses and anorthosites at Mount Narryer, Western Australia. Precambrian Research 38, 325–341.

Kositcin, N., Brown, S.J.A., Barley, M.E., Krapez, B., Cassidy, K.F., Champion, D.C., in press. SHRIMP U–Pb zircon age constraints on the Late Archaean tectonostratigraphic architecture of the Eastern Goldfields Superterrane, Yilgarn Craton, Western Australia. Precambrian Research.

Krogh, T.E., Davis, D.W., Corfu, F., 1984. Precise U–Pb zircon and baddeleyite ages for the Sudbury area. In: Pye, E.G., Naldrett, A.J., Giblin, P.E. (Eds.), The Geology and Ore Deposits of the Sudbury Structure. Ontario Geological Survey, Special Volume 1, pp. 431–446.

Kruger, F.J., Cawthorn, R.G., Meyer, P.S., Walsh, K.L., 1986. Sr-isotopic, chemical and mineralogical variations across the pyroxenite marker and in the Upper Zone of the western Bushveld Complex. Geo-congress '86, 21st Congress, Johannesburg. Geological Society of South Africa, Abstract, pp. 609–612.

Kuck, P.H., 2006. Nickel. United States Geological Survey, Mineral Commodity Summaries, January 2006. United States Geological Survey, pp. 116–117.

Lesher, C.M., 1989. Komatiite-associated nickel sulfide deposits. In: Whitney, J.A., Naldrett, A.J. (Eds.), Ore Deposition Associated with Magmas. Reviews in Economic Geology, vol. 4, pp. 45–101.

Lesher, C.M., 2004. Footprints of magmatic Ni–Cu(–PGE) systems. In: Muhling, J., Goldfarb, R., Vielreicher, N., Bierlein, F., Stumpfl, E., Groves, D.I., Kenworthy, S. (Eds.), SEG 2004: Predictive Mineral Discovery under Cover. Extended Abstracts. Centre of Global Metallogeny, The University of Western Australia, Publications No. 33, 27 September–1 October 2004, Perth, Western Australia, pp. 117–120.

Lesher, C.M., Keays, R.R., 2002. Komatiite-associated Ni–Cu–PGE deposits: geology, mineralogy, geochemistry, and genesis. In: Cabri, L.J. (Ed.), The Geology, Geochemistry, Mineralogy and Mineral Beneficiation of Platinum-Group Elements. Canadian Institute of Mining, Metallurgy and Petroleum, Special Volume 54, pp. 579–617.

Lesher, C.M., Burnham, O.M., Keays, R.R., Barnes, S.J., Hulbert, L., 2001. Geochemical discrimination of barren and mineralized komatiites associated with magmatic Ni–Cu–(PGE) sulphide deposits. Canadian Mineralogist 39, 673–696.

Li, X., Su, L., Song, B., Liu, D., 2004. SHRIMP U–Pb zircon age of the Jinchuan ultramafic intrusion and its geological significance. Chinese Science Bulletin 49, 420–422.

Liu, S.F., Champion, D.C., Cassidy, K.F., 2002. Geology of the Sir Samuel 1:250 000 sheet area, Western Australia. Geoscience Australia Record 2002/14, 57 pp.

Maier, W., 2004. Magmatic Ni–Cu–PGE sulfide deposits in southern and central Africa: recent exploration activities Abstract. Geological Society of Australia Abstracts, vol. 73, p. 9.

Marshall, A.E., 2000. Low temperature–low pressure ('epithermal') siliceous vein deposits of the North Pilbara granite–greenstone terrane, Western Australia. AGSO Record 2000/1,40 pp.

Marston, R.J., 1984. Nickel mineralization in Western Australia. Geological Survey of Western Australia. Mineral Resources Bulletin 14, 271 pp.

McCready, A.J., Stumpfl, E.F., Lally, J.H., Ahmad, M., Gee, R.D., 2004. Polymetallic mineralization at the Browns Deposit, Rum Jungle Mineral Field, Northern Territory, Australia. Economic Geology 99, 257–277.

McNaughton, N.J., Compston, W., Barley, M.E., 1993. Constraints on the age of the Warrawoona Group, eastern Pilbara Block, Western Australia. Precambrian Research 60, 69–98.

Meisel, T., Moser, J., Wegscheider, W., 2001. Recognizing heterogeneous distribution of platinum group elements (PGE) in geological materials by means of the Re–Os isotope system. Fresenius' Journal of Analytical Chemistry 370, 566–572.

Meixner, T., Hoatson, D.M., 2004. Geophysical interpretation of Proterozoic mafic–ultramafic intrusions in the Arunta Region, central Australia. Geoscience Australia Record 2003/29, 125 pp.

Miller, L.J., Smith, M.E., 1975. Sherlock Bay nickel–copper. In: Knight, C.L. (Ed.), Economic Geology of Australia and Papua New Guinea. 1. Metals. . Monograph, vol. 5. Australasian Institute of Mining and Metallurgy, pp. 168–174.

Mithril Resources Limited, 2005. Mithril Resources Limited Annual Report 2005, 56 pp.

Morris, P.A., Pirajno, F., 2005. Mesoproterozoic sill complexes in the Bangemall Supergroup, Western Australia: geology, geochemistry, and mineralization potential. Western Australia Geological Survey Report, vol. 99, 75 pp.

Morrison, K.C., Reed, A.R., Turner, N.J., 2003. Regional map set and geophysical signatures of major deposits. Western Tasmanian regional minerals program: Devonian granite aureoles project. Tasmanian Geological Survey Record 2003/13, pp. 1–23.

Mukasa, S.B., Wilson, A.H., Carlson, R.W., 1998. A multielement geochronologic study of the Great Dyke, Zimbabwe: significance of the robust and reset ages. Earth and Planetary Science Letters 164, 353–369.

Müller, S.G., Krapez, B., Barley, M.E., Fletcher, I.R., 2005. Giant ore-deposits of the Hamersley province related to the breakup of Paleoproterozoic Australia: new insights from in situ SHRIMP dating of baddeleyite from mafic intrusions. Geology 33, 577–580.

Myers, J.S., Shaw, R.S., Tyler, I.M., 1996. Tectonic evolution of Proterozoic Australia. Tectonics 15, 1431–1446.

Naldrett, A.J., 1981. Nickel sulfide deposits: classification, composition, and genesis. Economic Geology 628–685 (75th Anniversary Volume).

Naldrett, A.J., 1989. Magmatic Sulfide Deposits. Clarendon Press, New York, 177 pp.

Naldrett, A.J., 1993. Models for the formation of strata-bound concentrations of platinum-group elements in layered intrusions.

In: Kirkham, R.V., Sinclair, W.D., Thorpe, R.I., Duke, J.M. (Eds.), Mineral Deposit Modeling. Geological Association of Canada, Special Paper, vol. 40, pp. 373–387.

Naldrett, A.J., 1997. Key factors in the genesis of Noril'sk, Sudbury, Jinchuan, Voisey's Bay and other world-class Ni–Cu–PGE deposits: implications for exploration. Australian Journal of Earth Sciences 44, 283–315.

Naldrett, A.J., 2002. Requirements for forming giant Ni–Cu sulfide deposits. In: Cooke, D.R., Pongratz, J. (Eds.), Giant Ore Deposits: Characteristics, Genesis, and Exploration. . Centre for Ore Deposit Research Special Publication, vol. 4. University of Tasmania, Hobart, pp. 195–204.

Naldrett, A.J., 2004. Magmatic Sulfide Deposits; Geology, Geochemistry and Exploration. Springer-Verlag, Berlin, 727 pp.

Nelson, D.R., 1997a. Evolution of the Archaean granite–greenstone terranes of the Eastern Goldfields, Western Australia: SHRIMP U–Pb constraints. Precambrian Research 83, 57–81.

Nelson, D.R., 1997b. Compilation of SHRIMP U–Pb zircon geochronology data 1996. Western Australia Geological Survey Record 1997/2, 189 pp.

Nelson, D.R., 1998. Compilation of SHRIMP U–Pb zircon geochronology data 1997. Western Australia Geological Survey Record 1998/2, 242 pp.

Nelson, D.R., 2001. Compilation of geochronology data, 2000. Western Australia Geological Survey, Record 2001/2, pp. 81–86.

Nemchin, A.A., Pidgeon, R.T., 1998. Precise conventional and SHRIMP baddeleyite U–Pb age for the Binneringie Dyke, near Narrogin, Western Australia. Australian Journal of Earth Sciences 45, 673–675.

Nemchin, A.A., Pidgeon, R.T., Wilde, S.A., 1994. Timing of Late Archaean granulite facies metamorphism in the southwestern Yilgarn Craton of Western Australia: evidence from U–Pb ages of zircons from mafic granulites. Precambrian Research 68, 307–321.

Neradovsky, Y.N., Borisova, V.V., Sholokhnev, V.V., 1997. The Monchegorsk layered complex and related mineralization. In: Mitrofanov, F., Torokhov, F., Iljina, M. (Eds.), Ore Deposits of the Kola Peninsula, Northwestern Russia. Geological Survey of Finland Guide 45, Excursion Guidebook B4, pp. 13–17.

Newnham, L., 2003. Development of Avebury nickel sulphide deposit. Presentation at Australian Nickel Conference, Perth, October 2003. Report to Allegiance Mining NL, 1–6 (unpublished).

Paces, J.B., Miller Jr., J.D., 1993. Precise U–Pb ages of Duluth Complex and related mafic intrusions, northeastern Minnesota; geochronological insights to physical, petrogenetic, paleomagnetic, and tectonomagnetic processes associated with the 1.1 Ga Midcontinent Rift System. Journal of Geophysical Research, B, Solid Earth and Planets 98, 13997–14013.

Page, R.W., 1983. Chronology of magmatism, skarn formation, and uranium mineralization, Mary Kathleen, Queensland, Australia. Economic Geology 78, 838–853.

Page, R.W., Hoatson, D.M., 2000. Geochronology of the mafic–ultramafic intrusions. In: Hoatson, D.M., Blake, D.H. (Eds.), Geology and Economic Potential of the Palaeoproterozoic Layered Mafic–ultramafic Intrusions in the East Kimberley, Western Australia. Australian Geological Survey Organisation Bulletin, vol. 246, pp. 163–172.

Paktunc, A.D., 1987. Nickel, copper, platinum and palladium relations in Ni–Cu deposits of the St Stephen Intrusion, New Brunswick. Current Research—Geological Survey of Canada 87-1A, pp. 543–553.

Papunen, H., Gorbunov, G.I. (Eds.), 1985. Nickel–copper deposits of the Baltic Shield and Scandinavian Caledonides. Geological Survey of Finland Bulletin, vol. 333, 394 pp.

Papunen, H., Vorma, A., 1985. Nickel–copper deposits in Finland, a review. In: Papunen, H., Gorbunov, G.I. (Eds.), Nickel–Copper Deposits of the Baltic Shield and Scandinavian Caledonides. Geological Survey of Finland Bulletin, vol. 333, pp. 123–143.

Parrish, R.R., 1989. U–Pb Geochronology of the Cape Smith Belt and Sugluk Block, Northern Quebec. Geoscience Canada 16, 126–130.

Perring, C., Barnes, S., 2002. Nickel. CSIRO Exploration and Mining nickel www site at www.em.csiro.au/em/commodities/nickel/index.html.

Perring, R.J., Vogt, J.H., 1991. The Panton Sill. In: Barnes, S.J., Hill, R.E.T. (Eds.), Mafic-ultramafic complexes of Western Australia. Excursion Guidebook 3. Sixth International Platinum Symposium, July 1991, Perth, Western Australia. IAGOD and the Geological Society of Australia, p. 97–106.

Perring, C.S., Barnes, S.J., Hill, R.E.T., 1996. Geochemistry of Archaean komatiites from the Forrestania Greenstone Belt, Western Australia: evidence for supracrustal contamination. Lithos 37, 181–197.

Pidgeon, R.T., Cook, T.J.F., 2003. 1214±5 Ma dyke from the Darling Range, southwestern Yilgarn Craton, Western Australia. Australian Journal of Earth Sciences 50, 769–773.

Pidgeon, R.T., Hallberg, J.A., 2000. Age relationships in supracrustal sequences of the northern part of the Murchinson Terrane, Archaean Yilgarn Craton, Western Australia: a combined field and zircon U–Pb study. Australian Journal of Earth Sciences 47, 153–165.

Pidgeon, R.T., Nemchin, A.A., 2001. 1.2 Ga mafic dyke near York, southwestern Yilgarn, Craton, Western Australia. Australian Journal of Earth Sciences 48, 751–755.

Pidgeon, R.T., Wilde, S.A., 1990. The distribution of 3.0 and 2.7 Ga volcanic episodes in the Yilgarn Craton of Western Australia. Precambrian Research 48, 309–325.

Pirajno, F., 2004. Hotspots and mantle plumes: global intraplate tectonics, magmatism and ore deposits. Mineralogy and Petrology 82, 183–216.

Pirajno, F., Morris, P., 2005. Large igneous provinces in Western Australia: implications for Ni–Cu and Platinum Group Elements (PGE) mineralization. In: Mao, J., Bierlein, F.P. (Eds.), Mineral Deposit Research: Meeting the Global Challenge. Springer, pp. 1049–1052.

Pirajno, F., Smithies, H.R., Howard, H.M., in press. Mineralisation associated with the 1076 Ma Giles mafic–ultramafic intrusions, Musgrave Complex, central Australia: A review. SGA Newsletter.

Platinum Australia Limited, 2005. Platinum Australia Limited Report to the Australian Stock Exchange Limited, 7 December 2005 (unpublished).

Prendergast, M.D., 2003. The nickeliferous Late Archean Reliance Komatiitic Event in the Zimbabwe Craton — magmatic architecture, physical volcanology, and ore genesis. Economic Geology 98, 865–891.

Prendergast, M.D., Jones, M.J. (Eds.), 1989. Magmatic Sulphides — the Zimbabwe Volume. The Institution of Mining and Metallurgy, London, 254 pp.

Pratt, R., 1996. Australia's Nickel Resources. Bureau of Resource Sciences, Canberra, 52 pp.

Puchtel, I.S., Zhuraview, D.Z., Samsonov, A.V., Arndt, N.T., 1993. Petrology and geochemistry of metamorphosed komatiites and basalts from the Tungurcha greenstone belt, Aldan Shield. Precambrian Research 62, 399–418.

Purvis, A.C., Nesbitt, R.W., Hallberg, J.A., 1972. The geology of part of the Carr–Boyd Rocks complex, and its associated nickel mineralisation, Western Australia. Economic Geology 67, 1093–1113.

Reid, J.G., 1996. Laterite ores — nickel and cobalt resources for the future. In: Grimsey, E.J., Neuss, I. (Eds.), Nickel '96 Mineral to

Market. Kalgoorlie, 27–29 November 1996. Australasian Institute of Mining and Metallurgy, Publication Series 6/96, pp. 11–16.

Rosengren, N.M., Beresford, S.W., Grguric, B.A., Cas, R.A.F., 2005. An intrusive origin for the komatiitic–dunite hosted Mount Keith disseminated nickel sulfide deposit, Western Australia. Economic Geology 100, 149–156.

Ruddock, I., 1999. Mineral Occurrences and Exploration Potential of the West Pilbara. Western Australia Geological Survey Report, vol. 70, 63 pp.

Sanders, T.S., 1999. Mineralization of the Halls Creek Orogen, east Kimberley region, Western Australia. Geological Survey of Western Australia, Report 66 and Appendix, 44 pp.

Scoates, J.S., Mitchell, J.N., 2000. The evolution of troctolite and high Al basaltic magmas in Proterozoic anorthosite plutonic suites and implications for the Voisey's Bay massive Ni–Cu sulfide deposit. Economic Geology 95, 677–701.

Scoon, R.N., Mitchell, A.A., 2004. The platiniferous dunite pipes in the eastern limb of the Bushveld Complex; review and comparison with unmineralized discordant ultramafic bodies. South African Journal of Geology 107, 505–520.

Seabrook, C.L., Prichard, H.M., Fisher, P.C., 2004. Platinum-group minerals in the Raglan Ni–Cu–(PGE) sulfide deposit, Cape Smith, Quebec, Canada. Canadian Mineralogist 42, 485–497.

Seat, Z., Beresford, S.W., Gee, M.A.M., Grguric, B.A., Groves, D.I., Hronsky, J.M.A., Mathison, C.I., Waugh, R., 2005. Geological and geochemical architecture of the Nebo and Babel Ni–Cu–PGE deposit, West Musgrave, Western Australia. Proceedings, 10th International Platinum Symposium, Oulu, Finland, pp. 227–230.

Sheard, M.J., Robertson, I.D.M., 2002. Regolith morphology and geochemistry over greenstones; what works and what does not? Gawler Craton, South Australia: Gawler Craton 2002: State of Play Workshop, Regional concepts and data for targeting ore systems in the Gawler Craton, 5–6 December 2002, Adelaide. Minerals and Energy Resources of South Australia. CD-ROM.

Sherlock Bay Nickel Corporation Limited, 2005. Sherlock Bay Nickel Corporation Limited Annual General Meeting, Announcement to Australian Stock Exchange, 30 November 2005, 27 pp.

Solomon, M., Groves, D.I., 1994. The Geology and Origin of Australia's Mineral Deposits. Oxford Monographs on Geology and Geophysics, vol. 24. Oxford University Press Inc., New York, 951 pp.

Sproule, R.A., Lesher, C.M., Ayer, J.A., Thurston, P.C., Herzberg, C. T., 2002. Spatial and temporal variations in the geochemistry of komatiites and komatiitic basalts in the Abitibi greenstone belt. Precambrian Research 115, 153–186.

Stone, W.E., Archibald, N.J., 2004. Structural controls on nickel sulphide ore shoots in Archaean komatiite, Kambalda, WA; the volcanic trough controversy revisited. Journal of Structural Geology 26, 1173–1194.

Thornett, J.R., 1981. The Sally Malay deposit: gabbroid associated nickel–copper sulfide mineralization in the Halls Creek Mobile Zone, Western Australia. Economic Geology 76, 1565–1580.

Thorpe, R.I., Hickman, A.H., Davis, D.W., Mortensen, J.K., Trendall, A. F., 1992. U–Pb zircon geochronology of Archaean felsic units in the Marble Bar region, Pilbara Craton, Western Australia. Precambrian Research 56, 169–189.

Townsend, D.B., Preston, W.A., 1991. Reported nickel resources of Western Australia as at December 1990. Geological Survey of Western Australia Record 1991/9, 35 pp.

Tyler, I.M., Hocking, R.M., 2002. A revision of the tectonic units of Western Australia. Western Australia Geological Survey Annual Review 2000-01, pp. 33–44.

Van Kronendonk, M.J., 2000. Geology of the North Shaw 1:100 000 sheet. Western Australia Geological Survey, 1:100 000 Geological Series Explanatory Notes, 86 pp.

Vulcan Resources Limited, 2005. Vulcan Resources Limited Annual Report 2005, 65 pp.

Walker, R.J., Storey, M., Kerr, A.C., Tarney, J., Arndt, N.T., 1999. Implications of ^{187}Os isotopic heterogeneities in a mantle plume: evidence from Gorgona Island and Curaçao. Geochimica et Cosmochimica Acta 63, 713–728.

Wang, Q., Schiøtte, L., Campbell, I.H., 1996. Geochronological constraints on the age of komatiites and nickel mineralisation in the Lake Johnston greenstone belt, Yilgarn Craton, Western Australia. Australian Journal of Earth Sciences 43, 381–385.

Wilde, S.A., Pidgeon, R.T., 1986. Geology and geochronology of the Saddleback Greenstone Belt in the Archaean Yilgarn Block, southwest Australia. Australian Journal of Earth Sciences 33, 491–501.

Wingate, M.T.D., 1999. Ion microprobe baddeleyite and zircon ages for Late Archaean mafic dykes of the Pilbara Craton, Western Australia. Australian Journal of Earth Sciences 46, 493–500.

Wingate, M.T.D., Giddings, J.W., 2000. Age and palaeomagnetism of the Mundine Well dyke swarm, Western Australia: implications for an Australia–Laurentia connection at 755 Ma. Precambrian Research 100, 335–357.

Wingate, M.T.D., Campbell, I.H., Compston, W., Gibson, G.M., 1998. Ion microprobe U–Pb ages for Neoproterozoic basaltic magmatism in south-central Australia and implications for the breakup of Rodinia. Precambrian Research 87, 135–159.

Wingate, M.T.D., Campbell, I.H, Harris, L.B., 2000. SHRIMP baddeleyite age for the Fraser Dyke Swarm, southeast Yilgarn Craton, Western Australia. Australian Journal of Earth Sciences 47, 309–313.

Wingate, M.T.D., Pirajno, F., Morris, P.A., 2004. Warakurna large igneous province: a new Mesoproterozoic large igneous province in west-central Australia. Geology 32, 105–108.

Zang, W., 2003. Maitland special map sheet, South Australia. Geological Survey of South Australia. Geological Atlas 1:250 000 Series, sheet SI 53-12 and part of SI 53-16.